

Explaining excitable population dynamics in bark beetles: From life history to large, episodic outbreaks

Evan C. Johnson^{1,*}, Antonia Musso², José F. Negrón³, and Mark A. Lewis^{4,5}

¹*Mathematical and Statistical Sciences; University of Alberta; Edmonton, Alberta, Canada*

²*Biological Sciences; University of Alberta; Edmonton, Ontario, Canada*

³*USDA Forest Service; Rocky Mountain Research Station; Fort Collins, CO, USA*

⁴*Department of Mathematics and Statistics; University of Victoria; Victoria, British Columbia, Canada*

⁵*Department of Biology; University of Victoria; Victoria, British Columbia, Canada*

*Corresponding author: *Evan Johnson, ecjohns1@ualberta.ca*

Open Research statement

All code and data will be made available upon publication at [TBD](#)

Contents

1	Introduction	4
1.1	The biology of mountain pine beetle and lodgepole pine	7
1.2	Mountain pine beetle life history	9
1.2.1	Allee effect	9
1.2.2	Stand-Dependent dispersal mortality	10
1.2.3	Large-tree preference	14
1.2.4	Tree size-dependent fecundity	15
1.2.5	Time-scale separation	15
2	Methods	15
2.1	Overview	15
2.2	Data	17
2.3	Simulation model	17
2.4	Causal analysis	20
2.5	Describing population dynamics	20
3	Results	22
3.1	Model diagnostics and parameter estimates	22
3.2	Effects of life history on population dynamics	23
4	Discussion	30
4.1	Bark beetle comparative analysis	30
4.2	Mountain pine beetle dynamics	32
5	Acknowledgements	37
A	Statistical model description	37
A.1	Data	37
A.2	Model overview	38
A.3	Model-fitting	39
A.4	Lodgepole pine forest dynamics	40
A.5	Tree size-dependent preference sub-model	42
A.6	Converting beetle attacks to tree deaths	44
A.7	Tree size-dependent fecundity	44
A.8	Allee effect	45
A.9	Integrator model	47
B	Additional model justification	52
B.1	Stochastic perturbation size	52
B.2	Mass attack preference does not change	52
B.3	Increasing attack density does not affect population dynamics	53
B.4	Leave one year out cross validation	54
B.5	The Allee effect depends only on beetle density	58
C	Model fitting details and diagnostics	60
D	Landscape analysis of bark beetle damage	61
E	Additional supplementary figures	68

Abstract

Bark beetles are significant forest pests, with some species capable of causing widespread tree mortality. Among these, the mountain pine beetle (MPB) stands out for its exceptionally destructive outbreak in the 2000s. We use MPB as a case study to explore the concept of *excitable dynamics*, where ephemeral perturbations produce large excursions from equilibrium. Our empirically-calibrated model reveals five features of MPB biology: stand density-dependent dispersal, an Allee effect, time-scale separation between beetle and tree life cycles, tree size-dependent fecundity, and a large-tree preference. The first three features explain MPB's characteristic boom-bust dynamics, while the latter two explain outbreak magnitude. Other bark beetles lack one or more of these traits, partially explaining their generally lower impact. However, predicting bark beetle impact requires consideration of both life history and landscape factors: total damage increases linearly with host-tree biomass, but this relationship holds only for irruptive (i.e., excitable) beetle species. We distill our findings into a minimal mechanistic model that captures the essence of irruptive bark beetle dynamics. This model firmly establishes MPB as one of the first empirical examples of excitable dynamics in ecology.

Keywords: bark beetle, mountain pine beetle, outbreak, excitable dynamics, lodgepole pine, forest pest, population dynamics, density dependence

1 Introduction

Bark beetle (Coleoptera: Curculionidae, Scolytinae) outbreaks occur worldwide (Lantschner and Corley, 2023), with recent epidemics in western North America causing widespread tree mortality (Meddens et al., 2012; Taylor et al., 2006). These outbreaks exhibit a distinctive pattern: unpredictable and explosive population growth followed by rapid declines (Fig. E.1). The episodic “boom-bust” pattern contrasts sharply with the population dynamics of most species, which typically show either stochastic fluctuations around a weakly-attracting equilibrium or cycles driven by resource-consumer interactions (Louca and Doebeli, 2015; Hassell et al., 1976; Ellner and Turchin, 1995). In this paper, we demonstrate that certain bark beetle species are unique in that their population dynamics can be classified as “excitable”.

Excitable population dynamics are characterized by several features that set them apart from other types of dynamic behaviors (Murray, 1989; Morozov and Petrovskii, 2009; Hastings et al., 2021). Perturbations trigger large excursions from equilibrium, leading to dramatic population increases from minor or transient environmental changes. These excursions involve both positive and negative feedback mechanisms, creating a self-reinforcing cycle of growth followed by an eventual crash. Excitable systems often exhibit “slow-fast dynamics” (Hastings et al., 2018), where one state variable changes rapidly (e.g., beetle population size), while another changes slowly (e.g., tree population size). This results in a *refractory period*, the minimum time between excursions. In summary, the notion of excitability (while lacking a formal mathematical definition; Strogatz, 1994, pg. 118) involves perturbations causing large but ultimately transient deviations from a stable equilibrium. The canonical example of excitable dynamics is the action potential of a neuron (Hodgkin and Huxley, 1952): A perturbation (neurotransmitters from neighboring neurons) and positive feedback causes a neuron to fire, and slow-fast dynamics (related to conformational changes in ion channels) result in a refractory period. In the case of neurons, excitability is adaptive, ensuring unidirectional signal propagation and regulating firing frequency (Johnston and Wu, 1994).

Bark beetle outbreaks display these hallmarks of excitability. A perturbation such as drought or wind damage can increase tree susceptibility to beetle attack (Singh et al., 2024). This initiates a positive feedback loop: larger beetle populations overcome bigger, better-defended trees, further increasing their numbers. Irruptive bark beetles must mass attack host trees to overcome toxic resin defenses (Thalenhorst, 1958; Raffa and Berryman, 1983; Boone et al., 2011), using aggregation pheromones and tree volatiles to focus their efforts (Raffa, 2001; Seybold et al., 2006). Many bark beetle populations are thought to exhibit a *strong Allee effect*, wherein per capita growth rates become negative at sufficiently low population densities (Taylor, 2012). Negative feedback when beetles run out of suitable or detectable host trees. Post-outbreak, trees must grow until their phloem or cambium is thick enough to support beetle development, which generates a slow-fast dynamic and a minimum interval between outbreaks. The perturbation that triggers the outbreak, however, is effectively random — there is no maximum interval. Therefore, bark beetle outbreaks occur irregularly (episodic) rather than on a fixed schedule (cyclical).

We will demonstrate that bark beetles are unique in ecology as the only known taxonomic group known to exhibit excitable population dynamics. While the spruce budworm (*Choristoneura fumiferana*) is sometimes cited as an example, this is probably incorrect. An influential mathematical paper (Ludwig et al., 1978) proposed that excitability in the spruce budworm system could result from interactions between trees, spruce budworms, and their avian predators. Specifically, birds with a type III functional response (Holling, 1959) led to low predation rates at low budworm density due to prey-switching (preventing budworm extirpation between outbreaks), and saturating rates at high density due to handling time constraints (generating positive density dependence during incipient outbreaks). The slow part of the slow-fast dynamics is attributed to the fact forest quality rebounds slowly, and that avian

predation is assumed to be proportional to forest quality. However, current evidence indicates that spruce budworms undergo noisy cycles due to their interactions with parasitoids (Royama, 1984; Berryman, 1996; Royama, 1997; Régnière and Nealis, 2007; Pureswaran et al., 2016) rather than excitable dynamics. Although budworms may face mate-finding challenges at low densities (Régnière et al., 2013), there is little evidence for a demographic Allee effect over larger spatial scales.

Examples of excitable dynamics in ecology have been explored theoretically but lack empirical support. Models of algal blooms suggest the possibility of excitable dynamics triggered by a temporary influx of nutrients, with positive feedback arising from either top-down or bottom-up control. The top-down mechanism is a saturating functional response where zooplankton become satiated (Truscott and Brindley, 1994a,b); negative feedback comes from predation, and the slow-fast dynamics result from disparate generation times of zooplankton and phytoplankton. The bottom-up mechanisms involves the formation of algal mats, which improves nutrient cycling and accelerate algal growth (Huppert et al., 2002, 2004); the negative feedback comes from nutrient depletion, and the slow-fast dynamics result from slow replenishment of nutrients from runoff, decomposition, etc. Excitable algal blooms are likely to occur somewhere, given the diverse character of algal blooms worldwide (Glibert et al., 2018), anecdotes of threshold-effects (Pearsall, 1932; Lund, 1950), and correlations between the bloom occurrence and environmental fluctuations (e.g., Freund et al., 2006). To the best of our knowledge, however, there is no well-justified and empirically calibrated model that provides clear evidence for excitable algal blooms. Small mammal populations can experience severe outbreaks, but these are typically classified as pulse-driven rather than irruptive (Andreassen et al., 2021). Pulse-driven outbreaks occur due to significant increases in resource availability, such as abundant vegetation following unusually high precipitation, rather than small or transient perturbations characteristic of excitable systems (Holt, 2008).

Some bark beetle species undergo pulse-driven outbreaks triggered by logging, windfall, or drought. Definitionally, these outbreaks subside shortly after the disturbance ends. For example, prolonged drought in the western United States from 1995–2004 (Breshears et al., 2005) depleted trees’ defensive resin reserves, which led to an outbreak of *pinyon Ips* beetles. The outbreak peaked from 2002 to 2004, and infestation densities fell by nearly two orders of magnitude after the drought ended (Raffa et al., 2008). In contrast, excitable bark beetle outbreaks persist long after the initial disturbance subsides. An outbreak of the North American Spruce Beetle (*Dendroctonus rufipennis* Kirby) lasted 13 years following a single windthrow event in 1939 (Massey and Wygant, 1954; Anderson et al., 2010; Forest Health Protection, 2011) and an outbreak of the mountain pine beetle (MPB; *Dendroctonus ponderosae* Hopkins) continuing for 10–15 years after the initiating drought ended in 2000 (Creeden et al., 2014). Bark beetles that exhibit excitable dynamics are termed irruptive or aggressive, while those with pulse-driven outbreaks are classified as semi-aggressive or opportunistically aggressive (Lantschner and Corley, 2023; Weed et al., 2015).

In this paper, we ask: why do some bark beetles species display excitable population dynamics, and why are some outbreaks so large? To answer these questions, we examine the mountain pine beetle as a case study, using insights from this species and comparative analysis to better understand population patterns across bark beetle species. Our methodology involves four key steps:

1. Developing and validating a realistic model of mountain pine beetle dynamics, incorporating known biological features.
2. Performing a causal analysis through counterfactual simulations, manipulating various biological features to determine their impact on population dynamics.
3. Generalizing the results to other irruptive bark beetle species based on shared life history characteristics.

4. Building a minimal mechanistic model which contains only the necessary processes for excitability

Additionally, we explore the relationship between excitability and the magnitude of bark beetle outbreaks (i.e., the peak number of beetles). In theory, the two concepts are orthogonal — excitability only implies that outbreaks are large relative to the initiating perturbation. In practice, however, the two concepts are connected. Later, we show that the total area affected by a beetle species is proportional to the combined biomass of their host trees, but that this relationship only applies to excitable (also known as irruptive) species; the relationship does not hold for beetles with pulse-driven outbreaks.

The mountain pine beetle serves as our model species, chosen for its well-documented life history and its significant impact. The most recent outbreak of MPB (ca. 2000–2015) stands as the largest recorded insect outbreak in history (Taylor et al., 2006), killing up to 8.5 million hectares of tree crowns across western North America (Meddens et al., 2012), and killing > 50% of merchantable pine volume in British Columbia (British Columbia Government, 2016). This event had far-reaching consequences, including transforming British Columbia’s forests from a carbon sink to a source (Kurz et al., 2008), inflicting billions of dollars in economic damage (Corbett et al., 2016), and altering hydrological functioning (Schnorbus, 2011).

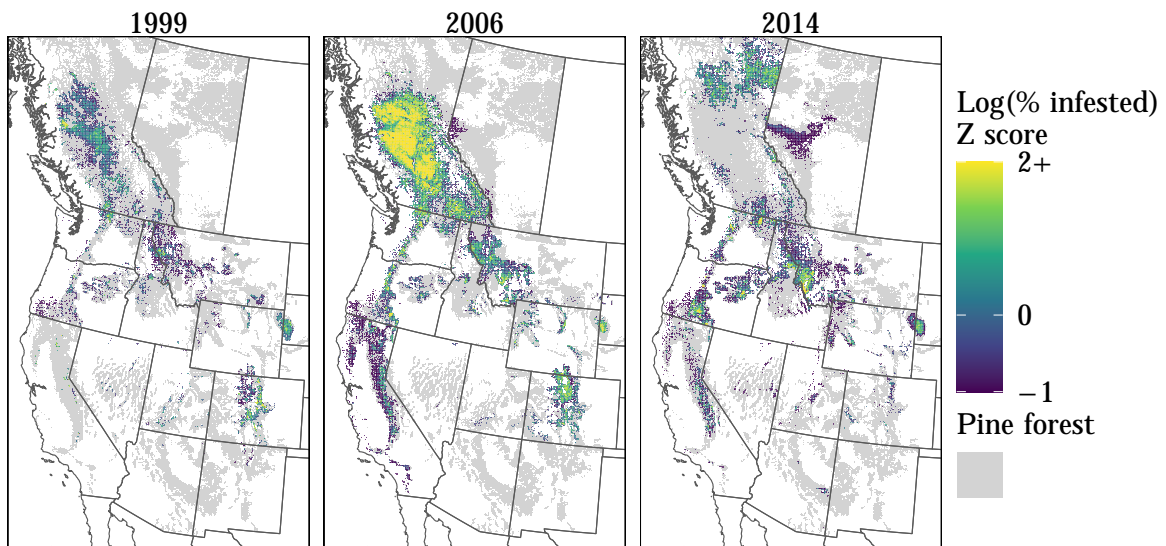


Figure 1: Progression of the latest large-scale mountain pine beetle outbreak. The data comes from fixed-wing Aerial Overview Surveys (United States and British Columbia) and Heli-GPS surveys (Alberta). Pine forest data comes from Beaudoin et al. (2014) and (Ellenwood et al., 2015).

Of course, the question of “Why is mountain pine beetle so destructive?” has been studied extensively. Climate change is the principal reason for the severity of the outbreak in the 2000s relative to past outbreaks (Carroll et al., 2006a; Alfaro et al., 2009; Creeden et al., 2014). Widespread drought conditions caused synchronized increases in tree susceptibility. At the same time, warmer winter temperatures reduced overwintering mortality in beetle larvae. Fire suppression has also played a role, by enabling the buildup of large-diameter pines (Taylor et al., 2006). Indeed, a comparative analysis of bark beetles found that the best predictor of outbreaks is the availability of susceptible host trees (Koricheva et al., 2012). Mountain pine beetle was far more destructive in British Columbia than the western United States (Meddens et al., 2012).

Although this spatial pattern is not well-researched, we suspect that it involves the high density and spatial continuity of lodgepole pine in the Chilcotin Plateau — the epicenter of the last two outbreaks in British Columbia.

Our approach differs from previous research on bark beetle dynamics in several key aspects. Rather than focusing on the (proximal) environmental causes of outbreaks, we focus on the (ultimate) beetle life-history causes of outbreaks. We present quantitative and empirically-calibrated models that offer more precision than the verbal descriptions found in other reviews of bark beetle dynamics (e.g. [Coulson et al., 1985](#); [Raffa et al., 2008](#); [Weed et al., 2015](#); [Biedermann et al., 2019](#); [Lantschner and Corley, 2023](#); [Singh et al., 2024](#)) and allow us to identify a minimal set of processes that generate characteristic boom-bust dynamics. Other studies have attempted to link life-history predictors to outbreaking behavior with statistical comparisons (e.g., [Nothnagle and Schultz, 1987](#); [Koricheva et al., 2012](#); [Kozlov et al., 2010](#)), but this approach faces significant limitations. It’s often unclear how certain predictors are mechanistically connected to outbreaks. For example, larger bark beetles are more prone to outbreaks, contradicting $r - K$ selection theory’s prediction that smaller beetles should have higher growth rates and thus greater outbreak potential ([Koricheva et al., 2012](#)). More critically, there is very little information available about the biology of non-outbreaking species ([Nothnagle and Schultz, 1987](#); [Johns et al., 2016](#)). To circumvent these difficulties, we build a mechanistic model of the bark beetle species for which the most information is available — the mountain pine beetle — and then extrapolate to other species based on shared life history .

The study of excitable dynamics in bark beetles has significant practical implications. The positive feedback mechanisms inherent in excitable systems mean that outbreaks can extend far beyond the spatial extent of an initial disturbance, making them widespread and difficult to manage. This suggests the existence of a “Goldilocks zone” of population densities where management efforts will be most effective — too low, and the strong Allee effect naturally limits population growth; too high, and the outbreak becomes unmanageable ([Hodge et al., 2017](#), Fig. 6). After a major outbreak occurs, there is a known window of time — a ticking clock — before the next outbreak could occur. This period offers forest managers a timeline for implementing preventive measures, such as creating diverse stands in terms of age structure and species composition ([Dymond et al., 2014](#); [Burton, 2010](#)).

1.1 The biology of mountain pine beetle and lodgepole pine

Adult beetles emerge in July or August and after emergence these beetles fly in search of new host trees, typically targeting large pines during the epidemic population phase. Mountain pine beetle has infested Jack pine and Rocky Mountain bristlecone pine, but the general suitability of these species is a matter of ongoing research ([Bentz, 2019](#); [Bentz et al., 2022](#); [Bleiker et al., 2023](#)). Individual beetles may fly around for several days, but few beetles survive more than 5–10 days outside of the tree ([Reid and Reid, 2008](#); [Fuchs and Borden, 1985](#)). Emergence from natal trees is synchronous due to temperature-dependent development thresholds ([Powell and Bentz, 2009](#); [Logan and Powell, 2001](#)), but the synchronicity is not perfect, and so the population-level flight period may last up to 6 weeks ([Bleiker and Van Hezewijk, 2016](#)).

Because individual beetles cannot be tracked, the dispersal phase of the life cycle is mildly mysterious. Available evidence points to three modes of dispersal: short-, medium-, and long-range dispersal. Most beetles disperse less than 30–50 meters under the canopy ([Safranyik et al., 1992](#); [Robertson et al., 2007](#); for the Douglas-fir beetle [Dodds and Ross, 2002](#)). A minority of beetles disperse up to 5 km ([Robertson et al., 2009](#); [Powell and Bentz, 2014](#); [Howe et al., 2021](#); [Koch et al., 2021](#)), performing pioneer attacks and aggregating to form semi-regular patterns of “spot infestations” (clusters of infested trees) across the landscape ([Strohm et al., 2013](#)). The smallest fraction of beetles (0–2.5%) fly above the canopy ([Robertson et al., 2009](#); [Safranyik et al., 1992](#)), where they may get carried up to 300 km by upper atmospheric winds ([Hiratsuka et al., 1982](#); [Cerezke, 1989](#); [Jackson et al., 2008](#)). Some experts have speculated that the fraction

may be higher in stands where most suitable host trees have already been killed (Carroll et al., 2003; de la Giroday et al., 2011; Bleiker, 2019).

Upon locating a suitable host, MPB females initiate attacks. The trees fight back by exuding resin, which serves to entrap or *pitch out* (i.e. expel) attacking MPB. Female pioneers release *trans* and *cis*-verbenol, aggregation pheromones that draw more beetles to the site (Pureswaran et al., 2000; Seybold et al., 2018). As males arrive, they emit *exo*-brevicomin, another aggregation pheromone that specifically attracts additional females (Rudinsky et al., 1974). Many bark beetle species use aggregation pheromones and host volatiles to coordinate *mass attacks*, where swarms of beetles overwhelm a single tree. Depending on the beetle population density, tree suitability, and the tree’s defensive capability, successful mass attacks may last from a couple of hours to a week, continuing until the tree’s resin supply is depleted.

Following a successful mass attack, females bore into the tree and excavate egg galleries. Mating occurs within the tree, and males will either seek out additional females or “settle down” to help with gallery defense. Eggs hatch within one to two weeks, and larvae immediately start feeding on the tree’s phloem. The beetles carry fungal spores in specialized mouthparts, thereby spreading and inoculating the phloem tissue with fungi. Beetle larvae and adults rely on fungal hyphae and spores for nutrition (Reid, 1958; Bleiker and Six, 2007). Tree death is hastened by MPB’s fungal symbionts, blue stain fungi *spp.*, which colonize the tree’s transport vessels (Arango-Velez et al., 2016). Larvae mine horizontal galleries that terminate in an oval pupal chamber which is lined with spores.

Mature larvae overwinter after accumulating cytoprotectants that allow them to survive temperatures as low as -30C (Bentz and Mullins, 1999). Other life stages are more susceptible to cold mortality particularly to cold snaps that are early or late in their overwintering period (Wygant, 1940; Safranyik and Linton, 1991; Logan et al., 1995). Other life stages are more susceptible to cold mortality particularly to cold snaps that are early or late in their overwintering period (Régnière and Bentz, 2007; Rosenberger et al., 2017). Come spring, surviving larvae resume feeding and pupate in the late spring or early summer. By the time of adult emergence, approximately one year after the initial attack, the needles of successfully-attacked trees have turned a rust-red color. This telltale diagnostic makes it possible to gather extensive data through aerial surveys.

Lodgepole pine and ponderosa pine are the predominant hosts of MPB, simply because they are the most abundant pine species in MPB’s geographic range. Lodgepole pine dominates in British Columbia, western Alberta, and the American Rocky Mountain states, whereas ponderosa pine is more abundant in the American southwest and the Sierra mountains (Beaudoin et al., 2014; Ellenwood et al., 2015). Both species are shade-intolerant and fire-resistant. They tend to be seral (i.e., persisting as a non-climax species in a fire cycle), taking advantage of high-light conditions following a stand-leveling fire (Fryer, 2018; Anderson, 2003; Lotan et al., 1985). Lodgepole pine has closed cones with seeds that remain viable for decades, effectively creating a seed bank (Teste et al., 2011a,b). Due to its abundant seeds and its ability to thrive in high-light conditions, lodgepole pine can take advantage of the light gaps created in the years following a mountain pine beetle attack, resulting in the recruitment of seedlings into approximately even-aged cohorts (Axelson et al., 2010). However, this regeneration pattern is not universal across MPB’s range; in Alberta, for example, the density of standing dead trees following MPB outbreaks prevents sufficient light penetration, leading to the replacement of lodgepole pine by more shade-tolerant species (Axelson et al., 2009).

During epidemics, MPB seeks out large healthy trees with abundant phloem resources. However, in their low-density endemic state, there are not enough beetles to mass attack a single healthy tree, and thus there is a collective behavioral switch where beetles seek out trees that are weakened or stressed, typically due to root disease, wind damage, or lightning (Tkacz and Schmitz, 1986; Carroll et al., 2006b). Endemic populations tend to remain at low density, primarily due to resource limitation, but also because of natural enemies and competition with

other bark and woodboring beetle species (Amman, 1983; Safranyik and Carroll, 2006). Endemic populations of MPB can transition into an incipient-epidemic state when they successfully breed within trees that have thick phloem. This scenario can occur if a healthy tree experiences acute stress (such as wind damage or lightning) right before the MPB flight period, such that pulse-driven bark beetles have not yet extensively colonized the tree (Bleiker et al., 2014). Such stressors can trigger local outbreaks (on the scale of square kilometers). However, widespread outbreaks are usually preceded by widespread drought conditions, which synchronously weaken the resin defenses of many trees (Alfaro et al., 2009; Creeden et al., 2014; Kolb et al., 2016).

1.2 Mountain pine beetle life history

A key element of this paper is a nonlinear dynamical model that captures key features of MPB biology. In this section, we review life history with a view toward features that should be emphasized in the model, like the ways in which MPB “decides” about what trees to attack, and how MPB responds to variation in the density of host trees and conspecific beetles. Our list is not exhaustive. Previous research has identified some biological processes that do not show up as a clear pattern in our data, or that we cannot feasibly incorporate into our models. These are discussed further in Appendix B.

1.2.1 Allee effect

Mountain pine beetle is subject to a strong Allee effect, a phenomenon where per capita growth rates become negative at a sufficiently low population density. The Allee effect arises because a threshold number of beetles must attack a single tree to successfully kill it. Another common mechanism of an Allee effect, poor mate finding in small populations, has been ruled out by previous research (Amman, 1980; Bleiker et al., 2014).

The Allee effect is mitigated by MPB’s ability to aggregate. In general, aggregation counteracts the negative effects of positive density dependence, just as dispersal counteracts the negative effects of negative density dependence (Crowley, 1981; Briggs and Hoopes, 2004). Aggregation pheromones and volatile monoterpene from attacked trees attract additional beetles. However, this chemical signal may be dampened by unsuitable host-tree chemistry (Hynum and Berryman, 1980; Boone et al., 2011), unsuitable natal-tree chemistry (which negatively affects aggregation pheromone production; Chiu et al., 2018), or simply a limited ability to detect aggregation pheromones at-distance. Evidence from small-scale spatial maps, as well as mechanistic pheromone diffusion models, suggest that beetles primarily respond to aggregation pheromones that are 20-100 meters from their tree-of-origin (Mitchell and Preisler, 1991, Fig. 4–5); Strohm et al., 2013). There is limited evidence that the detection limit is 500-1000 meters under the right wind conditions (Barclay et al., 1998). In summary, the Allee effect persists due to various physical and chemical factors that constrain the strength of aggregation.

It has long been recognized that the size disparity between beetles and trees means that many beetles must attack a single tree, and therefore, that outbreaks require a threshold or critical density of beetles (Thalenhorst, 1958; Safranyik et al., 1975; Berryman, 1978). However, explicit evidence for the Allee effect in MPB is not always forthcoming. Studies have detected an Allee effect when focusing on tree-level attack density (e.g., beetle entry holes per unit tree surface area). An Allee effect is implied by a positive relationship between attack density and the probability of tree death (Waring and Pitman, 1983, 1985; Peterman, 1974), a positive relationship between attack density and the probability of reproduction (Raffa and Berryman, 1983, Fig. 5), or a positive relationship between the number of attacked trees and the probability of tree death (Boone et al., 2011). On the other hand, studies *do not* detect an Allee effect when they focus solely on the density of infested trees, treating this quantity as a proxy for beetle population size (MacQuarrie and Cooke, 2011; Tunnock et al., 1970; Trzcinski and Reid, 2009).

1.2.2 Stand-Dependent dispersal mortality

Mountain pine beetle predominantly disperses from stands only after most large-diameter trees are killed. The vast majority of these emigrants die on their journey due abiotic elements or an inability to find a suitable host tree. Beetles that do survive may be less likely to attack suitable host trees, given the low energetic conditions resulting from a long flight (Jones et al., 2020). Since stand-dependent dispersal and the associated mortality are somewhat obscure features of MPB dynamics, we will take a moment to discuss supporting evidence.

The most likely explanation for stand-dependent dispersal is chemosensory constraints: MPB is simply unable to sense and aggregate on small and medium-sized trees. Multiple lines of evidence support this explanation — MPB primarily attacks small or non-host trees when they are adjacent to large host trees (Mitchell and Preisler, 1991; Preisler and Mitchell, 1993; Amman et al., 1985; Huber et al., 2009), and studies have shown large trees have higher monoterpene concentrations, which may be the main determinant of whether pioneer female beetles initiate an attack (Boone et al., 2011; Seybold et al., 2006; Howe et al., 2022a).

Alternative explanations for stand-dependent dispersal have less support. One considers the fact that beetle infestations alter the forest microclimate (Bartos, 1989; Amman and Logan, 1998). As stands are thinned, increased wind disrupts MPB aggregation pheromone plumes, and increased light may induce MPB to fly. However, the microclimate hypothesis is undermined by timing — trees take 5-20 years to fall (Lewis and Hartley, 2006; Hansen, 2014) and 2–7 years to lose needles (Klutsch et al., 2009; Audley et al., 2021), while populations crash within 1–2 years (Fig.,E.1). The inclusive fitness hypothesis suggests beetles refuse to consider medium-sized trees because large trees engender higher fitness, but this is unlikely given high dispersal mortality and positive fitness in medium trees (Fig.,3).

Even though we cannot track individual beetle dispersal, there is robust evidence for stand-dependent dispersal. In addition to the previously discussed evidence, trapping experiments have shown that far more beetles are caught in unthinned stands than thinned stands, regardless of whether pheromone traps (Bartos, 1989; Schmitz et al., 1989), or passive traps are used (Fig. 2). Sallé and Raffa (2007) have shown that beetles with low body weight had proportionally more lipids. Since beetles are more reactive to aggregation pheromones once lipids are depleted, this explicates a physiological mechanism by which beetles can escape depleted stands. Several modeling studies explicitly infer substantial stand-dependent dispersal (Powell and Bentz, 2014; Powell et al., 2018; Howe et al., 2021). Other, more complicated models implicitly assume stand-dependent dispersal, and then show that this assumption leads to realistic population dynamics (e.g., Powell et al., 2018; Bone and Altaweel, 2014; Kautz et al., 2016).

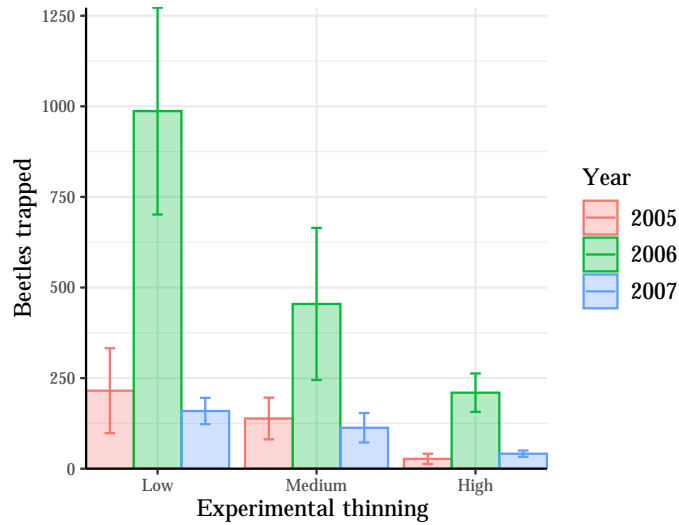


Figure 2: Fewer beetles are trapped in heavily thinned stands, suggesting that beetles disperse away from sparse forests. The y-axis displays the mean and standard errors of beetles in passive traps in Fraser Experimental Forest’s (Colorado) managed stands over the full flight period. Thinning levels are categorized as ‘Low’, ‘Medium’, and ‘High’, with corresponding Growth Stocking Levels (GSL) of 120, 80, and 40, respectively. The small size of the experimental blocks (0.2 ha) suggests that captured beetles predominantly originated from adjacent unmanaged forest, in turn suggesting that the data reflect the impact of tree density on dispersal behavior, not on the within-block infestation density. Data comes from [Negrón \(2018\)](#).

The most compelling evidence for stand-dependent dispersal is the fact that outbreaks invariably end before the vast majority of medium-sized trees are killed (Fig. 4), even though beetles have positive fitness on medium-sized trees (Fig. 3). Previous research ([Goodsman et al., 2018](#)) has explained this pattern — where an outbreak ends sooner than expected — as a result of *overcompensatory density dependence*, a phenomenon where increased population size now leads to a decreased population size in the next generation. However, there is no evidence for overcompensatory density dependence in MPB. Attacking beetles pack themselves into trees at a density that roughly optimizes individual fitness ([Raffa and Berryman, 1983](#)). When attack densities do exceed the theoretical optimum, there is no clear change in emergence densities (Fig. E.3; [Berryman, 1974](#), Fig. 2c; [Berryman, 1976](#); Fig. 2, [Raffa and Berryman, 1983](#), Fig. 6 shows a slight increase) and there is no clear change in population dynamics (Appendix A.6).

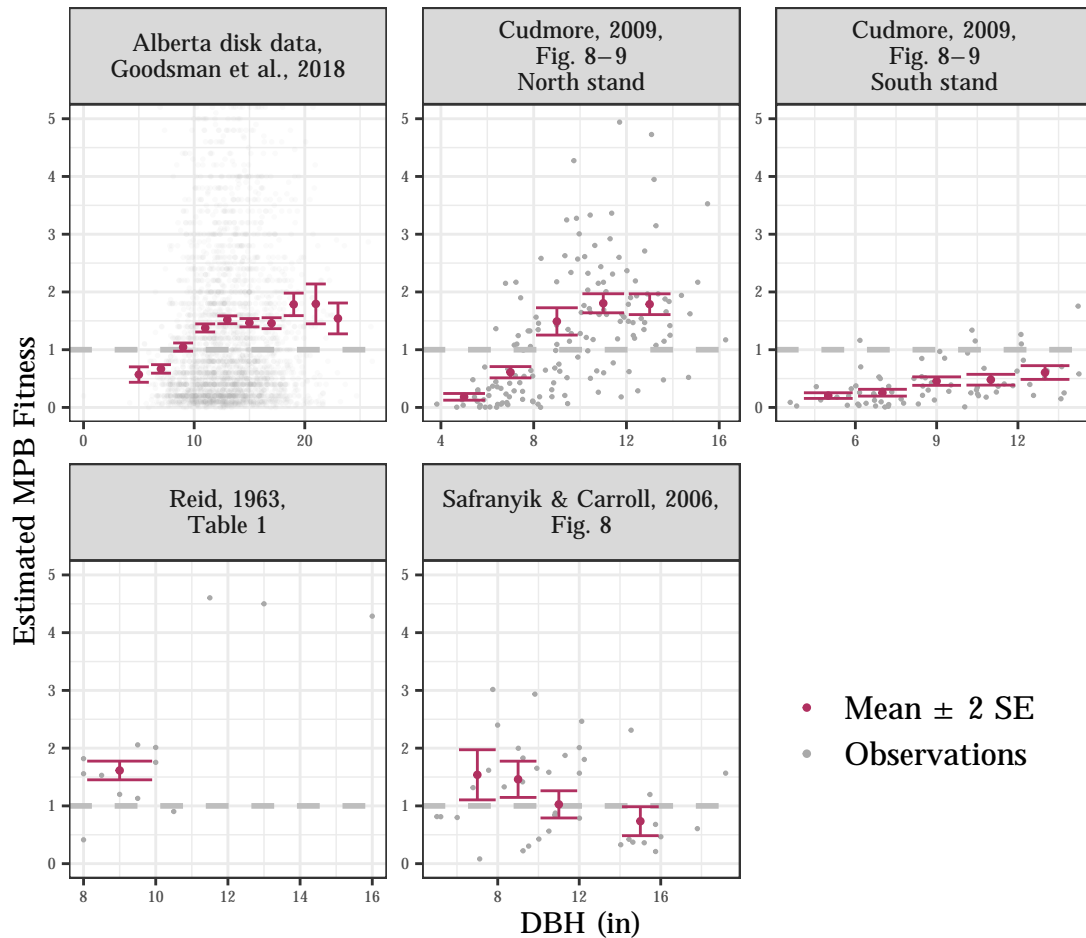


Figure 3: Mountain pine beetle tends to have positive fitness when attacking medium-sized trees (approx. 8–14 inches DBH). Ecological fitness is estimated with $(0.3) \times \text{females out of the tree} / \text{females into the tree}$, where the factor 0.3 is the approximately the median dispersal-phase survival in the dataset from Klein et al. (See Fig. E.4). Depending on the study, gallery starts or entry holes serve as estimates for *females into the tree* (note that only females initiate galleries). $(2/3) \times (3/2) \times$ Emergence holes, or $(2/3)$ of the overwintered brood serve as estimates of *females out of the tree*. Note that $(2/3)$ is the typical proportion of females (Reid, 1962; Cole et al., 1976), and that $(3/2)$ is the average number of beetles emerging from each hole (Safranyik and Linton, 1985; Peterman, 1974, Fig. 13). Data comes from Goodsman et al. (2018); Cudmore et al. (2009); Reid (1963); Safranyik and Carroll (2006). The means and standard errors were only computed for bins with at least 5 observations.

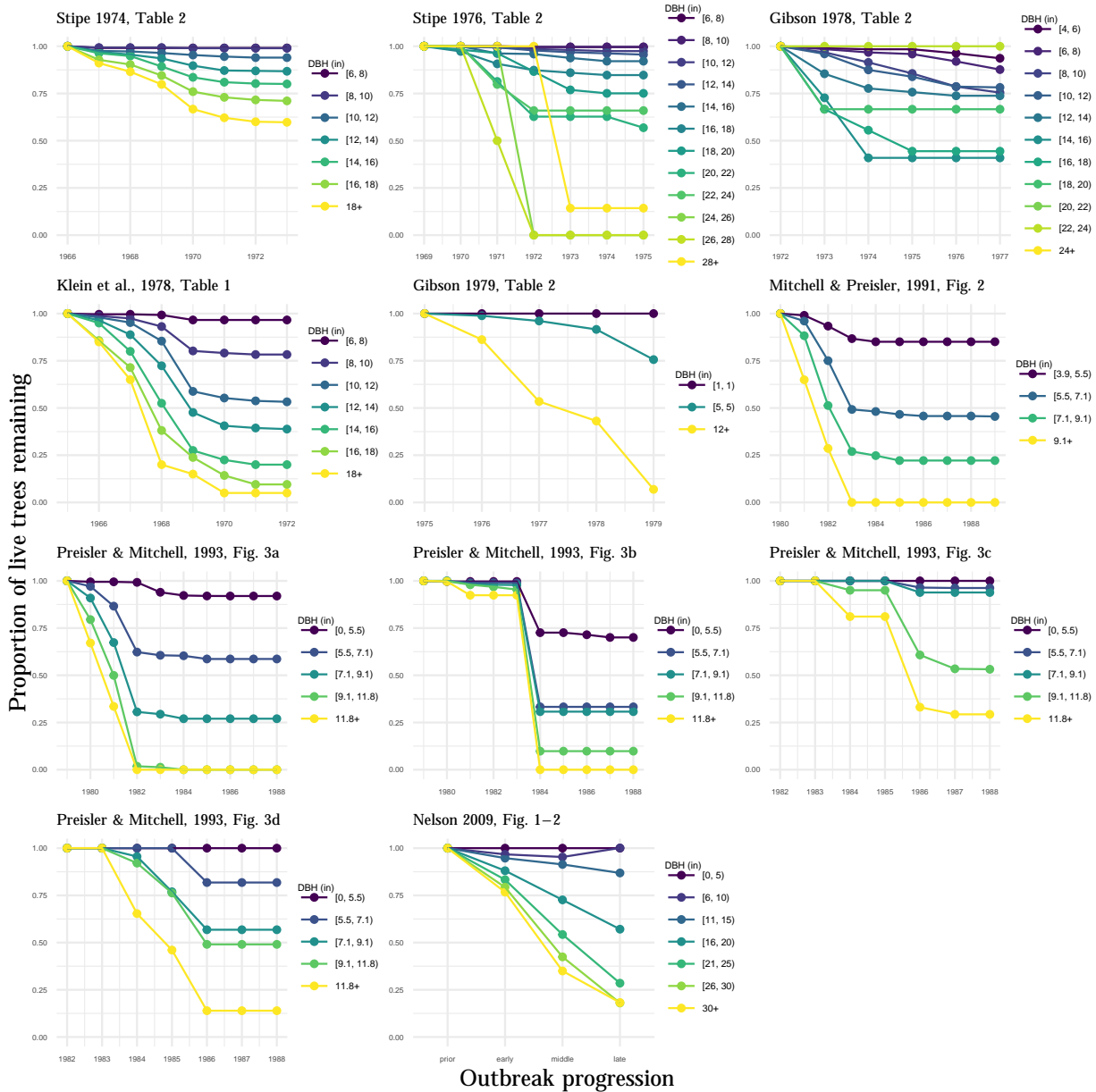


Figure 4: Outbreaks typically end before a majority of medium-sized trees (approx. 8–14 inches DBH) are killed. The figure depicts the proportion of remaining live trees as a function of time, stratified by diameter class (diameter at breast height, DBH). Data comes from [Stipe \(1974, 1976\)](#); [Gibson and Bennett \(1978\)](#); [Gibson et al. \(1979\)](#); [Klein et al. \(1978\)](#); [Preisler and Mitchell \(1993\)](#); [Nelson \(2009\)](#).

There is also evidence that stand-dependent dispersal mostly results in mortality, although this evidence is indirect. First, it is our observation (based on Aerial Overview Survey data) that outbreaks do not last substantially longer in areas with high contiguous pine biomass. If dispersing beetles were not dying in such areas, emigrating beetles would be replaced by immigrating beetles, and thus outbreaks would be prolonged. Second, mortality is already substantial for beetles traveling short distances: baseline dispersal mortality is estimated to be around 40–80% ([Safraiyik, 1989](#); [Latty, 2007](#); [Pope et al., 1980](#)); Fig. E.4). Third, dispersal puts beetles in a low energetic condition, leading to decreased aggregation pheromone production, and making them less likely to attack trees ([Jones, 2019](#); [Jones et al., 2020](#)). Fourth, lab experiments indicate that most beetles only survive several days outside of a tree ([Fuchs and Borden, 1985](#); [Reid and Reid, 2008](#)). Fifth, longer flights increase exposure to natural enemies,

most notably avian predators (Rust, 1930; Stallcup et al., 1963).

1.2.3 Large-tree preference

Mountain pine beetle exhibits a strong preference for large-diameter trees during their dispersal/host-selection phase, driven by both proximate sensory cues and ultimate evolutionary benefits. From an evolutionary perspective, large trees offer two key advantages: primarily, they have thicker phloem, which serves as the primary food source for MPB larvae, and secondarily, their thicker bark may provide better insulation during cold winters.

The proximate mechanisms driving a large-tree preference are evident across different stages of host selection. In the initial landing phase, beetles display a mix of random movement and slight preference for large, vertically-oriented black silhouettes (Shepherd, 1966; Billings et al., 1976), indicating that visual cues play a role. Chemo-sensory cues play a relatively minor role during the initial landing phase (Billings et al., 1976; Hynum and Berryman, 1980; Moeck and Simmons, 1991). For pioneer attacks, females use physical and gustatory cues associated with tree diameter, such as terpene concentrations (Raffa and Berryman, 1982) and bark roughness (Reid, 1963). During mass attacks, larger trees become even more attractive due to increased concentrations of aggregation pheromones and host volatiles, both of which correlate positively with tree size. These sensory preferences align with the evolutionary advantages of large trees, ensuring that beetles select hosts that offer the best resources for their offspring.

Mountain pine beetle’s large-tree attack preference is extremely well-established. The probability of tree death increases logistically with tree diameter (Buonanduci et al., 2023; Rodman et al., 2022; Morris et al., 2022; Negrón, 2020; Negrón et al., 2017; Björklund and Lindgren, 2009 and 15 sources therein, see Table 1), and stand susceptibility indexes invariably use variables that correlate with tree diameter: tree age, pine volume, or basal area (Shore et al., 1992; Chojnacky et al., 2000; Randall et al., 2011; Bentz et al., 1993, and sources therein). Depending on site-specific factors, the probability of tree mortality is near-zero for 4–8-inch trees and near-100% for 12–16-inch trees.

Despite their preference for large trees, MPB have developed strategies to maintain a near-optimal attack density and avoid strong intraspecific competition. Mountain pine beetle will “fill up” trees to an approximately invariant density, measured in beetles per square meter of tree trunk surface area, before moving on to the next tree. Interestingly, this attack density is close to being optimal in terms of the population growth rate (Raffa and Berryman, 1983). The mechanism for attaining (approximate) optimality is a suite of aggregation and anti-aggregation pheromones, and the relationship between such pheromones and host tree defenses. Beetles are attracted to the combination of terpenoid aggregation pheromones and volatilized terpenes. Because both are derived from tree resin, trees become less attractive as their resin defenses are depleted (Raffa and Berryman, 1983; Raffa, 1988). Anti-aggregation pheromones, which are only detected by beetles at short distances (around a meter; Bentz, 1996), redirect beetles to nearby trees, while rivalry stridulations (noises produced by males) help ensure that galleries are evenly spaced. Raffa (2001) puts forward several hypotheses for the apparent lack of cheaters — beetles who ignore the anti-aggregation pheromones and enter a “full” tree.

Beetle attack density remains relatively constant across tree diameters and beetle population sizes. Killed trees receive an approximately invariant number of attacks per unit surface area (Fig. A.9, Reid, 1963, Table 1, Peterman, 1974, Figs. 4–7). There is less literature on the relationship between attack density and beetle population size, but any such relationship is likely weak, given that 1) Negrón (2018) found no relationship; 2) there is a clear mechanism for limiting attack density (see the previous paragraph), and 3) that attack density varies in the range of 50–100 females per square meter (see Fig. E.5 in the *Results*), despite beetle population sizes varying by several orders of magnitude.

1.2.4 Tree size-dependent fecundity

Mountain pine beetle has higher effective per capita fecundity in larger trees. Large trees have thick phloem, which is the primary food source of larvae and teneral adults. Thin phloem can slow larval development, which can cause mortality if a cold snap occurs before the cold-resistant third & fourth-instar stages are attained; if larvae do manage to fully develop within a small tree, they may have small body sizes and low energetic condition upon emergence (Amman, 1983). Additionally, the thick bark of large trees protects against cold winter temperatures.

From a more abstract perspective, there are two ways in which large trees lead to more beetles: 1) they offer higher emergence densities (per unit of susceptible tree surface area); 2) they have lots of susceptible surface area. We use the term *effective fecundity* specifically to the former, diameter-dependent emergence density; we use “effective” because tree diameter doesn’t affect brood density per se, but rather brood density after overwintering but before the dispersal phase. Emergence density has a piecewise-linear relationship with tree diameter (Reid, 1963, Table 1; Safranyik, 1968, Fig. 25; Cole, 1969, Fig. 5; Cudmore et al., 2009, Fig. 6). Small trees produce next-to-zero beetles, whereas large trees produce thousands of beetles per square meter. Susceptible tree surface area also increases linearly with tree diameter, implying that total beetle brood size increases quadratically with tree diameter.

1.2.5 Time-scale separation

Trees live longer than beetles. Although this is evident, it sets the MPB-lodgepole system apart from most predator-prey and host-parasitoid systems. Typically, predators live longer than prey, and parasitoids have lifespans that are similar to their hosts’ lifespans.

2 Methods

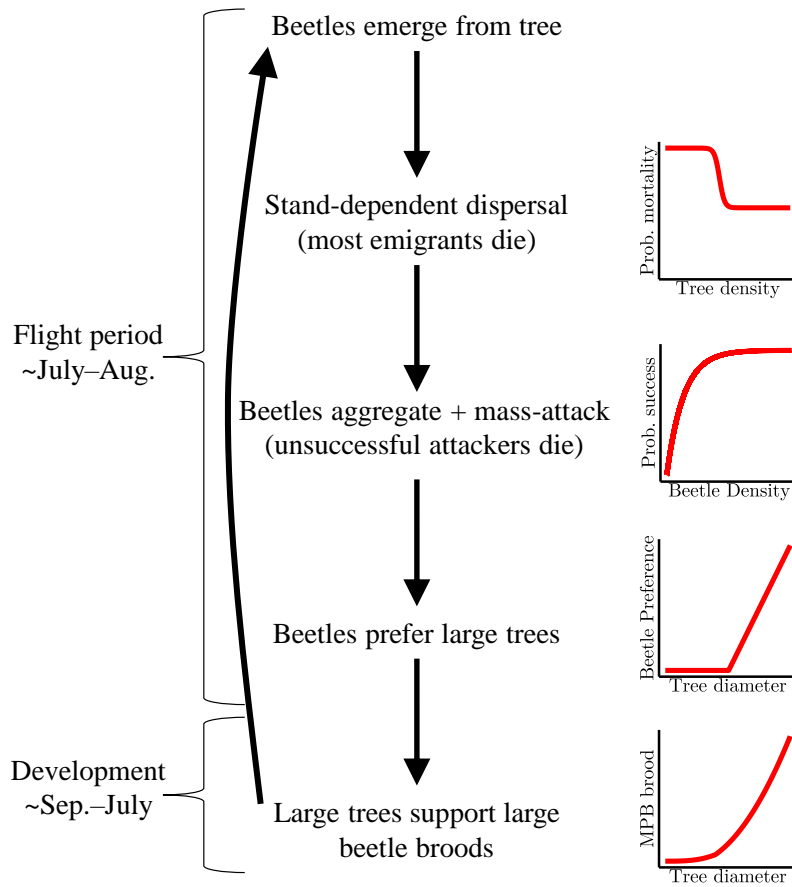
2.1 Overview

To understand how MPB life history affects MPB population dynamics, we will build a mechanistic model of MPB dynamics (summarized in Fig. 5), then simulate the model under counterfactual scenarios where various biological features have been turned on or off. If a population-dynamical phenomenon (e.g., episodic outbreaks) disappears when a certain feature is turned off (e.g., stand-dependent dispersal mortality), we can say that the feature is a necessary condition for the phenomenon. If two features being turned off makes the difference, then the two features are jointly necessary. As always, our inferences are conditional on the approximate veracity of the model.

Approximate timing

Outbreak processes

Cartoon representation



Pine forest processes

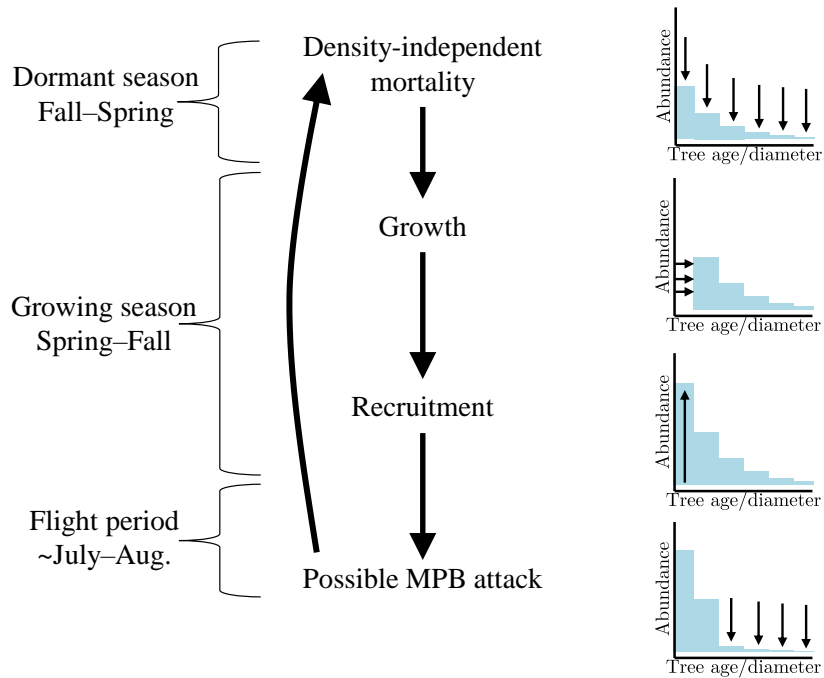


Figure 5: Depiction of the beetle/forest simulation model, and of the sub-models therein.

“Our model” is actually constituted by two types of related models: a simulation model

and a set of statistical models. The statistical models are used for model-building and for parameter estimation. The parameter estimates feed into the simulation model, which is then used to explore system behavior under various scenarios. The description of the statistical model is quite long, due to a large number of sub-models, equations describing error distributions, and the extensive use of graphical evidence to justify model structure. Therefore, the statistical models are described in Appendix A, while the simulation model is described below (in Section 2.3).

Realism is the key feature of our model — we intend to emulate the actual ecological system so that we can conduct virtual experiments. Many models of MPB have been published, but many are too simple for our purposes, having favored mathematical tractability over realism. Other models are too complex, containing functional forms that cannot be reasonably parameterized given available data. For further discussion of previous MPB models, see the *Discussion* and Appendix B.5. In contrast, our models are thoroughly justified via clear patterns in the data and/or a preponderance of evidence from previous research (see Appendices A & B). All models were fit to data with *Stan* (Stan Development Team, 2020), a Bayesian model-fitting software that implements Hamiltonian Monte Carlo (details in Appendix C).

2.2 Data

The model was parameterized using data from Boone et al. (2011) and Klein et al. (1978). All data was extracted from figures and tables using the *GraphGrabber* software and *Microsoft Excel's* digitizing features. Specific variables are described in Table A.1. The Boone et al. dataset contains the number of mass-attacked trees and the number of *successfully* mass-attacked trees, across a range of attack years, stands, and attack densities. This data justifies a functional form for the Allee effect. The second dataset, courtesy of Klein et al. (Fig. A.1), is one of the only datasets that contain beetle attacks, beetle emergence, and tree deaths, all stratified by year and tree diameter class. Our statistical model of MPB outbreak dynamics is primarily calibrated with this dataset, with the notable exception being that a Bayesian prior for the Allee effect parameter is derived from the Boone et al. data.

2.3 Simulation model

Mountain pine beetle outbreak dynamics (fast):

1. Beetle survival during the dispersal phase depends on forest conditions. The survival probability is a logistically increasing function of the total surface area of susceptible trees:

$$s_y = s_0 (1 + \exp(-\lambda_1 ((\text{relative surface area})_y - \lambda_0)))^{-1} \quad (1)$$

where s_y is the survival probability in the year y , and s_0 is the maximum survival probability. The parameters λ_0 λ_1 respectively control the intercept and slope of the logistic function. The *relative surface area* is the ratio of the current total surface area of trees with a diameter at breast height (DBH) of 8 inches or greater to the maximum possible surface area for such trees in an equilibrium forest without mountain pine beetle outbreaks.

2. Beetle populations experience stochastic perturbations. To obtain the density of attacking beetles, we multiply the number of emerging females per acre, B_y , and the dispersal-phase survival probability, s_y . Potentially, with probability P_I , we also add I beetles per acre:

$$(\text{attacks per acre})_y = s_y B_y + I \times \text{Bernoulli}(P_I). \quad (2)$$

The Bernoulli random variable simulates the stochastic endemic \rightarrow incipient-epidemic transition. Because most outbreaks occur during regional epidemics, beetle immigration

is the proximal catalyst for many endemic \rightarrow incipient-epidemic transitions on the local scale. But because drought is responsible for region-wide outbreaks, drought is the ultimate catalyst for most local-scale outbreaks. Drought conditions are somewhat unpredictable, but the best predictor of drought in western North America is the Pacific Decadal Oscillation (McCabe et al., 2004; Hidalgo, 2004), which has a quasi-period of 15-30 years (Mantua and Hare, 2002). The last two drought periods preceded the last two continent-scale outbreaks and were 20 years apart, (Creeden et al., 2014, Fig. 5d). Therefore, we set $P_I = 1/20 = 0.05$. We also set $I = 300$ based on a back-of-the-envelope calculation (Appendix B.1).

3. The probability of a successful mass attack is an exponential saturating function of attack density (i.e., beetles per acre). The density of successful attacks is

$$(\text{succ. attacks per acre})_y = (\text{attacks per acre})_y \overbrace{\left(1 - \exp\left(-2.3 \frac{(\text{attacks per acre})_y}{a}\right)\right)}^{\text{Probability of success}}, \quad (3)$$

where a is the Allee threshold parameter (defined as the attack density where the success probability equals 0.9). Unsuccessful beetles die without attacking additional trees.

4. Beetles prefer larger trees. Beetle preference is a piecewise linear function of tree diameter where “preference” is operationalized as the proportion of beetle attacks within a particular diameter class, divided by the proportion of total tree surface area belonging to that class:

$$(\text{preference})_j = \begin{cases} \beta_0 + \beta_1 \cdot \text{DBH}_j & \text{if } \text{DBH}_j > -\beta_0/\beta_1 \\ 0 & \text{otherwise.} \end{cases} \quad (4)$$

Here, β_0 and β_1 are intercept and slope parameters; and DBH_j is the diameter at breast height of the j^{th} discrete diameter class. Thus, $-\beta_0/\beta_1$ is the susceptible DBH threshold for beetle attacks.

5. Beetles distribute among tree diameter classes based on preference. The number of beetles per acre that successfully attack the j^{th} DBH class is:

$$(\text{succ. attacks per acre})_{j,y} = \frac{(\text{succ. attacks per acre})_y \cdot (\text{preference})_j \cdot (\text{prop. area})_{j,y}}{\sum_{k=1}^J (\text{preference})_k \cdot (\text{prop. area})_{k,y}} \quad (5)$$

where $(\text{succ. attacks per acre})_y$ is the total density of successfully attacking beetles, and $(\text{prop. area})_{j,y}$ is the proportion of susceptible tree surface area belonging to the j^{th} DBH class in year y .

6. A tree is killed once it is “filled-up” to a density of $1/\gamma$ female beetles per m^2 . The number of killed trees per acre (KTPA) in each diameter class is:

$$(\text{KTPA})_{j,y} = \min\left(\gamma \frac{(\text{succ. attacks per acre})_{j,y}}{(\text{surface area per tree})_{j,y}}, (\text{TPA})_{j,y}\right) \quad (6)$$

where γ a slope parameter, and $(\text{TPA})_{j,y}$ is trees per acre. If “successfully” attacking beetles kill all of the trees within a size class, the excess beetles are assumed to die (hence the “min” function).

7. The number of beetles produced by a single tree increases quadratically with tree diameter. Beetle emergence density (emerging female beetles per m^2) is a piecewise linear function of tree DBH:

$$(\text{emerge density})_{j,y} = \begin{cases} \zeta_0 + \zeta_1 \cdot \text{DBH}_j & \text{if } \text{DBH}_j > -\zeta_0/\zeta_1 \\ 0 & \text{otherwise} \end{cases} \quad (7)$$

Here, ζ_0 and ζ_1 are intercept and slope parameters. Thus, $-\zeta_0/\zeta_1$ is the DBH threshold for beetle reproduction. The expected number of female beetles per acre in next year, $y + 1$, is obtained with simple accounting:

$$\mathbb{E}[B_{y+1}] = \sum_{j=1}^J (\text{emerge density})_{j,y} \cdot (\text{surface area per tree})_j \cdot (\text{KTPA})_{j,y}. \quad (8)$$

8. The realized number of beetles is stochastic. To capture temporal variation in overwintering mortality, we assume that the realized number of beetles is drawn from a zero-truncated normal distribution:

$$B_{y+1} \sim \text{Normal}_{\text{Trunc.}}(\mathbb{E}[B_{y+1}], \sigma_{\text{env}} \cdot \mathbb{E}[B_{y+1}]). \quad (9)$$

The scale of environmental stochasticity is fixed at $\sigma_{\text{env}} = 0.2$, which is roughly consistent with the $\pm 40\%$ deviations of survival seen in the literature (Safranyik and Vithayasai, 1971; Reid, 1963, Tables 4 & 7; Amman, 1983, Fig. 34; Régnière and Bentz, 2007, Table 1).

Lodgepole pine dynamics (slow):

1. Trees grow at a constant rate until maturity. Tree growth is 4 mm (0.157 inches) DBH increase per year until trees reach 20 inches DBH, after which growth stops.

Although lodgepole pine trees are capable of indeterminate growth, intraspecific competition in dense stands constrains the maximum diameter. The vast majority of lodgepole pine trees in even-aged stands do not exceed 20–24 inches DBH (Rodman et al., 2022; Negrón, 2020; Huang, 1999), and many U.S. Forest Service reports use a “> 18 inches” category to describe lodgepole diameters (e.g., Cole, 1969; Stipe, 1974; McGregor, 1973). The DBH growth rate is consistent with empirical estimates (Mata, 2003; Heath and Alfaro, 1990; McLane et al., 2011). However, like all pines, lodgepole pine grows faster in youth and slower in age, so 4mm here is a convenient approximation, representing the average increment over a tree’s lifespan.

2. Trees experience constant background mortality. A fixed proportion (m) of trees die each year, regardless of size:

$$(\text{TPA})_{j+1,y+1} = (1 - m) \times (\text{TPA}')_{j,y} - (\text{KTPA})_{j,y} \quad (10)$$

where $(\text{TPA})_{j,y}$ is trees per acre in diameter class j and year y , and $(\text{TPA}')_{j,y}$ is trees per acre remaining after beetle-induced mortality.

3. Forest maintains constant density through recruitment. Recruitment into the smallest diameter class (0.157 inches DBH) ensures a K standing trees per acre, which includes live trees and MPB-killed trees that have not yet dropped their needles:

$$(\text{TPA})_{1,y+1} = K - \sum_{j=1}^J (1 - m) \times (\text{TPA}')_{j,y} + \sum_{s=y-2}^y \sum_{j=1}^J (\text{KTPA})_{j,s}. \quad (11)$$

4. Dead trees temporarily occupy canopy space. Trees killed by MPB retain needles for 3 years, occupying forest canopy and suppressing recruitment as a live tree would.

2.4 Causal analysis

When the simulation model is instantiated with realistic parameter values, the five focal biological features are turned on. To turn the features off, we alter specific parameter values.

To turn off the Allee effect, we set the Allee threshold, a , to infinity. As a consequence, the probability of a successful attack is always one, or equivalently, the number of initial attacks equals the number of successful attacks. To turn off stand-dependent dispersal mortality, we set λ_0 to infinity, such that the $s_y = s_0$ in Eq. 35. To turn off the large-tree preference, the piecewise linear function for attack preference, Eq. 4, becomes a step function,

$$(\text{preference})_j = \begin{cases} 1 & \text{if } \text{DBH}_j > -\beta_0/\beta_1 \\ 0 & \text{otherwise.} \end{cases} \quad (12)$$

All trees above the attack threshold, $-\beta_0/\beta_1$, are equally attractive. An alternative approach would be to make all trees (susceptible or not) equally attractive, but this approach would vastly increase the number of trees available to the beetles. In doing so, we would be modulating two key ecological factors — size-dependent host-feeding *and* resource availability — which which diverges further from the real-world scenario and is therefore less causally relevant (Lewis, 1979)

To turn off tree size-dependent fecundity, we set $\zeta_1 = 0$ and set ζ_0 to the average emergence density (across killed tree surface area in the Klein et al. dataset), which is calculated as

$$\sum_{y=1}^{Y'} \sum_{j=1}^{J'} \begin{cases} \frac{(\zeta_0 + \zeta_1 \text{DBH}_j)(\text{KTPA}_{j,y} \times (\text{surface area per tree})_j)}{\sum_{z=1}^{Y'} \sum_{k=1}^{J'} (\text{KTPA}_{k,z} \times (\text{surface area per tree})_k)}, & \text{if } \text{DBH}_j > -\frac{\zeta_0}{\zeta_1} \\ 0, & \text{otherwise.} \end{cases} \quad (13)$$

Note here that J' and Y' are the number of diameter classes and years in the Klein et al. dataset, and should not be confused with the more granular diameter classes and the indeterminate number of years in the simulation model.

Finally, we turn off time-scale separation by forcing lodgepole pine to grow quickly. To accomplish this, we iterate density-independent pine mortality, growth, and recruitment (Eq. 10–Eq. 11) 50 times between bouts of beetle attacks, such that year-old trees have 8-inch diameters.

We create simulation scenarios where either 0, 1, or 2 of features have been turned off. The result is 10 simulation scenarios: 9 counterfactual and 1 realistic (i.e., all of the features are turned on). For each scenario, we draw 1,000 sets of parameters from the joint posterior distribution of the statistical models. For each parameter set, we simulate 3,000 years of data, starting with zero beetles and equilibrium forest conditions.

2.5 Describing population dynamics

We track 5 key metrics of MPB population dynamics: peak beetle density, length of the outbreak growth phases, outbreak period, large tree density, and proportion of time spent in the endemic state. To compare model predictions to the real world, we also calculated *observation-based estimates* of these 5 features.

As a preliminary step to quantifying the 5 features, we must distinguish persistent fluctuations (i.e., outbreaks and/or population cycles) from noisy fluctuations. First, we create a smoothed time series by applying a centered moving average with a three-year window. Second, we find peaks and troughs in the smoothed time series; these serve as initial guesses for the true peaks and troughs. Third, we go back to the original time series and identify the true peaks and troughs, e.g., a true trough is the minimum value between successive “guess peaks” identified in the smoothed time series. To prevent sub-critical immigration from being classified as an outbreak, we disregard sets of peaks and troughs where the $B_{\text{peak}} - B_{\text{trough}} < 600$; note that 600 is twice the stochastic immigration parameter I (see Eq. 2).

Two of the metrics require an operational definition of an endemic MPB population. There are multiple definitions in the literature: less than 40 female beetles per ha (Carroll et al.,

2006b), less than 5 attacked trees per ha (Boone et al., 2011), and less than 0.025 infested large-diameter trees per ha (Amman, 1984). Of these, we select the smallest value (40 females/ha \approx 16 females/acre) to operationalize the endemic state. This choice is based on two considerations: a) smaller values align more closely with aerial survey data, where the majority of stands appear to have no infestation; and b) our simulation model does not explicitly represent endemic beetle populations, leading to a slight underestimate of beetle density.

1. **Peak beetle density.** For each simulated time series, we take the third quartile of all peak values of B_y , the density of emerging female beetles. The third quartile represents a typical large outbreak, which is relevant because large local outbreaks disproportionately contribute to spatial spread and range expansion (see the *Discussion*, Section 4).

Because beetles or emergence holes are rarely observed across multiple years, the only *observation-based estimate* of peak beetle density comes from the Klein et al. dataset. This dataset is also used to parameterize the simulation model, so the predictions and observations are not independent.

2. **Outbreak growth phase length** For each outbreak in a simulated time series times, we calculate the difference between the year of peak beetle density and the year before beetle density first exceeds the endemic threshold of 16 females/ha. Then, we take the mean of this quantity across all outbreaks.

An observation-based estimate is calculated using British Columbia’s Aerial Overview Survey data from 1990-2021. First, we estimate the number of infested trees using the methodology in Fig. E.1 caption, aggregate data into 1km^2 pixels, and subset to locations with moderate-to-severe outbreaks (cumulative infestations in the upper quartile). Next, we calculate the difference between the year with the maximum number of infested trees and the year before infested trees were first detected. Finally, we take the mean of this quantity across all locations.

3. **Outbreak period.** This quantity is simply the mean number of years between peaks (whether cycles or outbreaks) in the simulated time series. The observation-based estimate was sourced from studies that have reconstructed region-wide outbreaks with tree ring data (Alfaro et al., 2003; Negrón and Huckaby, 2020; Jarvis and Kulakowski, 2015; Alfaro et al., 2009; Axelson et al., 2009). More precisely, the observation-based estimate is the median (across studies) of the mean outbreak recurrence time.

4. **Large tree density.** The large tree density is simply the temporal average of trees per acre with $DBH \geq 8$ inches. Here, there are two observation-based estimates. The first comes from the Klein et al. dataset, and is therefore not independent of the simulation-based predictions. The second is the median (across several studies) of trees per acre with $DBH \geq 8$ inches, prior to a MPB outbreak (McGregor, 1973; Gibson and Bennett, 1978; Hamel et al., 1975; Stipe, 1974, 1976; Mitchell and Preisler, 1991; Amman, 1969; Negrón, 2020; Evenden and Gibson, 1940). This is an overestimate of the temporal average of large-tree density, but it may be a sensible approximation, given that MPB populations are usually in the endemic state.

5. **Proportion of time spent in the endemic state.** This is straightforwardly computed as the proportion of years with less than 16 emerging females per acre. The observation-based estimate comes from British Columbia’s Aerial Overview Survey data (years: 1962–2021). Specifically, we aggregated data into 1km^2 pixels, subsetting to locations with moderate-to-severe outbreaks (cumulative infestations in the upper quartile), and computed the proportion of years where no infestations were detected.

The five metrics above can be used heuristically to classify simulated time series with respect to their population dynamical behavior: excitable dynamics (i.e., episodic boom-bust dynamics), population cycles, or equilibrium dynamics. If the proportion of time spent in the endemic states is $\geq 1/2$, then the time series has *excitable* dynamics. If the proportion of time spent in the endemic states is $< 1/2$, and the outbreak period is < 50 years, then the time series has *Cycles*. If the proportion of time spent in the endemic states is $< 1/2$, and the outbreak period is ≥ 50 years, then the time series has *Equilibrium* dynamics.

3 Results

3.1 Model diagnostics and parameter estimates

The statistical models performed well across multiple assessment criteria. Various diagnostics indicated that the models converged to the global posterior distribution, with most prior distributions having negligible impact on the results (Appendix A.3). The models successfully recreated the original outbreak trajectory and out-of-sample data (Appendix B.4).

The parameter estimates produced by the statistical models align with previous research (Table 1). The posterior distributions of attack density and emergence density (from a 10-inch diameter tree) are consistent with over a dozen studies across British Columbia, Alberta, and the western United States (Figures E.5 & E.6). The mean overstory density, 338 trees per acre or 835 trees per hectare, agrees with estimates from regenerating stands in southern British Columbia (Nigh et al., 2008, mean = 893 stems/ha) and lodgepole-dominated stands in the U.S. Rocky Mountains (Pfeifer et al., 2011; Meddens et al., 2011, 2012; mean = 1065 stems/ha). The minimum susceptible tree diameter is estimated at 7.46 inches, which is consistent with the often-cited 8-inch (or 20 cm) threshold (Hopping and Beall, 1948; Cole, 1969; Safranyik, 1988). The baseline dispersal mortality (i.e., $1-s_0$) is 0.52, which is consistent with the 0.5–0.7 range provided by previous studies of bark beetles (Schmid, 1977; Safranyik, 1989; Latty, 2007; Pope et al., 1980). Finally, the mean attack density of 71 females per square meter in the Klein et al. dataset is close to the optimal value of 60 females per square meter, proposed by Raffa and Berryman (1983).

Parameter	Short description	Mean	SD	CI _{2.5%}	CI _{97.5%}
a	Allee threshold	432	363	13.5	1338.88825
s_0	max dispersal survival	0.477	0.0701	0.363	0.639
λ_{resid}	dispersal threshold	0.652	0.0353	0.579	0.708
λ_1	dispersal sensitivity	49.7	96.6	17.2	262
β_0	pref.~DBH intercept	-3.42	0.773	-4.84	-1.93
β_1	pref.~DBH slope	0.453	0.0688	0.319	0.580
γ	dead tree~attack slope	0.0151	0.000878	0.0134	0.0168
ζ_0	emerge~DBH intercept	-9.86	49.2	-106	87.8
ζ_1	emerge~DBH slope	25.4	5.21	15.3	35.5
K	forest carrying capacity	904	313	413	1630.37825
m	annual tree mortality	0.0518	0.00637	0.0376	0.0634
Derived quantities	Short description	Mean	SD	CI _{2.5%}	CI _{97.5%}
$-\beta_1/\beta_0$	susc. DBH threshold	7.46	0.666	5.98	8.47
$1/\gamma$	attack density	66.3	3.88	59.4	74.4
$\zeta_0 + \zeta_1 * 10$	emerge density (10 in. DBH)	244	25.1	191	296
$K - \sum_{t=0}^{17} (1 - m)^t m K$	Overstory density	338	86.0	193	529
Fixed parameter	Short description	value			
P_I	Prob. immigration	0.05			
I	immigrating females	300			
σ_{env}	Environmental stochasticity	0.2			
Symbol N/A	max DBH	20			
Symbol N/A	annual DBH growth	0.157			

Table 1: Summary statistics of marginal posterior distributions for model parameters, including the Mean, standard deviation, and credible intervals (CI_{2.5%}, CI_{97.5%}). The table also includes derived quantities, including the diameter at breast height (DBH) of the smallest susceptible trees; the model-based estimate of successful attack density (gallery starts per square meter); the emergence density (females per square meter) for 10-inch DBH tree; and the density of overstory trees (stems per acre). Overstory trees are operationalized with a standard cutoff: $\text{DBH} \geq 7\text{cm} \approx 2.76\text{in}$. This explains the summation from 0 to 18 in the formula: $\frac{2.76\text{in cutoff}}{0.157\text{in per year}} \approx 18$ years. Finally, the table contains fixed parameters, whose values were obtained via literature search. For more elaborate descriptions and parameter units, see supplementary Table A.1. For the summary statistics of sub-model noise parameters, see supplementary Table C.1.

3.2 Effects of life history on population dynamics

Three key features are essential for excitable population dynamics in MPB: stand-dependent dispersal mortality, an Allee effect, and time-scale separation (Fig. 6, Fig. 7). Without the stand-dependent dispersal mortality, MPB and lodgepole pine attain a noisy equilibrium where there is a consistently low density of beetles (Fig. 6C), but not low enough to technically be endemic. Without the Allee effect, a classic population cycle appears (Fig. 6D). Without time-scale separation, MPB and lodgepole pine attain a noisy equilibrium with large numbers of beetles and susceptible trees (Fig. 6 E).

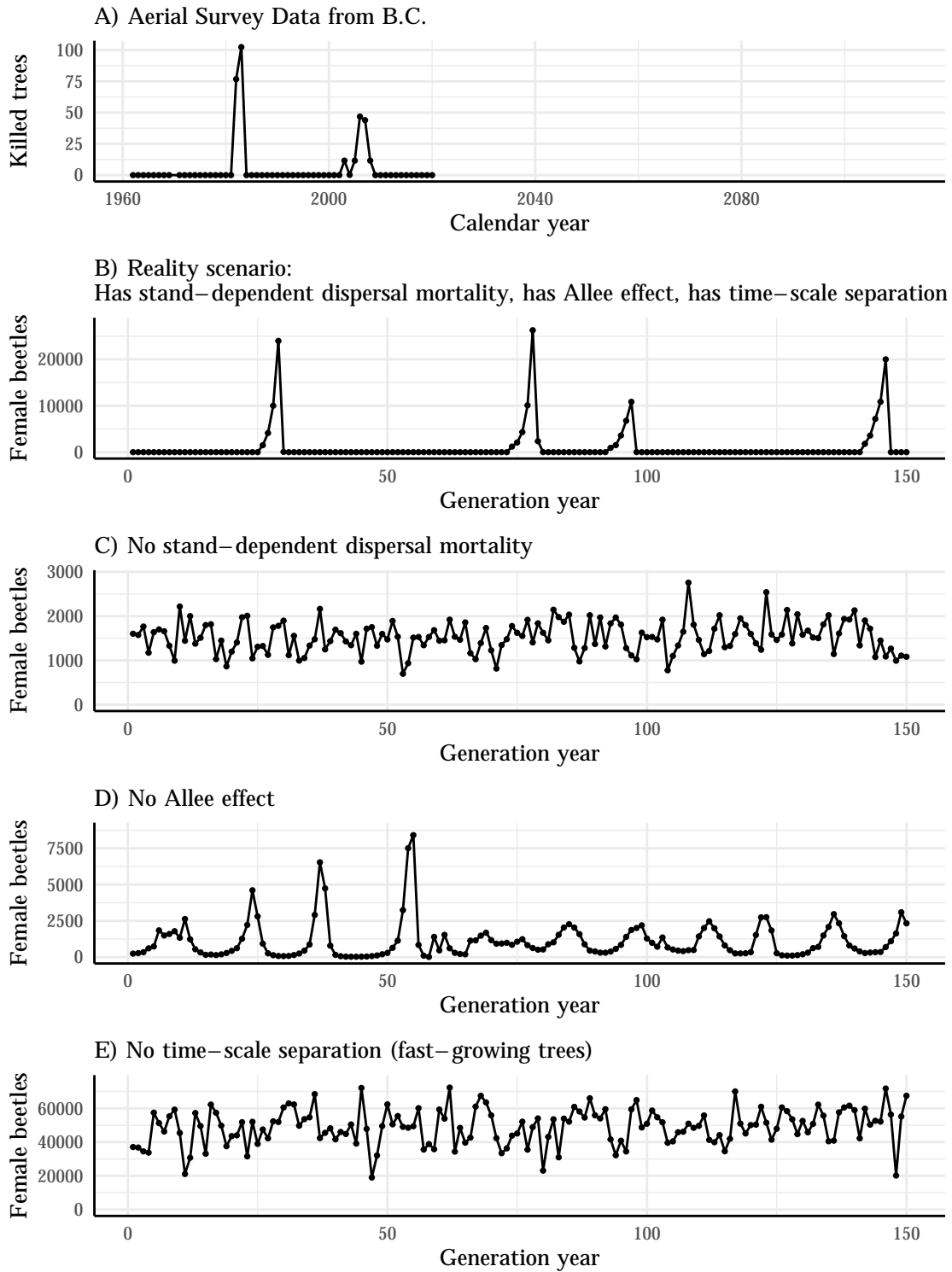


Figure 6: Time series of mountain pine beetle infestations, real vs. simulated. The real data comes from Aerial Overview Survey data in British Columbia, aggregated across a representative 1 km^2 patch. Simulated time series are representative of various simulation scenarios.

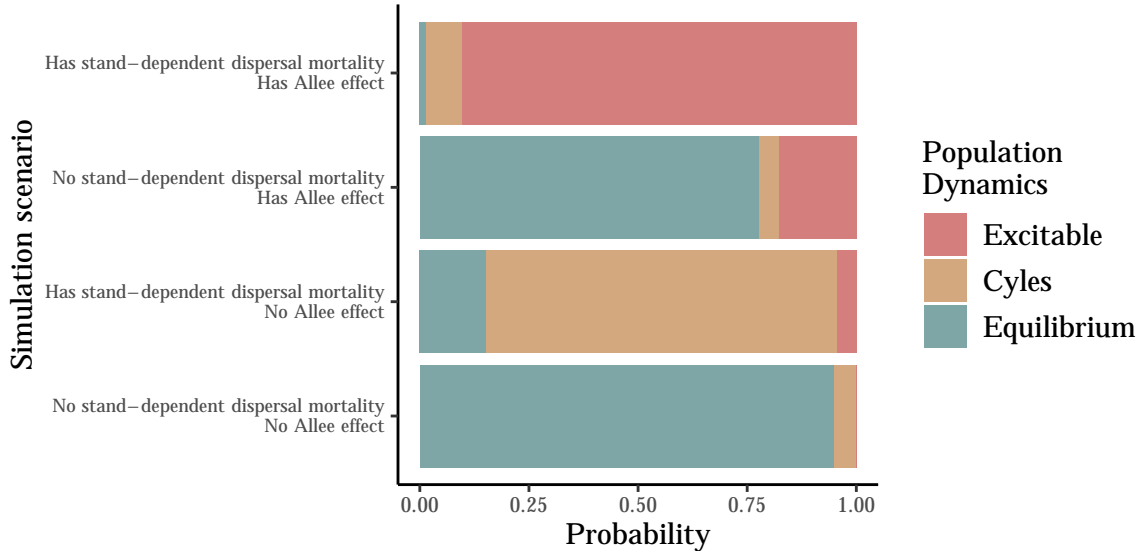


Figure 7: Stand-dependent dispersal mortality and the Allee effect lead to excitable boom-bust dynamics. Barplot proportions represent the posterior probabilities of different dynamical behaviors, classified using the methodology in Section 2.5.

The process of stand-dependent dispersal mortality explains why beetles don’t overexploit trees. It is perhaps trivial to say that if beetles disperse away and die before they have killed all the trees, then the beetles won’t kill all the trees. However, the lack of over-exploitation, or equivalently, the seemingly premature “bust” phase of the “boom-bust cycle”, is a ubiquitous feature of outbreaks (Fig. 4) and is thus worth connecting to MPB life-history. This also suggests an optimistic perspective: outbreaks are much less destructive than they theoretically could be. Stand-dependent dispersal probably occurs because chemo-sensory constraints prevent beetles from aggregating on small trees (Section 1.2.2), even though beetles have positive fitness when they do successfully attack small trees. Without stand-dependent dispersal mortality, the system would reach a stochastic equilibrium, creating a forest with few large pine trees.

The Allee effect explains why outbreaks are so extreme when they do occur. The Allee effect suppresses MPB populations, keeping them in their endemic state until enough large trees have accumulated that a small inoculum of beetles — either from long-distance dispersal or a stochastic successful attack — can grow explosively. Without the Allee effect, lodgepole pine and MPB enter a predator-prey cycle.

Classic predator-prey theory predicts that long-lived prey should make predator-prey cycles unlikely (Murdoch et al., 2003). One might naively expect that the time-scale separation between beetles and trees would allow MPB to grow rapidly enough to prevent an unchecked proliferation in pine abundance, thus preventing the *prey-escape phase* of a population cycle (De Roos et al., 1990) wherein the prey species can grow unimpeded by the predator. Even though pines live much longer than beetles, we still see population cycles in the counterfactual

simulations (when the Allee effect is turned off). This can be explained by the phenomenon of cohort resonance (Bjørnstad et al., 2004). During an outbreak, many pines are killed at roughly the same time. Subsequently, pines are recruited at the same time, and then become susceptible to MPB at the same time. Thus, there are a brief few years where the pines that MPB can “see” are growing faster than exponentially.

The two remaining features — size-dependent tree preference and tree size-dependent fecundity — do not affect the qualitative nature of MPB population dynamics, i.e., whether a simulation was classified as *Excitable* or *Cycles*. However, they do have quantitative effects on some of the fine-grained properties of outbreaks: the combination of both size-dependent tree preference and tree size-dependent fecundity led to a 40% increase in the peak beetle density (from 15 to 21 thousand) and an 8% decrease in the length of growth phase (from 5.8 years to 5.4 years). In other words, the combination of these life-history traits makes outbreaks moderately more explosive and slightly more rapid.

The inclusion of stand-dependent dispersal mortality leads to better predictions of outbreak magnitude and large-tree density (Fig. 8). The Allee effect leads to better predictions of the outbreak recurrence time and growth phase length. Specifically, without the Allee effect, the cycles occur too frequently and the growth phase of each cycle is too long. Stand-dependent dispersal mortality primarily explains the fact that a portion of large trees remain despite MPB outbreaks.

Biological features					Metrics		Mean \pm (SD)					Probability of Dynamics		
Has stand-dependent dispersal mortality	Has Allee effect	Has large-tree preference	Has tree size-dependent fecundity	Has time-scale separation	Peak beetle density, 1000s	Outbreak growth phase, years	Outbreak period, years	Large tree density, trees ≥ 8 in DBH per acre	Prop. time endemic	Prop. sims without peaks	Prop. sims without outbreaks	Excitable	Cycles	Equilibrium
✓	✓	✓	✓	✓	21 (9.0)	5.4 (1.2)	44 (34)	44 (9.7)	0.68 (0.16)	0.00 (0.00)	0.00	0.90	0.08	0.01
✓	✓	✓	✓	✓	10 (10)	7.3 (1.1)	174 (295)	11 (13)	0.18 (0.25)	0.00 (0.06)	0.44	0.18	0.05	0.78
✓	✓	✓	✓	✓	6.4 (3.1)	9.7 (2.2)	26 (10)	38 (9.2)	0.07 (0.15)	0.00 (0.00)	0.06	0.05	0.80	0.15
✓	✓	✓	✓	✓	16 (7.1)	5.9 (1.4)	57 (136)	43 (10)	0.66 (0.16)	0.00 (0.00)	0.00	0.89	0.07	0.04
✓	✓	✓	✓	✓	16 (7.0)	5.9 (1.4)	60 (157)	45 (10)	0.65 (0.16)	0.00 (0.00)	0.00	0.88	0.10	0.03
✓	✓	✓	✓	✓	72 (18)	8.0 (2.4)	4.8 (1.2)	46 (9.1)	0.00 (0.04)	0.00 (0.00)	0.99	0.00	1.0	0.00
		✓	✓	✓	3.3 (0.90)	13 (1.4)	293 (374)	2.6 (4.0)	0.00 (0.01)	0.01 (0.08)	1.0	0.00	0.05	0.95
	✓	✓	✓	✓	11 (12)	8.5 (1.2)	221 (402)	12 (15)	0.19 (0.26)	0.01 (0.08)	0.45	0.19	0.07	0.74
	✓	✓	✓	✓	4.6 (2.2)	8.9 (1.9)	1076 (876)	4.8 (9.9)	0.04 (0.15)	0.09 (0.29)	0.85	0.04	0.00	0.96
	✓	✓	✓	✓	73 (16)	NA	4.7 (0.12)	46 (8.8)	0.00 (0.00)	0.00 (0.00)	1.0	0.00	1.0	0.00
✓			✓	✓	5.7 (2.7)	10 (2.4)	30 (17)	37 (10)	0.06 (0.14)	0.00 (0.00)	0.05	0.04	0.74	0.23
✓		✓	✓	✓	6.1 (2.9)	9.9 (2.7)	29 (36)	39 (10)	0.06 (0.15)	0.00 (0.00)	0.13	0.05	0.75	0.21
✓		✓	✓		72 (16)	NA	4.7 (0.12)	47 (9.7)	0.00 (0.00)	0.00 (0.00)	1.0	0.00	1.0	0.00
✓	✓			✓	15 (7.0)	5.8 (1.3)	63 (200)	42 (10.0)	0.65 (0.16)	0.00 (0.06)	0.00	0.87	0.09	0.05
✓	✓		✓		76 (20)	7.4 (1.8)	9.9 (125)	42 (9.0)	0.01 (0.07)	0.00 (0.04)	0.99	0.01	0.99	0.00
✓	✓	✓			66 (15)	13 (3.9)	4.9 (0.30)	46 (9.0)	0.01 (0.05)	0.00 (0.04)	0.98	0.00	1.0	0.00

Table 2: Results of the simulation study. A check mark indicates that a biological feature is present in the simulation scenario. The quantitative values take the format of “Mean \pm (SD)”, where both summary statistics are calculated across the posterior distribution. In addition to the 5 metrics of population dynamics (presented in Section 2.5), there are two extra metrics: 1) the proportion of simulations where neither peaks nor troughs were detected after applying the moving-average smoothing and various thresholds described in Section 2.5; 2) the proportion of simulations where no outbreaks were detected, where an outbreak is defined as a *trough* \rightarrow *peak* \rightarrow *trough* sequence where the population attains the endemic state (< 16 females per acre) before and after the peak. If a simulation scenario produced both NA and non-NA values for a particular metric, then the NA values were omitted when calculating that metric.

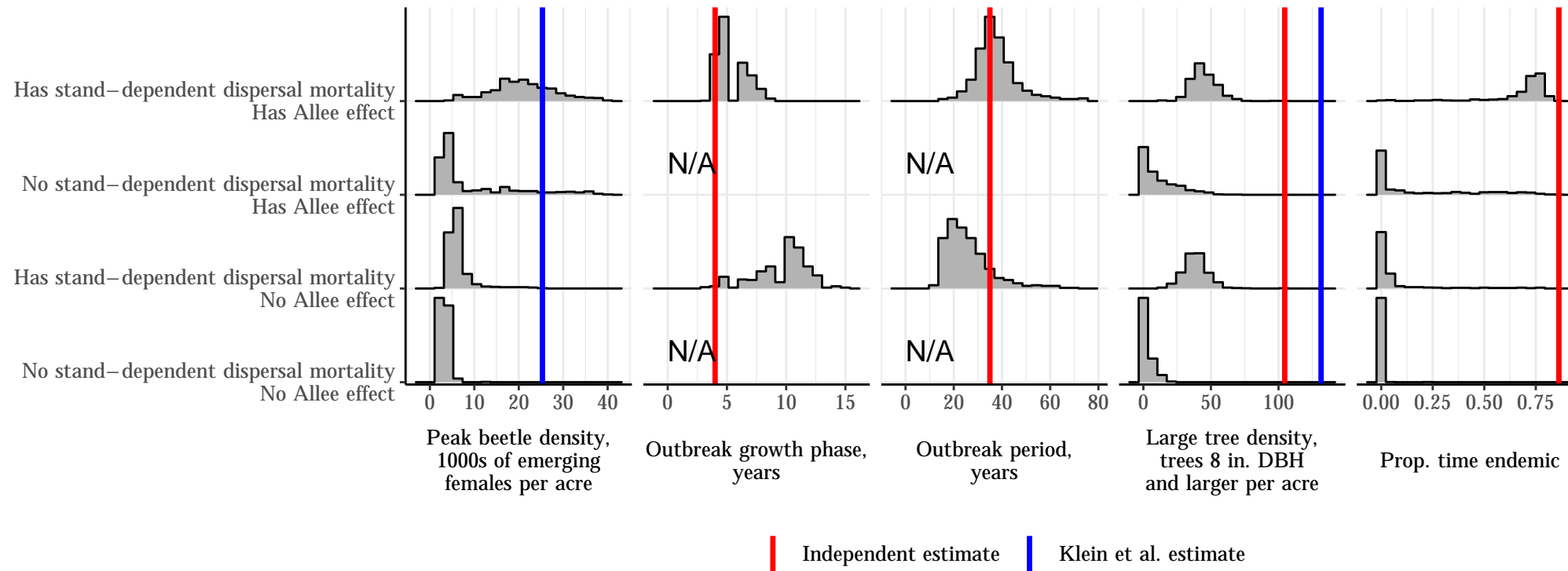


Figure 8: A comparison of population dynamic metrics for various combinations of stand-dependent dispersal mortality and the Allee effect. The histograms show the frequency of predicted values across posterior samples. The vertical lines show observation-based estimates from the [Klein et al.](#) dataset or independent sources. Simulation scenarios without stand-dependent dispersal mortality resulted in few peaks and outbreaks (see Table 2), hence the “N/A” label. The five metrics and the observation-based estimates are explained in Section 2.5.

4 Discussion

Excitable population dynamics are related to five features of bark beetle ecology: stand-dependent dispersal mortality, an Allee effect, time-scale separation between beetle and tree life cycles, tree size-dependent fecundity, and a large-tree preference. Time-scale separation (i.e., trees grow slower than beetles) ensures that killed trees cannot be immediately replaced by new mature pines, thus preventing equilibrium dynamics. Stand-dependent dispersal (i.e., beetles disperse farther through sparse forests) leads to high levels of mortality, which is exacerbated by the Allee effect (i.e., not enough beetles to mass attack healthy trees), bringing beetle populations to an endemic, low-density state. The two inhibitory processes — stand-dependent dispersal mortality and a strong Allee effect — explain why populations spend the vast majority of time in their endemic state, and why subsequent outbreaks are so explosive: with suppressed beetle populations, large trees accumulate, providing proverbial fuel for the beetle fire.

The two remaining traits, tree size-dependent fecundity and a large-tree preference, explain the large magnitude of outbreaks, i.e., the peak number of beetles. Larger trees provide more resources for beetle reproduction and are preferentially attacked, leading to rapid population growth during outbreaks. While not essential for MPB’s excitable population dynamics due to MPB’s high baseline fecundity, these traits may be crucial for other bark beetle species that lie on the boundary between pulse-driven and irruptive behaviors. Bark beetles can be categorized as either “outbreaking” or “non-outbreaking”, with the former category further divided into “pulse-driven” and “irruptive” (equivalent to excitable) categories.

4.1 Bark beetle comparative analysis

Aggregation behavior is a key distinguishing factor between outbreaking and non-outbreaking bark beetle species. Non-outbreaking species are poor aggregators, with few individuals attacking simultaneously and pheromones used primarily for mate-finding. Examples include the greater European spruce beetle (*Dendroctonus micans*) and the black turpentine beetle (*Dendroctonus terebrans*); more are listed in [Reeve et al. \(2012\)](#) Table 2. To survive in living trees, non-outbreaking beetles often have adaptations such as resistance to toxic tree resin ([Weed et al., 2015](#)). Interestingly, *Dendroctonus micans* adults do not aggregate, but larvae do ([Grégoire, 1988](#); [Deneubourg et al., 1990](#)), leading to greater larval survival in small pockets of tree phloem ([Storer et al., 1997](#)). Although most bark beetles are non-outbreaking ([Wood, 1982](#)), aggregation and mass-attacks appear to be the ancestral state for *Dendroctonus* bark beetles ([Reeve et al., 2012](#)).

The distinction between pulse-driven and irruptive species is less clear-cut. Instead, differences lie in the magnitude of various life history traits and environmental factors. For example, the Douglas-fir beetle (*Dendroctonus pseudotsugae*), a pulse-driven species, prefers large trees that are downed ([Hood and Bentz, 2007](#)) or recently defoliated by the Douglas-fir tussock moth, *Orgyia pseudotsugata* ([Wright et al., 1984](#); [Negrón et al., 2014](#)). During outbreaks, it may attack healthy trees, but these are typically adjacent injured trees ([Cunningham et al., 2005](#); [Cole et al., 2022](#)). This behavior, contrasting with the irruptive MPB’s strong preference for healthy trees, contributes to the Douglas-fir beetle’s classification as a pulse-driven species.

The western balsam bark beetle (WBBB; *Dryocoetes confusus*) presents an intriguing case that further blurs the lines between these categories. The WBBB likely has excitable population dynamics: it is generally considered irruptive (e.g. [Lantschner and Corley, 2023](#)) and causes large destruction in response to drought perturbations ([Maclauchlan et al., 2023](#)). Further, WBBB shares many life history traits with the MPB, including a preference for large trees, tree-size-dependent fecundity, and the mass-attack-based Allee effect. Despite these similarities, their population dynamics look quite different. WBBB often attacks less than 5% of a given stand in one year, with chronic infestations slowly killing many mature trees over time ([Maclauchlan et al., 2003](#); [McMillin et al., 2003](#)). One possible explanation is that WBBB

carries a fungus, *Grosmannia dryocoetidis*, that is truly pathogenic to host trees (Molnar, 1965; Zipfel et al., 2006). Therefore, sub-critical or initially unsuccessful attacks can kill trees simply by inoculating the fungus. Another possible explanation is that WBBB’s primary host, subalpine fir, often grows in mixed-age stands (Antos and Parish, 2002; Maclauchlan, 2016) wherein younger trees are less susceptible. This contrasts with MPB’s primary host, lodgepole pine, which typically experiences clearcut logging or stand-leveling fires, resulting in even-aged stands prone to explosive outbreaks. The highly clustered nature of WBBB’s outbreaks (Howe et al., 2022a) suggest it may lack *stand-dependent dispersal mortality*.

A beetle species’ status as irruptive or pulse-driven can change over space and time in response to environmental conditions. One example is the red turpentine beetle (*Dendroctonus valens*), which is considered non-outbreaking in its native range in North America but has become irruptive in China. This shift is attributed to novel fungal symbionts aiding host tree mortality, the higher susceptibility of the Chinese host *Pinus tabulaeformis*, more attractive host volatiles, prevalent monoculture plantations, and warmer weather (Yan et al., 2005; Sun et al., 2013). This case highlights the importance of considering traits (e.g., aggregation and large-tree preference due to attractive host volatiles), abiotic factors (e.g., climate), and idiosyncratic elements (e.g., fungal symbionts) in determining outbreak potential.

The European spruce beetle (*Ips typographus*) provides another interesting comparison to MPB. *I. typographus* experiences significantly higher intraspecific competition among larvae, resulting in consistently lower fitness (KärvEmo and Schroeder, 2010). This difference may explain why the European spruce beetle is less destructive than MPB (KärvEmo and Schroeder, 2010), despite both species being considered irruptive. The likely mechanism behind this disparity is *I. typographus*’ much lower emission of the anti-aggregation pheromone verbenone (Birgersson et al., 1984; Ramakrishnan et al., 2022). Another way to conceptualize the disparity (in terms of our “biological features”), is that the European spruce beetle lacks strong *tree size-dependent fecundity*, since high competition undermines the benefits of thicker phloem.

Environmental conditions and interspecific interactions significantly influence outbreak potential. The spruce beetle (*Dendroctonus rufipennis*) in Alaska’s interior rarely outbreaks despite favorable conditions. Less precipitation in the interior leads to lower phloem moisture, thus favoring competitive non-eruptive insects like *Ips perturbatus* (Werner et al., 2006). Similarly, the roundheaded pine beetle (*Dendroctonus adjunctus*) outbreaks in areas where trees are stressed by drought and other bark beetles, specifically western pine beetles (*Dendroctonus brevicomis*) and *Ips* species (Negrón et al., 2000; Negrón, 2008).

We conducted a comparative analysis of bark beetle damage using aerial survey data from western North America and maps of host-tree biomass (Appendix D). Our analysis reveals that classification as “irruptive” is a necessary condition for causing extensive damage, but the total amount of beetle damage scales linearly with the total biomass of host trees (Fig. 9). Previous research has found an approximately linear relationship between tree biomass and tree damage across sites, within species (Negrón et al., 1999; Negrón and Klutsch, 2017); here we show that this relationship also applies *between* species. Together, both life history traits and environmental factors determine if a bark beetle population is capable of overcoming an Allee effect (i.e., overcoming the defenses of healthy trees) and growing explosively; then landscape-level factors determine the overall impact of bark beetle outbreaks. This analysis adds a layer of nuance to Rudinsky’s 1962 claim that the “Abundance of suitable breeding material has recently been definitely identified as the decisive factor in outbreaks of bark beetles.”

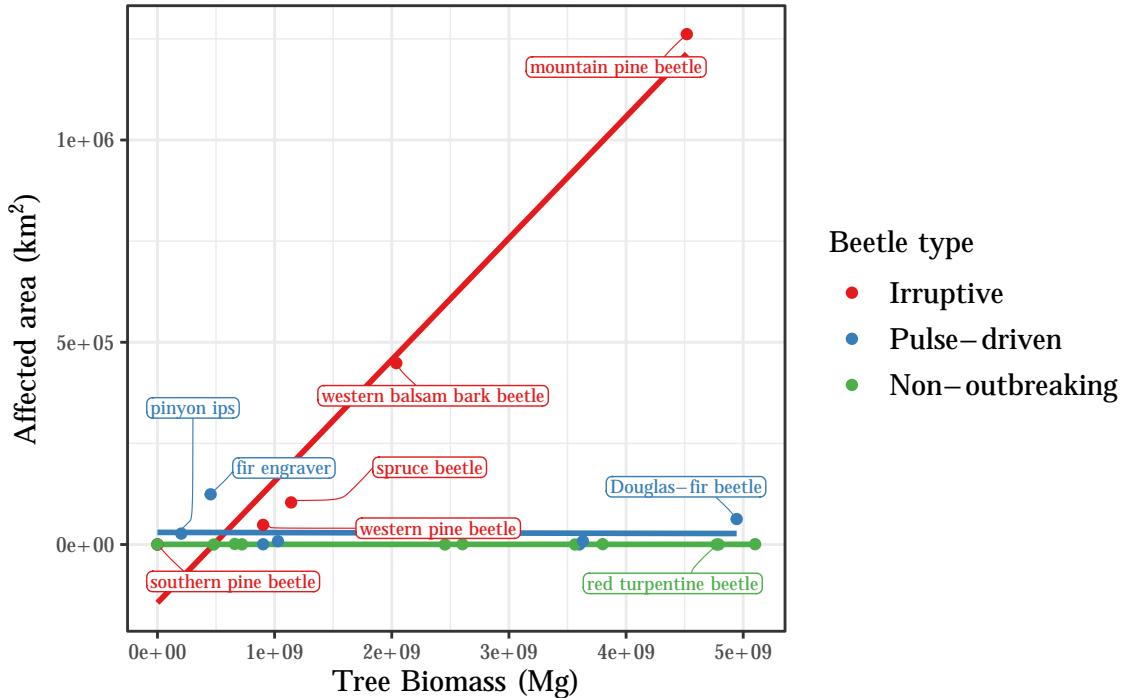


Figure 9: Total bark beetle damage is determined by life-history traits and landscape characteristics. Cumulative damaged area is a linear function of the total biomass of host trees, across British Columbia and the western United States (i.e., regions 1–6 as defined by the US Forestry Service); however, this relationship only holds true for bark beetles classified as irruptive. Methodological details in Appendix D.

The western pine beetle (*Dendroctonus brevicomis*) provides an illustrative example of how landscape characteristics can influence the impact of even highly irruptive species. Unlike MPB, which can attack any pine species within its native range, the western pine beetle’s outbreaks are limited due to its high specificity to ponderosa pine (Homicz et al., 2022). Recent trends in southern pine beetle (*Dendroctonus frontalis*) damage illustrate how management practices can affect landscape characteristics and total beetle impact. Despite being considered irruptive, the total area affected by southern pine beetle has declined significantly over time (Fettig et al., 2022). Asaro et al. (2017) attribute this decline to silvicultural practices, namely rapidly removing infested trees and limiting connectivity between high-risk host stands.

Other bark beetle species lack the unique life history of MPB, either in kind or in degree, resulting in pulse-driven outbreaks or less destructive irruptive outbreaks. We have examined examples of bark beetles lacking MPB’s key traits: the great European spruce beetle lacks the ability to aggregate (implicating the Allee effect), the western balsam bark beetle possibly lacks stand-dependent dispersal mortality, and the European spruce beetle lacks size-dependent fecundity. The Douglas-fir beetle prefers large trees Sturdevant et al. (2022), but prefers these to be downed or otherwise unhealthy. Consequently, these species have slow-moving outbreaks (e.g., the western balsam bark beetles) or are unable to achieve self-driving growth without sustained perturbations.

4.2 Mountain pine beetle dynamics

Our model accurately predicts the return time of MPB outbreaks, which is somewhere between 20–50 years according to tree-ring-based reconstructions. Our counterfactual simulations with no Allee effect, resulting in classic population cycles, predict an outbreak return time that is too short (approximately 20 years). Other models in the literature claim an outbreak return time that is too long (Powell and Bentz, 2009; Duncan et al., 2015; Brush and Lewis, 2023).

The period of MPB outbreaks is primarily determined by the time it takes lodgepole pine to grow into a susceptible age class. In an idealized scenario where MPB kills all trees, outbreaks would occur approximately every 55 years: 50 years for new trees to become vulnerable, plus a few years for the outbreak and subsequent growth of pine seedlings. However, there are two real-world complications. First, stand-dependent dispersal mortality results in a large number of medium-sized trees surviving the outbreak, so the observed periodicity of 35 years partially reflects the time it takes for medium-sized trees to become large trees, e.g., it takes approximately 25 years for an 8-inch tree to become a 12-inch tree. The 2000s outbreak in British Columbia killed more medium-sized trees than usual, which suggests a longer-than-usual wait time for the next outbreak. Second, widespread outbreaks require widespread perturbations (usually drought), which are functionally stochastic. Thus, tree growth and climate patterns imply a right-skewed distribution of waiting times between outbreaks, where the minimum time is determined by tree growth, and the shape of the right tail is determined by drought probability.

Tree size influences both MPB fecundity and attack preference, explaining about 40% of peak beetle numbers. The outbreak peak is relevant because it is thought to drive MPB range expansion (Bleiker, 2019). Only a minuscule fraction of emerging beetles undergo long-distance dispersal (estimated at 2.5%; Safranyik et al., 1992), so outbreak expansion via long-distance dispersal requires severe local infestations, such that emigrating beetles are numerous enough to mass-attack trees at their destination. In other words, range expansion requires that peak beetle density exceeds the *donor threshold* (terminology introduced by Johnson et al., 2006).

The donor threshold concept may explain regional patterns of MPB spread. Outbreaks are spatially correlated at greater distances in British Columbia than in the western United States, where lower pine biomass leads to smaller peak beetle populations and fewer successful long-distance dispersers. The donor threshold may also explain why MPBs expanded into central Alberta from British Columbia, rather than gradually moving northward from Montana along the eastern Canadian Rockies. British Columbia is more climatically suitable than the eastern Rockies (Safranyik et al., 2010), thus leading to large MPB populations and successful long-distance dispersal.

Our research offers a revised perspective on the density-dependent dynamics of MPB, challenging established assumptions. In previous work, the number of new infestations is assumed to be proportional to both beetles and trees (e.g. Burnell, 1977; Heavilin et al., 2007; Křivan et al., 2016), as in the classic Lotka-Volterra model. Yet, our analysis shows that for intermediate-to-high tree density (i.e., before stand-dependent dispersal mortality kicks in) the number of new infestations is only proportional to beetles, reflecting the fact that outbreaking beetles are limited by their ability to overcome tree defenses, not by their ability to find susceptible trees. While overcompensatory density dependence has been a common assumption in past studies (e.g. Goodsman et al., 2017, 2018; Lewis et al., 2010; Duncan et al., 2015), we argue that MPB experiences near-perfect compensatory density dependence (see Section 1.2.2). Previous research has assumed that the probability of a successful mass attack depends on the quotient of beetle and tree density (e.g., Burnell, 1977; Goodsman et al., 2016; Brush and Lewis, 2023). Instead, we propose that beetle density alone is a more significant determinant of the success probability, as detailed in Appendix B.5.

Putting all of these results together, we can simplify our simulation model (Section 2.3) to formulate a minimal mechanistic model of MPB dynamics. Because the large-tree preference and tree size-dependent fecundity are non-essential (for excitability in MPB, specifically), we drop explicit age structure and only track the density of all susceptible trees (i.e., trees with DBH > 8 inches). All susceptible trees are equally preferred for mass attacks, and all killed trees give rise to the same number of beetles. For simplicity, stochasticity is eliminated. The

minimal mechanistic model can be written as

$$\begin{aligned}
 \underbrace{A_{y+1}}_{\text{Attacking females per acre}} &= \underbrace{A_y}_{\text{Attacking females per acre}} \times \underbrace{\left(1 - e^{-\frac{2.3A_y}{a}}\right)}_{\text{Allee effect}} \times \underbrace{(\zeta^* \gamma^*)}_{\text{Emerging females per succ. attack}} \times \underbrace{s_0 \left(1 + \exp\left(-\lambda_1 \left(\frac{S'_y}{S_{max}} - \lambda_0\right)\right)\right)^{-1}}_{\text{Survival after stand-dependent dispersal}} + \underbrace{\epsilon}_{\text{Endemic beetles}} \quad (14)
 \end{aligned}$$

$$\begin{aligned}
 \underbrace{S_{y+1}}_{\text{Susceptible trees per acre}} &= \underbrace{g(K^* - S_y)}_{\text{Recruitment of susceptible trees}} - \underbrace{A_y \times \left(1 - e^{-\frac{2.3A_y}{a}}\right) \times \gamma^*}_{\text{Trees killed by MPB}}. \quad (15)
 \end{aligned}$$

Here, A_y is the female attack density in the y^{th} year, S_y is the density of susceptible trees, S'_y is the density of susceptible trees remaining after beetle attack (i.e., $S'_y = S_y - A_y \times \left(1 - e^{-\frac{2.3A_y}{a}}\right)$), the parameter ζ^* is the average emerging females per killed tree, γ^* is the average number of killed trees per successful attack, K^* is redefined as the carrying capacity of the susceptible trees, ϵ is the now-explicit number of endemic female beetles, g modulates the rate of recruitment into the class of susceptible trees, and all other parameters have their original meanings (see Table A.1). When simulating the model, a floor at $S = 0$ may be necessary to avoid negative trees.

The minimal model has several purposes. 1) It is descriptive, compactly representing the density-dependent dynamics of MPB and lodgepole pine. 2) It demonstrates that there are two stable equilibria: an endemic equilibrium with few beetles, and an epidemic equilibrium with many beetles. This *bistability* is typical of systems with a strong Allee effect (Taylor, 2012), so it is no surprise that the endemic equilibrium disappears when the Allee effect is turned off (Fig. 10C) 3) It shows the MPB/lodgepole system is an instance of an *excitable dynamical system*, where perturbations can lead to long excursions in phase space, before returning to a resting state (Fig. 10A). Typically, excitable systems have a single stable equilibrium (Strogatz, 1994, pg. 118), whereas our system has two. However, the endemic equilibrium is globally-attracting as a practical matter, since the epidemic equilibrium has a minuscule basin of attraction (Fig. E.7). Previous papers proposed two stable equilibria for irruptive bark beetles (e.g., Berryman, 1979; Mawby et al., 1989; Brush and Lewis, 2024). Our model corroborates this while adding crucial nuance: while it is possible to temporarily attain beetle densities at (or above) epidemic equilibrium, it is not possible to stay at the epidemic equilibrium.

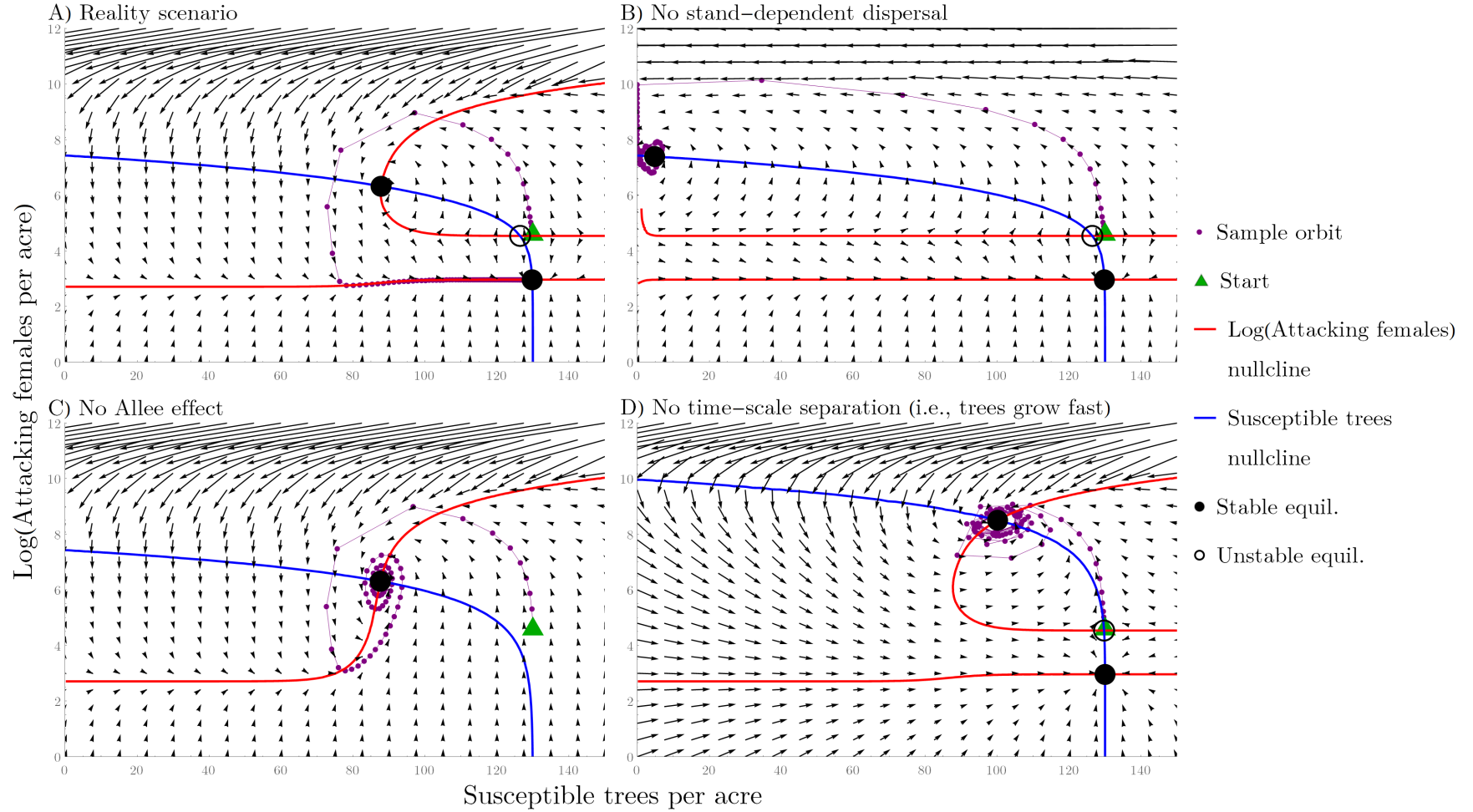


Figure 10: Phase portraits of the minimal mechanistic model (Eq. 14 & Eq. 15), across various simulation scenarios **Panel A**: Stand-dependent dispersal, an Allee effect, and time-scale separation leads to excitable dynamics. Nullclines show curves where $\log(A_{y+1}) = \log(A_y)$ and $S_{y+1} = S_y$, and arrow directions are $\log(A_{y+1}) - \log(A_y)$ and $S_{y+1} - S_y$. Most model parameters were set to their respective posterior means (see Table 2). The exceptions are $\gamma^* = 1/360$ and $\zeta^* = 1300$, which are approximately the respective means (across trees) of attacks and emergences in the [Klein et al.](#) dataset. The carrying capacity's value, $K^* = 130$, is approximately the density of trees with $\text{DBH} \geq 8\text{in}$ in the [Klein et al.](#) dataset. The recruitment parameter's value, $g = 0.036$, was obtained by solving the differential equation $dS(t)/dt = g(K - S(t))$ with initial condition $S(0) = 0$, then solving for the g where 90% of carrying capacity is attained in $t = 50$ years; lodgepole pine attains an 8-inch DBH and becomes susceptible after approximately 50 years.

Through the development and analysis of our age-structured simulation model, we have shed light on the life history and biological processes underlying outbreaks, and challenged established ideas in the MPB modelling literature. A comparative analysis of bark beetles reveals that MPB’s life history traits contribute to its uniquely destructive nature. However, to accurately predict total damage, it’s necessary to consider host-tree biomass (Fig. 9) and idiosyncratic factors, such as fungal symbionts and interspecific competition. Our findings are succinctly summarized in a minimal mechanistic model (Eq. 14 & Eq. 15), which establishes the MPB/lodgepole system as the first empirical examples of an excitable dynamical system in ecology. This work underscores the importance of detailed case studies and looking beyond traditional predator-prey models to understand complex population dynamics.

5 Acknowledgements

We would like to thank Micah Brush for insightful discussions; and Xiaoqi Xie for obtaining the Biosim data (Figs. B.7 & B.6). This research was funded through a grant to the TRIA-FoR Project to ML from Genome Canada (Project No. 18202).

Appendix A Statistical model description

A.1 Data

Boone et al.’s study was conducted from 2000–2005 in the mature lodgepole pine stands of southern British Columbia. Six stands were selected for the study, with an average area of 15.3 hectares per stand, and an average of 1225 canopy trees per hectare. Each year, until the beetle population waned and attained its endemic condition, every tree in each stand was inspected to determine the number of attacked trees and the success or failure of these attacks.

Klein et al.’s study was conducted from 1965–1972 in the southwest corner of Yellowstone National Park in Idaho. Data was collected and aggregated across 85 permanent plots that spanned a square mile. Trees were grouped into six 2-inch diameter classes, ranging from 8 to ≥ 16 inches. For each of the 106 sampled trees, paired 6x6-inch sample squares were marked on opposite sides of the bole at regular height intervals. Within these squares, emergence holes and successful attacks (operationalized as egg-gallery starts) were measured (Fig. A.1). Some of this data was originally presented by Parker (1973), but a more thorough reporting is given by Klein et al. (1978).

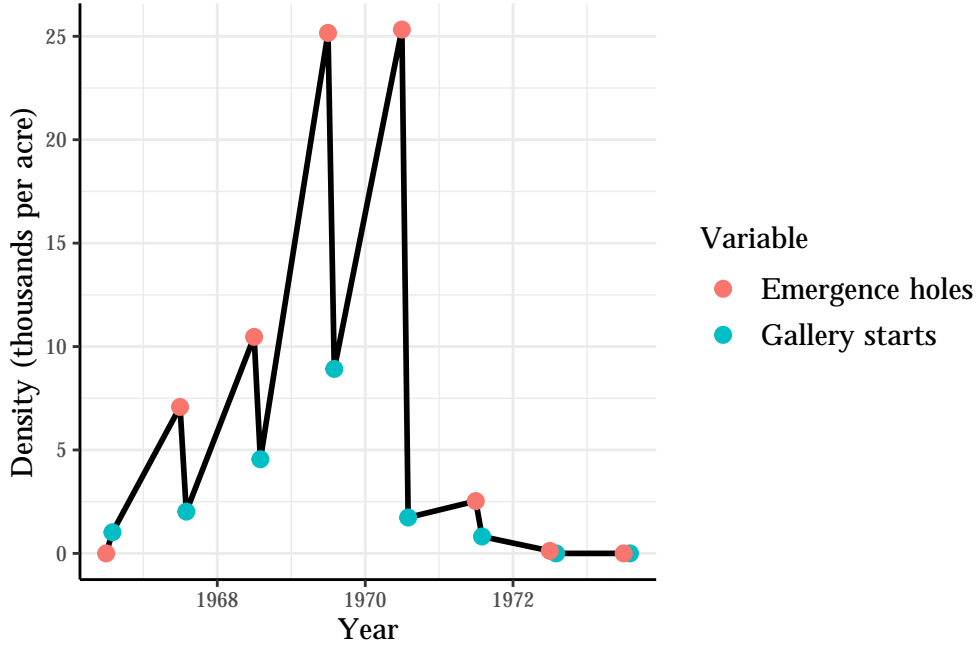


Figure A.1: Time series of emergence holes and gallery starts in the Klein et al. dataset. Emergence and subsequent attacks are assumed to take place in July and August respectively. There are always far fewer gallery starts than emergence holes, suggesting high levels of dispersal mortality.

A.2 Model overview

There are three statistical models. 1) The tree growth model (Appendix A.4); 2) The simple Allee effect model (Appendix A.8), which is fit to the Boone et al. dataset; and 3) the complex outbreak model (Appendices A.5–A.9), which is fit to the Klein et al. dataset. Table A.1 describes all relevant notation, including subscripts, data, intermediate quantities, and bonafide parameters.

The tree growth model (Appendix A.4) estimates the demographic parameters of lodgepole pine: density-independent mortality and forest carrying capacity (m and K). This model was fit with the 1965 pre-outbreak tree diameter distribution in the Klein et al. dataset (sample size = 7). The simple Allee effect model (Appendix A.8) describes the Allee effect and was fit with Boone et al. data (sample size = 28). The posterior distribution of the Allee threshold parameter was used to create an informative prior for the Allee effect in our third statistical model.

The third statistical model (Appendices A.5–A.9), which is by far the most complex, uses the Klein et al. dataset (sample size = 91) to model the outbreak dynamics of MPB. This outbreak model contains several *sub-models*, simple models that are used to resolve one aspect of MPB’s life cycle. For example, tree diameter and beetle attack preference, are used to estimate the parameters β_0 and β_1 . A variety of such sub-models provide direct estimates of the parameters β_0 , β_1 , γ , ζ_0 , ζ_1 , and additional noise parameters. The remaining parameters (a , s_0 , λ_0 , and λ_1), are estimated by stringing together the deterministic aspects of the sub-models to predict the number of gallery starts in the following year; we call this the *integrator model*. All of the sub-models, along with the integrator model are combined and fit simultaneously. The result is a hierarchical model structure, where information is partially pooled across sub-models, because all parameters must work cohesively to predict next year’s gallery starts.

In the third statistical model, the Allee threshold parameter is given a half-normal prior,

with a standard deviation equal to half of the point estimate of a (the mean of the marginal posterior) from the second model (which estimates the Allee effect in the [Boone et al.](#) data). This prior expresses the belief that the Allee threshold in the [Boone et al.](#) data is an upper bound on the threshold in the [Klein et al.](#) dataset, since the [Klein et al.](#) data are averages over a much larger spatial scale (259 hectares vs. 15 hectares) and MPB are known to be highly spatially aggregated. All other parameters are given weakly-informative priors, which are later shown to have negligible influence on the results.

In the main text, we presented the simulation model with each time-step beginning and ending with the density of emerging beetles. This approach was chosen for two reasons: Firstly, flying beetles are a noticeable aspect of actual outbreaks. Secondly, emergence ties directly into our discussion of the interaction between peak beetle density and long-distance dispersal. In contrast, the outbreak statistical model ends each step with beetles that have successfully mass-attacked a tree. This structure yields an extra year of data at the beginning of the outbreak's. Later years, dominated by stand-dependent dispersal, offer less insight into non-dispersal parameters.

Throughout this appendix, we will refer to the surface area over which beetles may attack as the *susceptible surface area*; note that beetles do not attack the upper part of the bole due to thin phloem. To convert between tree diameter and susceptible surface area, we use a simple linear model,

$$SA = -3.792 + 0.821 \times DBH, \quad (16)$$

where DBH is the diameter at breast height in inches, and SA is the susceptible surface area in square meters. Eq. 16 was first published by [Burnell \(1977\)](#), who claims an excellent fit ($R^2 = 0.94$) and attributes the parameterization to William Klein.

A.3 Model-fitting

The parameters of the simulation model are estimated with three *statistical models*: the lodgepole-dynamics model, the Allee-effect model, and the outbreak-dynamics model. The combined statistical models are conceptually identical to the simulation model.

The first statistical model (Appendix A.4) estimates the demographic parameters of lodgepole pine: density-independent mortality and forest carrying capacity (m and K). This model was fit with the 1965 pre-outbreak tree diameter distribution in the [Klein et al.](#) dataset (sample size = 7). Our second statistical model (Appendix A.8) describes the Allee effect and was fit with [Boone et al.](#) data (sample size = 28). The posterior distribution of the Allee threshold parameter was used to create an informative prior for the Allee effect in our third statistical model.

The third statistical model (Appendices A.5–A.9), which is by far the most complex, uses the [Klein et al.](#) dataset (sample size = 91) to model the outbreak dynamics of MPB. This outbreak model contains several *sub-models*, simple models that are used to resolve one aspect of MPB's life cycle. For example, tree diameter and beetle attack preference, are used to estimate the parameters β_0 and β_1 . A variety of such sub-models provide direct estimates of the parameters β_0 , β_1 , γ , ζ_0 , ζ_1 , and additional noise parameters. The remaining parameters (a , s_0 , λ_0 , and λ_1), are estimated by stringing together the deterministic aspects of the sub-models to predict the number of gallery starts in the following year; we call this the *integrator model*. All of the sub-models, along with the integrator model are combined and fit simultaneously. The result is a hierarchical model structure, where information is partially pooled across sub-models, because all parameters must work cohesively to predict next year's gallery starts.

In the third statistical model, the Allee threshold parameter is given a half-normal prior, with a standard deviation equal to half of the point estimate of a (the mean of the marginal posterior) from the second model (which estimates the Allee effect in the [Boone et al.](#) data). This prior expresses the belief that the Allee threshold in the [Boone et al.](#) data is an upper

bound on the threshold in the [Klein et al.](#) dataset, since the [Klein et al.](#) data are averages over a much larger spatial scale (259 hectares vs. 15 hectares) and MPB are known to be highly spatially aggregated. All other parameters are given weakly-informative priors, which are later shown to have negligible influence on the results.

A.4 Lodgepole pine forest dynamics

We begin by deriving tree ages in a stable population, undisturbed by mountain pine beetle. Let K be the carrying capacity (units: trees/acre). Let m be the annual probability of density-independent mortality, constant across all ages. When a tree dies, a seedling is immediately recruited in its place, such that there are always K trees per acre. The asymptotic density of trees of age t is given by:

$$N_t = Km(1 - m)^t \quad (17)$$

Here, $K \times m$ is the density of recruits into the first age class, and $(1 - m)^t$ is the probability that a tree survives up to age t .

The [Klein et al.](#) dataset does not contain tree ages, but it does contain densities of trees within diameter classes. To convert diameter to age, we divide DBH (in inches) by 0.15748, the average annual diameter increment of lodgepole pine.

The response variable is the pre-outbreak (1965) density of trees in the j -th age bin, which is defined by the age range interval $\left[(\text{lower age})_j, (\text{upper age})_j \right]$. The expected density $\mu_{j,\text{tree}}$ for the j^{th} age bin can be defined as:

$$\mu_{j,\text{tree}} = \sum_{t=(\text{lower age})_j+1}^{(\text{upper age})_j} Km(1 - m)^t \quad (18)$$

Finally, the likelihood for the observed tree density, denoted, $(\text{TPA})_j$, is given by the normal PDF:

$$\log(\text{TPA})_j \sim \text{Normal}(\log(\mu_{j,\text{tree}}), \sigma_{\text{tree}}). \quad (19)$$

Residual errors in the densities of small and large-diameter trees are made commensurate through the logarithmic transformation. The noise parameter is σ_{tree} . The model provides a good fit to the data ([Fig. A.2](#)), though there is substantial uncertainty ([Fig. A.3](#)) due to the high quotient of parameters and data (i.e., 3/7).

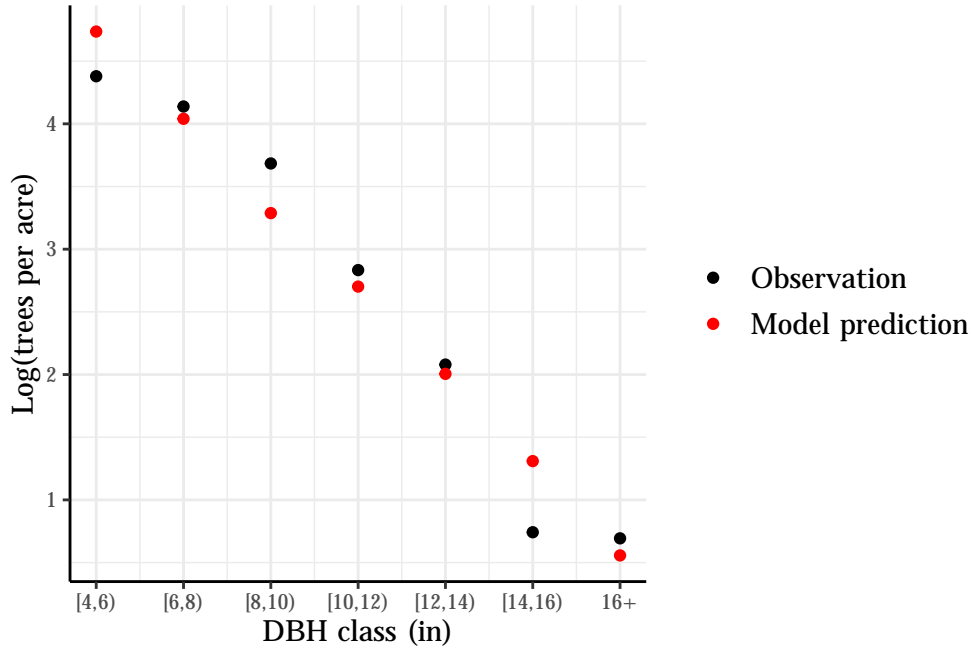


Figure A.2: The pre-outbreak diameter distribution of lodgepole pine is effectively modeled by assuming density-independent mortality and instant recruitment. The theoretical distribution of trees per acre in the j^{th} diameter class is $(\text{TPA})_{j,\infty} = (1 - m)^{(j-1)}mK$, so the logarithm of trees per acre within should be approximately linear with respect to diameter at breast height (DBH). Data from Klein et al. (1978). The predictions were generated with posterior means of model parameters.

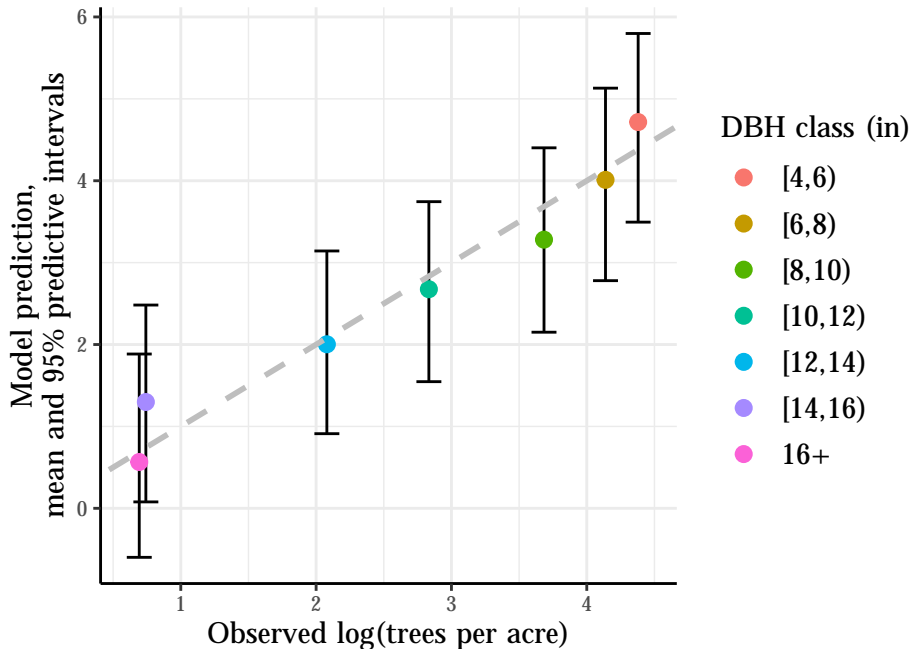


Figure A.3: Observations vs. predictions for the lodgepole pine forest model. The error bars give the 95% predictive interval, representing both parameter and sampling uncertainty. The dashed grey line represents perfect agreement between observed and predicted values. Data from Klein et al. (1978).

A.5 Tree size-dependent preference sub-model

We define *mass attack preference* for trees in the the j^{th} diameter class, in the y^{th} year, as

$$(\text{preference})_{j,y} = \frac{(\text{proportion of successful attacks received})_{j,y}}{(\text{proportion of total tree surface area})_{j,y}}. \quad (20)$$

High values of preference indicate that beetles like to attack a DBH class disproportionately, in relation to the surface area that is “owned” by that DBH class. The preference variable can be calculated directly from the Klein et al. data. The data clearly show that that preference increases linearly with tree diameter (Fig. A.4, A.5).

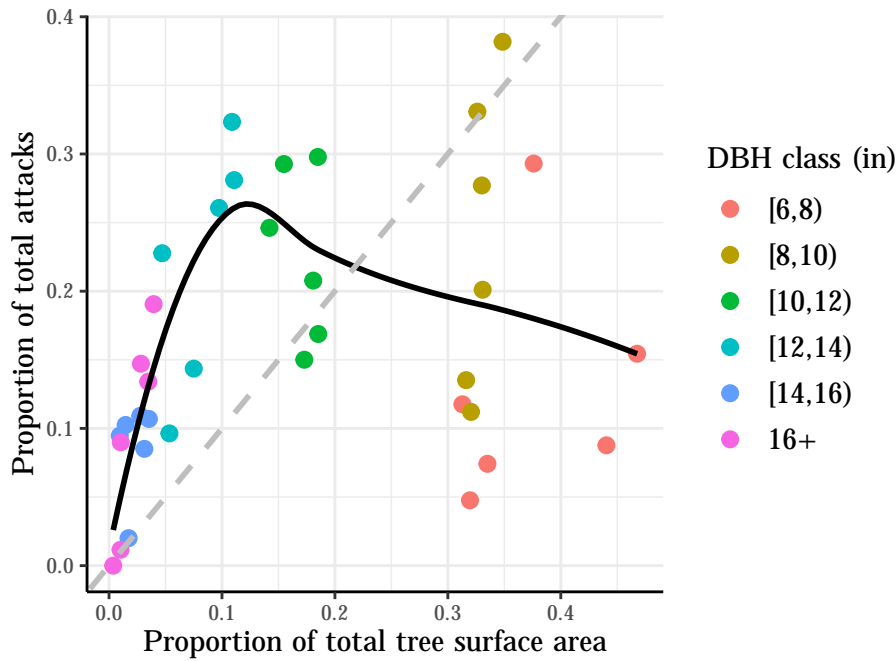


Figure A.4: Beetles disproportionately kill large trees. The x-axis is the proportion of susceptible surface area belonging to live trees of a particular diameter class, within a year. The y-axis is the proportion of total attacks received by the same diameter class, within a year. The black line is a LOESS model prediction. The grey dashed line is the one-to-one line, representing the *no-mass-attack-preference hypothesis*. Data from Klein et al. (1978).

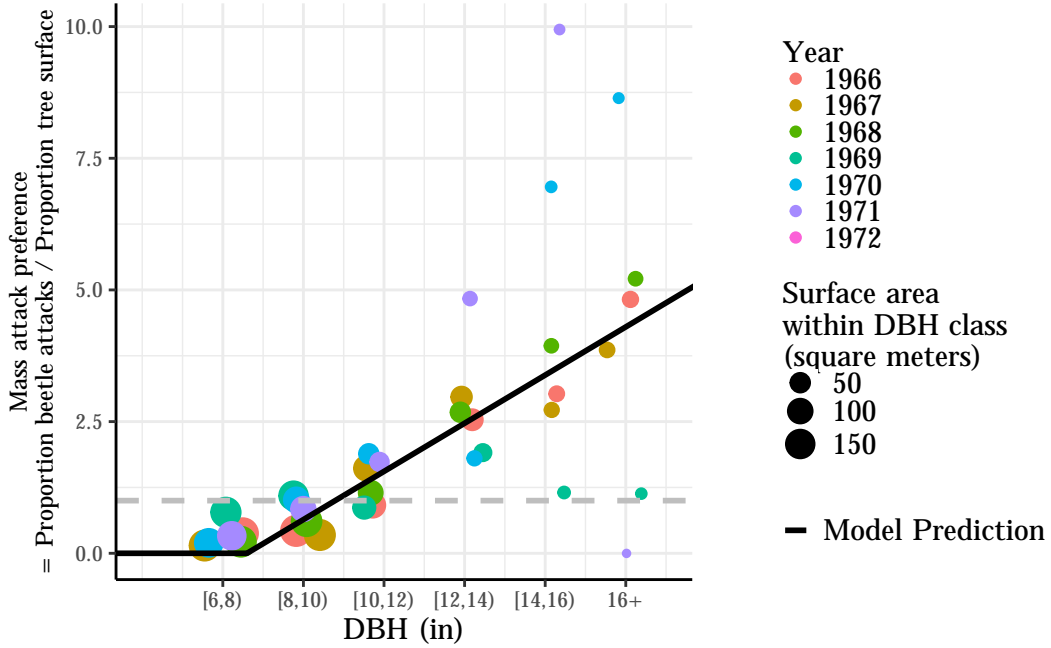


Figure A.5: Beetle preference is an increasing function of tree diameter. The data (from Klein et al., 1978) is well-modeled by a piecewise linear function (see Eq. 22). There is clear heteroskedasticity in the data, which is likely due to smaller sample sizes within classes of large-diameter trees. The exact number of samples is not available, so we use the within-DBH-class surface area as a proxy for sample size, visualized as scatter-plot point size. The prediction was generated using posterior means of model parameters.

Preference is normally distributed with mean $\mu_{j,\text{pref}}$ and standard deviation $\sigma_{j,y,\text{pref}}$:

$$(\text{preference})_{j,y} \sim \text{Normal}(\mu_{j,\text{pref}}, \sigma_{j,y,\text{pref}}). \quad (21)$$

The mean is a piecewise linear function,

$$\mu_{j,\text{pref}} = \begin{cases} \beta_0 + \beta_1 \cdot \text{DBH}_j & \text{if } \text{DBH}_j > -\beta_0/\beta_1 \\ 0 & \text{otherwise.} \end{cases} \quad (22)$$

Above, we assume that DBH_j is the diameter at breast height for the middle of a diameter class, e.g., if we are considering all trees where $\text{DBH} \in [10, 12)$, then DBH_j in the above equation is 11 inches. In the Klein et al. dataset, there are six 2-inch DBH classes. In the simulation model, each tree age is associated with a unique DBH, separated by intervals of 0.157 inches.

The standard deviation of preference is

$$\sigma_{j,y,\text{pref}} = \sqrt{\frac{\sigma_{\text{pref}0}^2}{(\text{total surface area})_{j,y}} + \sigma_{\text{pref}1}^2}, \quad (23)$$

where $\sigma_{\text{pref}0}$ accounts for a baseline level of variability, and $\sigma_{\text{pref}1}$ accounts for increasing variability with smaller sample sizes (clearly visible in Fig. A.5), with the typical inverse square root scaling that would be expected under the central limit theorem. We do not know the exact sample sizes, so we treat the total tree surface area (within the j^{th} diameter class) as a proxy for sample size.

A.6 Converting beetle attacks to tree deaths

We model killed trees as a linear regression through the origin, with a dynamic noise term to account for some obvious heteroskedasticity (Fig. A.6). The killed trees per acre, denoted $(KTPA)_{j,y}$ is normally distributed:

$$(\text{dead})_{j,y} \sim \text{Normal}(\mu_{j,y,\text{dead}}, \sigma_{j,y,\text{dead}}). \quad (24)$$

The mean and standard deviations are given by the equations,

$$\mu_{j,y,\text{dead}} = \gamma \frac{(\text{succ. attacks per acre})_{j,y}}{(\text{surface area per tree})_j}, \quad \text{and} \quad (25)$$

$$\sigma_{j,y,\text{dead}} = \sigma_{\text{dead}0} \frac{(\text{succ. attacks per acre})_{j,y}}{(\text{surface area per tree})_j}, \quad (26)$$

We fit variants of the above model where the standard deviation increased as a square of the independent variable, where the standard deviation was constant, and where the standard deviation contained both constant and dynamics parts (as in the Eq. 23). The model presented above was the best according to Leave-One-Out Cross Validation with expected log predictive density.

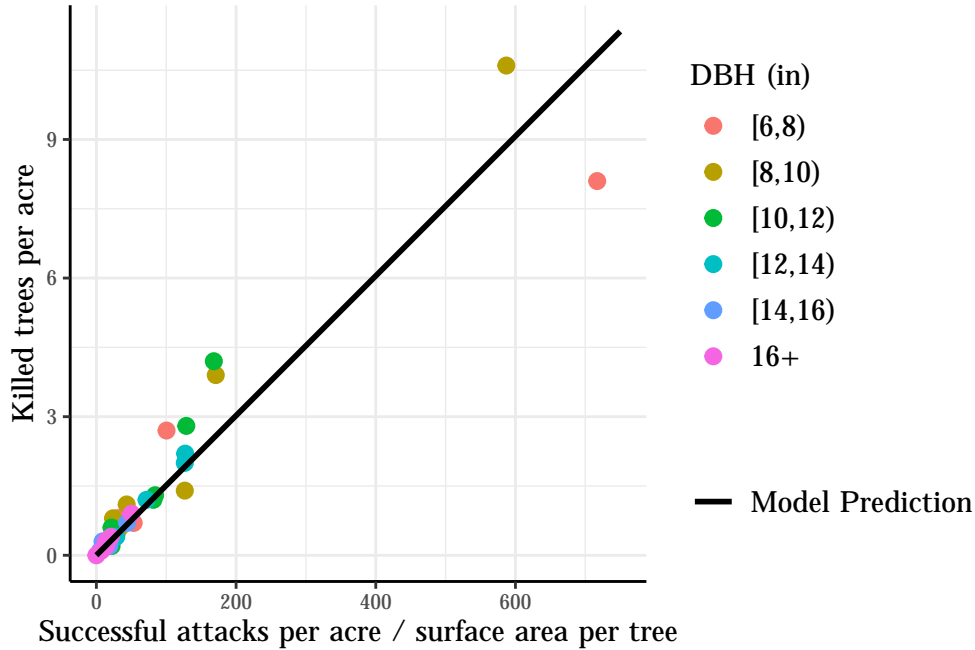


Figure A.6: The number of killed trees is a linear function of successful beetle attacks (corrected for DBH-specific surface area), suggesting that beetles “fill up” a tree to a universal density, and then move on to the next tree. The prediction was generated using posterior means of model parameters. Data from Klein et al. (1978).

A.7 Tree size-dependent fecundity

The Klein et al. dataset does not contain DBH-specific emergence data. The total number of emergence holes per acre is normally distributed:

$$(\text{exit density})_{y+1} \sim \text{Normal}(\mu_{y,\text{exit}}, \sigma_{\text{exit}}), \quad (27)$$

where the mean is a sum over DBH classes:

$$\mu_{y+1,\text{exit}} = \sum_{j=1}^J \begin{cases} \overbrace{(\zeta_0 + \zeta_1 \cdot \text{DBH}_j)}^{\text{Emergence density}} \cdot \overbrace{(\text{KTPA})_{j,y} \cdot (\text{surface area per tree})_j}^{\text{surface area of killed trees}}, & \text{if } \text{DBH}_j > -\frac{\zeta_0}{\zeta_1} \\ 0, & \text{otherwise.} \end{cases} \quad (28)$$

Emergence occurs after the MPB brood overwinters, so the calendar year index for the response variable and the mean prediction is $y + 1$. The standard deviation is simply a constant. Refining the error structure would require unjustifiable assumptions, given the absence of DBH-specific emergence data. The model predictions are in agreement with the data (Fig. A.7).

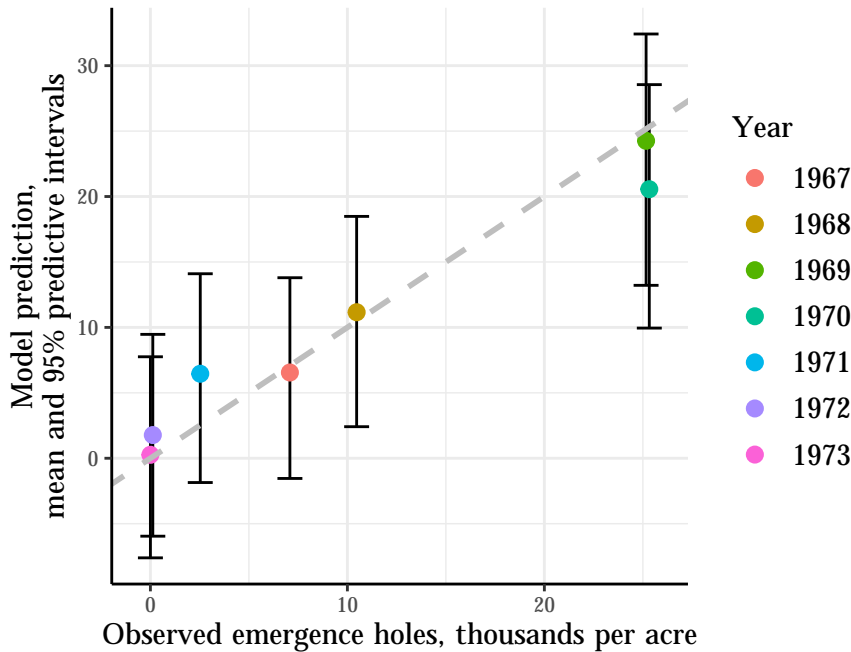


Figure A.7: Observations vs. predictions for the tree size-dependent fecundity sub-model. The error bars give the 95% predictive intervals, representing both parameter and sampling uncertainty. The dashed grey line diagonal line represents perfect agreement between observed and predicted values. Data from Klein et al. (1978).

We cannot justify the functional form of Eq. 28 with graphical evidence, since the Klein et al. dataset only contains total emergence holes (not stratified by diameter class). However, the linear nature of the relationship has been well-established (Reid, 1963, Table 1; Safranyik, 1968, Fig. 25; Cole, 1969, Fig. 5; Cudmore et al., 2009, Fig. 6). The linear relationship also implicitly accounts for the fact that the male:female sex ratio of emerging beetles increases with tree diameter (Cole et al., 1976, Fig. 5). Note that emergence only depends on killed trees, not attacking beetles, because a slightly above-optimal attack density is balanced by intraspecific density dependence, manifesting as a decrease in per capita oviposition or early-instar survival. In other words, there is perfectly compensatory density dependence at the tree scale (Fig. E.3; Berryman, 1974, Fig. 2c; Berryman, 1976, Fig. 2).

A.8 Allee effect

The Boone et al. dataset contains two pertinent variables: density of trees attacked and proportion of attacked trees that are killed. As a first step, we convert the number of attacked trees to the number of attacking beetles. This is done primarily for practical reasons, as we aim

to model the [Klein et al.](#) data, which lacks information on the number of attacked trees (only successfully attacked trees are reported)

To estimate the number of attacking beetles, we multiply the attacked trees by 360, the average number of attacks per successfully attacked tree in the [Klein et al.](#). Since successfully attacked trees receive more attacks, this is probably an overestimate of beetles per attacked tree, which would ultimately lead to a less informative prior for the Allee threshold parameter, a , when modeling the [Klein et al.](#) data.

The probability of a female successfully killing a tree, denoted by (prob. of success) $_y$, is modeled as a normal random variate with mean $\mu_{y,\text{allee}}$ and a standard deviation parameter σ_{allee} , as shown by the following equation,

$$(\text{prob. of success})_y \sim \text{Normal}(\mu_{y,\text{allee}}, \sigma_{\text{allee}}). \quad (29)$$

The mean probability of success is an exponential saturating function of (attacks per acre) $_y$, parameterized with the Allee threshold, denoted a :

$$\mu_{y,\text{allee}} = 1 - \exp\left(-2.3 \cdot \frac{(\text{attacks per acre})_y}{a}\right). \quad (30)$$

The exponential saturating function above is justified by the [Boone et al.](#) dataset (Fig. A.8). The Allee effect sub-model is first fit to the [Boone et al.](#) data; the subsequent estimate of a is used to set an informative prior for the full statistical outbreak model (constituted by the Allee effect sub-model, other sub-models, and the integrator model), which is fit to the [Klein et al.](#) data. Specifically, we choose a half-normal prior with a standard deviation equal to half of the posterior mean of a .

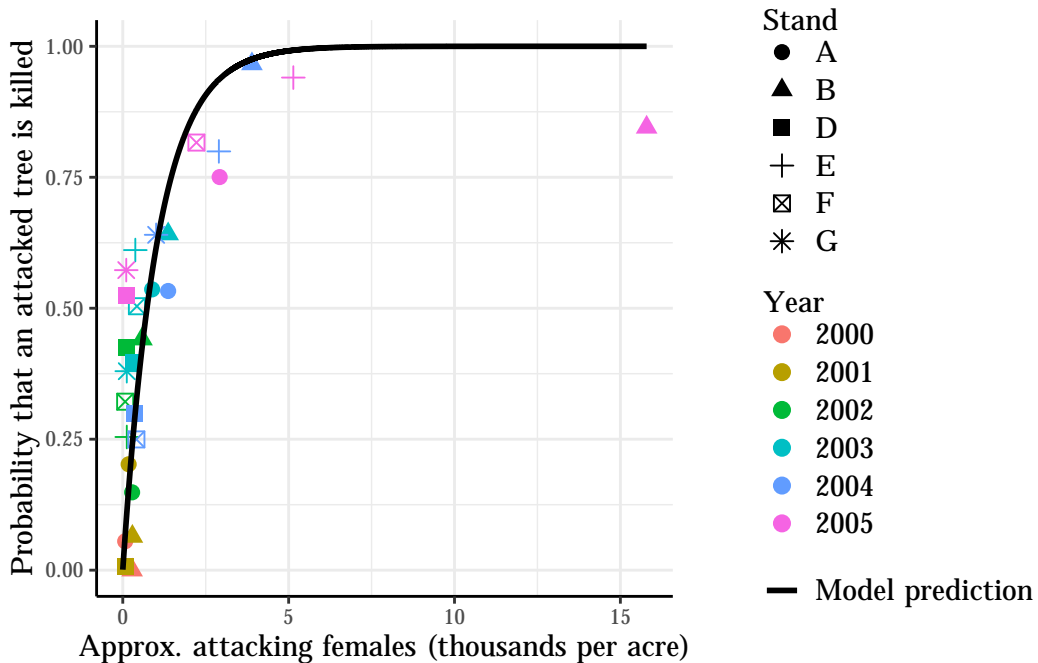


Figure A.8: The probability of an attacked tree being killed is an increasing function of beetle density. The data is effectively modeled by an exponential saturating function (see Eq. 3, “Probability of success” term). The prediction was generated using posterior means of model parameters. Data from the [Boone et al.](#) dataset.

The normal distribution in Eq. 29 is unrealistic because it implies that probabilities outside of the interval $[0, 1]$ are possible. Additionally, the normal distribution assumes constant variance,

whereas the [Boone et al.](#) data clearly shows heteroskedasticity. That being said, a more realistic error structure would unnecessarily complicate the model. The normality of errors and constant variance are the least important assumptions when trying to estimate the conditional expectation ([Gelman and Hill, 2007](#), Sec. 3.6). This is exactly what we are trying to do: only the mean probability of success (i.e., Eq. 30) is used to model the [Klein et al.](#) data.

Another unrealistic aspect of the Allee effect sub-model is that the probability of success approaches an asymptote of 100%, whereas visual inspection of the data suggests an approximate maximum of 80-90% Fig. A.8. However, in the integrator model (Section A.9), an additional parameter for the maximum probability of successful attacks would be non-separable with the maximum dispersal-phase survival, s_0 . Thus, our estimate of s_0 not only represents maximum survival during the dispersal phase, but also the fact that some mass attacks are unsuccessful despite high beetle density. Additionally, s_0 captures the phenomenon where low-vigor females successfully attack trees but do not oviposit (5–30% of females could fall into this category; [Amman, 1975, 1980](#)).

A.9 Integrator model

The integrator model combines the deterministic skeletons of all sub-models (Appendices A.5–A.8) to predict the next year’s gallery starts, solely from this year’s gallery starts. In doing so, we can estimate several parameters that cannot be estimated from singular sub-models: a , s_0 , λ_0 , λ_1 , and a residual noise parameter, σ_{resid} .

First, we predict the distribution of successful beetle attacks among diameter classes. The predicted mass attack preference is

$$\widehat{\text{preference}}_{j,y} = \begin{cases} \beta_0 + \beta_1 \cdot \text{DBH}_j & \text{if } \text{DBH}_j > -\beta_0/\beta_1 \\ 0 & \text{otherwise.} \end{cases} \quad (31)$$

Note that the $\widehat{\text{preference}}_{j,y}$ has a “hat”, which will be used throughout this section to distinguish model-based predictions from data.

Next, we use the total number of successful beetle attacks — denoted (succ. attacks per acre) $_y$ and operationalized as gallery starts per acre — to predict the number of successful beetle attacks within the j^{th} DBH class, denoted (succ. attacks per acre) $_{j,y}$:

$$(\widehat{\text{succ. attacks per acre}})_{j,y} = \frac{(\text{succ. attacks per acre})_y \cdot (\widehat{\text{preference}})_{j,y} \cdot (\text{prop. area})_{j,y}}{\sum_{k=1}^J (\widehat{\text{preference}})_{k,y} \cdot (\text{prop. area})_{k,y}}, \quad (32)$$

The quantity $(\text{prop. area})_{j,y}$ is the proportion of total tree surface area belonging to a particular diameter class.

The equation for successful attacks, Eq. 4, shows how beetles are distributed among tree diameter classes, but not how beetles are distributed among individual trees. As it turns out, killed trees receive an approximately invariant number of attacks per unit surface area (Fig. A.9; see further discussion in Section 1.2.3).

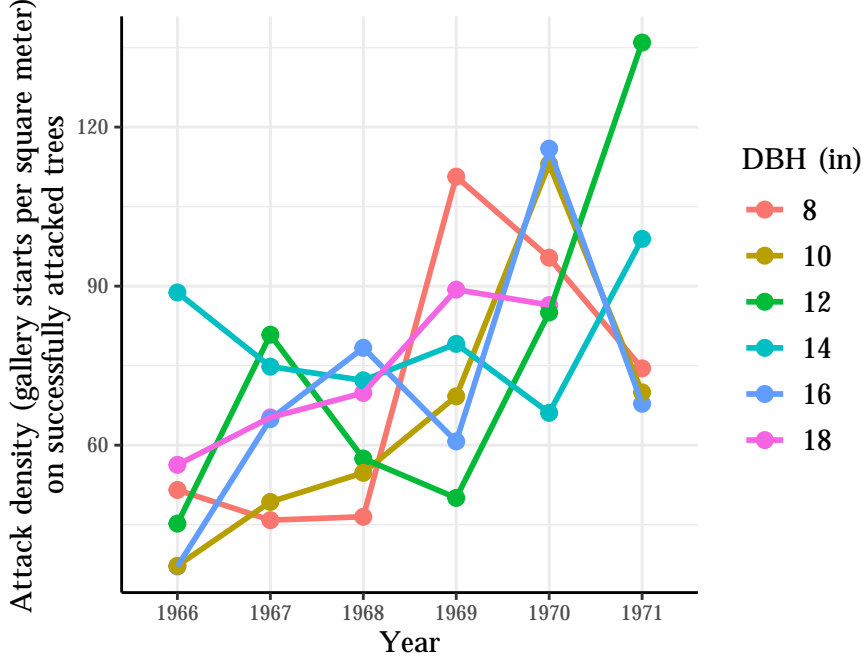


Figure A.9: Successful attack density (gallery starts per square meter) increases slightly over time, but does not depend on tree diameter at breast height (DBH). Data from Klein et al. (1978).

If beetles are unsuccessful, the tree survives and the beetles are assumed to die. This is a simplifying assumption because unsuccessful beetles could attack other trees. The assumption is perhaps justifiable because some beetles will be killed by the first tree, the remainder face increased mortality risk during secondary dispersal, and late-arriving beetles have low fitness (Raffa, 2001).

Successful beetle attacks are converted into killed trees with

$$\hat{\text{dead}}_{j,y} = \min \left(\gamma \frac{(\text{successful attacks per acre})_{j,y}}{(\text{susceptible surface area per tree})_{j,y}}, \text{TPA}_{j,y} \right), \quad (33)$$

and killed trees are converted into emerging females with

$$(\text{exit density})_{y+1} = \sum_{j=1}^J \begin{cases} \overbrace{(\zeta_0 + \zeta_1 \cdot \text{DBH}_j)}^{\text{Emergence density}} \overbrace{((\text{KTPA})_{j,y} (\text{surface area per tree})_j)}^{\text{surface area of killed trees}}, & \text{if } \text{DBH}_j > -\frac{\zeta_0}{\zeta_1} \\ 0, & \text{otherwise.} \end{cases} \quad (34)$$

To predict the number of attacking beetles, we multiply the exit hole density by the predicted probability of survival during the dispersal phase. This quantity is a logistically increasing function (from 0 to the maximum s_0) of “relative surface area” which is defined as the susceptible surface area of all trees with $\text{DBH} \geq 8$ inches in year y , divided by the total susceptible surface area when MPB is absent and the forest is at equilibrium. We use the *relative* surface area mostly for interpretability (e.g., 0.5 means the forest is half-depleted) but also for computational reasons (the Bayesian model-fitting program *Stan* prefers all parameters to be on the unit-scale). Unlike the simulations, there are no stochastic influxes of beetles:

$$(\text{attacks per acre})_{y+1} = \frac{s_0 (\text{exit density})_{y+1}}{1 + \exp(-\lambda_1 ((\text{relative surface area})_{y+1} - \lambda_0))}. \quad (35)$$

We cannot directly justify the functional form of Eq. 35 — say, by plotting total emergence against subsequent total attacks — because Klein et al. only reported attacks on successfully killed trees. However, we note that the logistic function is a standard way to model probabilities, and that the extreme limit of the function (i.e., dispersal mortality is near 100% when there are few trees) is supported by both the Klein et al. dataset (Fig. E.4) and the literature (see Section 1.2.2). In particular, Powell and Bentz (2014) estimated that mean dispersal distance increased from several meters to several kilometers as tree density decreased.

To complete the virtual life-cycle and predict the number of successful attacks next year, denoted $\mu_{y+1,\text{full}}$, the Allee effect is applied to the predicted attack density:

$$\mu_{y+1,\text{full}} = (\text{attacks per acre})_{y+1} \times \left(1 - \exp \left(-2.3 \cdot \frac{(\text{attacks per acre})_{y+1}}{a} \right) \right). \quad (36)$$

Finally, the likelihood of the integrator model is given by a normal distribution with a residual noise parameter.

$$(\text{succ. attacks per acre})_{y+1} \sim \text{Normal}(\mu_{y+1,\text{full}}, \sigma_{\text{resid}}). \quad (37)$$

Table A.1: Statistical model notation

Symbol	Description	Units	submodel(s)
Subscript			
t	Tree age in years	N/A	Lodgepole, A.4
j	The DBH-class index, uniquely identifies a tree diameter class	N/A	All
y	The year index,	N/A	All
tree	Pertaining to the lodgepole pine dyanamics sub-model	N/A	Lodgepole, A.4
pref	Pertaining to the tree size-dependent preference sub-model	N/A	Attack pref., A.5
dead	Pertaining to the tree to killed tree sub-model	N/A	Killed trees, A.6
exit	Pertaining to the tree size-dependent fecundity sub-model	N/A	Fecundity, A.7
allee	Pertaining to the Allee effect sub-model	N/A	Allee effect, A.8
Data			
$(\text{upper age})_j$	Upper age limit of trees within a particular diameter class	years	Lodgepole, A.4
$(\text{lower age})_j$	Lower age limit of trees within a particular diameter class	years	Lodgepole, A.4
TPA_j	Density of trees within the ages corresponding to the j^{th} diameter class	trees · acres ⁻¹	Lodgepole, A.4
$(\text{preference})_{j,y}$	Mass attack preference, defined as the attack density within a particular diameter class, divided by the attack density across all trees (within a year)	unitless	Attack pref., A.5
DBH_j	Diameter at breast height	inches	Attack pref., A.5
$(\text{KTPA})_{j,y}$	Killed trees per acre	trees · acres ⁻¹	Killed trees, A.6
$(\text{succ. attacks per acre})_{j,y}$	Gallery starts per acre	(gallery starts) · acres ⁻¹	Killed trees, A.6
$(\text{surface area per tree})_j$	Susceptible surface area per individual tree, defined by Eq. 16	meters ² · trees ⁻¹	Killed trees, A.6
$(\text{exit density})_y$	Emergence holes per acre	(exit holes) · acres ⁻¹	Fecundity, A.7
J	Total number of unique diameter classes,	unitless	Fecundity, A.7
Y	Total number of years in the data set	unitless	Fecundity, A.7
$(\text{attacks per acre})_{j,y}$	Attacking female beetles per acre	beetles · acres ⁻¹	Allee effect, A.8
$(\text{prop. area})_{j,y}$	Proportion of total susceptible tree surface area belonging to a particular diameter class	unitless	Integrator, A.9
Derived quantities			
$\mu_{j,\text{tree}}$	Expected tree density in the j^{th} diameter class	trees · acres ⁻¹	Lodgepole, A.4
$\mu_{j,y,\text{pref}}$	Predicted mean of the mass attack preference	unitless	Attack pref., A.5
$\sigma_{j,y,\text{pref}}$	Standard deviation of the mass attack preference	unitless	Attack pref., A.5
$\mu_{j,y,\text{dead}}$	Predicted mean of the killed trees density	trees · acres ⁻¹	Killed trees, A.6
$\sigma_{j,y,\text{dead}}$	Standard deviation of the killed trees density	trees · acres ⁻¹	Killed trees, A.6

$\mu_{y,exit}$	Predicted mean of emergence hole density	(exit holes)acres ⁻¹	Fecundity, A.7
$\mu_{j,y,allee}$	Mean proportion of successful attacks	unitless	Allee effect, A.8
s_y	Actual survival probability for beetles during the dispersal phase	unitless	Integrator, A.9
$\mu_{y,full}$	Expected density of successful beetle attacks (across all DBH classes)	(gallery starts) · acres ⁻¹	Integrator, A.9
Model parameters			
K	Tree carrying capacity	trees · acres ⁻¹	Lodgepole, A.4
m	Annual probability of tree death (not caused by MPB)	unitless	Lodgepole, A.4
σ_{tree}	Noise parameter	trees · acres ⁻¹	Lodgepole, A.4
β_0	Y-intercept of the piecewise linear preference-DBH function	unitless	Attack pref., A.5
β_1	Slope of the piecewise linear preference-DBH function; the DBH threshold for attacks is $-\beta_0/\beta_1$	unitless	Attack pref., A.5
σ_{pref0}	noise parameter; accounts for a baseline level of variability in mass attack preference	unitless	Attack pref., A.5
σ_{pref1}	Noise parameter; accounts for increasing variability with smaller sample sizes in mass attack preference	unitless	Attack pref., A.5
γ	Proportionality constant for number of killed trees; the reciprocal of the average attack density	meters ² · (gallery starts) ⁻¹	Killed trees, A.6
σ_{dead0}	noise parameter; the effect of the relative attack density on the standard deviation	meters ² · (gallery starts) ⁻¹	Killed trees, A.6
ζ_0	Y-intercept of the piecewise linear emergence-DBH function	(exit holes) · (meters) ⁻² · (acres) ⁻¹	Fecundity, A.7
ζ_1	Slope of the diameter-emergence regression; the DBH threshold for emergence is $-\zeta_0/\zeta_1$	(exit holes) · (meters) ⁻² · (acres) ⁻¹ · (inches) ⁻¹	Fecundity, A.7
σ_{exit}	Standard deviation parameter for emergence holes	(exit holes) · acres ⁻¹	Fecundity, A.7
a	Allee threshold (density of beetles at which probability of attack success is 0.9)	beetles · acres ⁻¹	Allee effect, A.8
σ_{allee}	Standard deviation parameter for proportion of successful attacks	unitless	Allee effect, A.8
s_0	Maximum survival probability for beetles during the dispersal phase	unitless	Integrator, A.9
λ_1	Sensitivity of dispersal mortality on tree surface area; controls the speed of the transition from low to high dispersal mortality as trees are killed.	unitless	Integrator, A.9
λ_0	Transition point parameter; controls the level of tree death at which dispersal mortality becomes significant	unitless	Integrator, A.9
σ_{resid}	Residual noise parameter, to account for error in the predicted density of successful beetle attacks next year	(gallery starts) · acres ⁻¹	Integrator, A.9

Appendix B Additional model justification

B.1 Stochastic perturbation size

To simulate the influx of female beetles corresponding to the incipient-epidemic transition, we set $I = 300$ (see Eq. 2 in the main text). This number was obtained with a back-of-the-envelope calculation: the median emergence density of females across several studies and Forest Service reports (*Other Studies* in Fig. E.6), multiplied by the susceptible surface area of typical killed tree (10 inches DBH as an input to Eq. 16), multiplied by the median estimate of the dispersal-phase survival probability (using gallery-starts/emergence-holes quotient from the Klein et al. dataset, Fig. E.4), multiplied by 0.81, which is the number of successfully attacked trees per acre that corresponds to an incipient-epidemic state (according to Carroll et al., 2006c). The chosen values of P_I and I are educated guesses, but we re-ran our analysis with several different values and obtained qualitatively identical results.

B.2 Mass attack preference does not change

One potential shortcoming of our model is that preference only depends on tree diameter, whereas previous papers have shown that MPB’s preference for large-diameter trees increases as outbreaks progress (Boone et al., 2011; Howe et al., 2022b). To investigate further, we separately fit our preference sub-model to each year of data and plotted β_1 (the slope of the preference \sim DBH regression) against beetle pressure, as measured by the density of emerging females, and the number of emerging females per unit of susceptible tree surface area (Fig. B.1). There was no clear pattern, indicating that dynamic changes to the DBH preference are small or nonexistent. Similarly, there was no relationship between beetle pressure and the residuals of our original preference model (Fig. B.2).

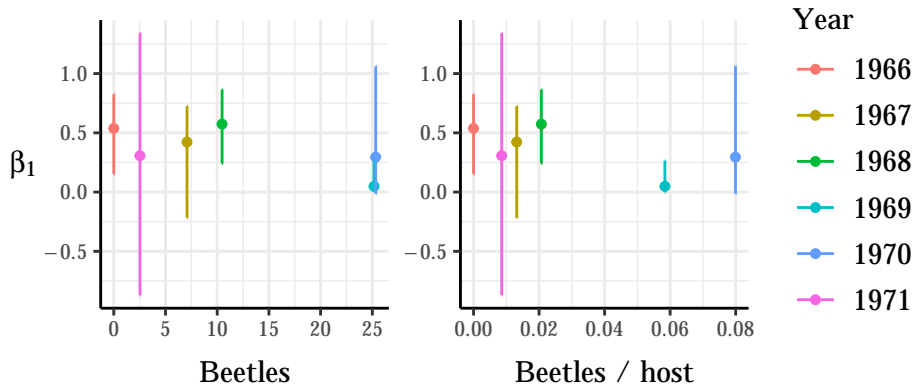


Figure B.1: The mean and 95% credible intervals of β_1 — the slope parameter in the preference \sim DBH model — as a function of beetle pressure. To obtain multiple estimates of β_1 , the tree size-dependent preference sub-model was fit independently to each year of data. Two metrics of beetle pressure are used: *Beetles*, i.e., recently emerging female beetles (units: thousands per acre), and *Beetles/host*, i.e., the quotient of emerging female density and within-DBH-class surface area (units: females per acre per square meter). There is no clear relationship between β_1 and beetle pressure. Data from Klein et al. (1978).

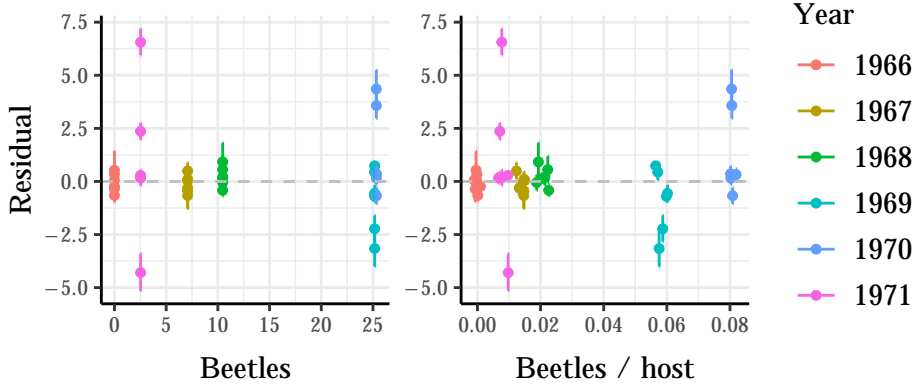


Figure B.2: The mean and 95% credible intervals of the $(\text{preference})_{j,y}$ residuals — from the tree size-dependent preference sub-model — as a function of beetle pressure. Two metrics of beetle pressure are used: *Beetles*, i.e., recently emerging female beetles (units: thousands per acre), and *Beetles/host*, i.e., the quotient of emerging female density and within-DBH-class surface area (units: females per acre per square meter). There is no clear relationship between residual values and beetle pressure. Data from Klein et al. (1978).

There are a couple of ways to explain the absence of evidence for dynamic DBH-preferences. First, it could be that MPB’s large-tree preference “kicks in” at an early, unobserved stage of the Klein et al. outbreak. In Fig. 6. of the publication by Boone et al. (2011), the ratio of DBH of trees entered and not entered increases from 1.2 to 1.6 as an outbreak progresses from endemic to eruptive conditions. However, based on Boone et al.’s classification scheme, the Klein et al. outbreak is approximately in the eruptive condition until the very end of the outbreak (calculations in supplementary files). Second, dynamic changes to DBH-preferences could be small. In Fig. 3D of Howe et al. (2022b), the mean DBH of attacked trees only increased a few centimeters as infestation severity increased from 1 to 1000 attacked trees per hectare.

B.3 Increasing attack density does not affect population dynamics

Figure A.9 in the main text shows that the density of attacks on killed trees (e.g., gallery starts per square meter) increases over time. This pattern can potentially be explained by a positive relationship between attack density and beetle population size, an assumption made by several models in the literature. To investigate further, we fit the killed-tree sub-model (Appendix A.6) to each year of data and plotted $1/\gamma$ (the model-based estimate of attack density) against beetle pressure, as measured by the density of emerging females, and the number of emerging females per unit of susceptible tree surface area (Fig. B.3). The plots are suggestive of a positive relationship if the data from 1971 are excluded, but the nature of the relationship is ultimately inconclusive.

Even if beetle pressure does affect attack density, this has negligible influence on population dynamics. The killed-tree sub-model provides an excellent fit to the data, and the residual variation cannot be explained by beetle pressure (Fig. B.4). This is likely because variation in attack density is swamped by variation in $\frac{(\text{succ. attacks per acre})_{j,y}}{(\text{surface area per tree})_{j,y}}$ (see Eq. 6 in the main text).

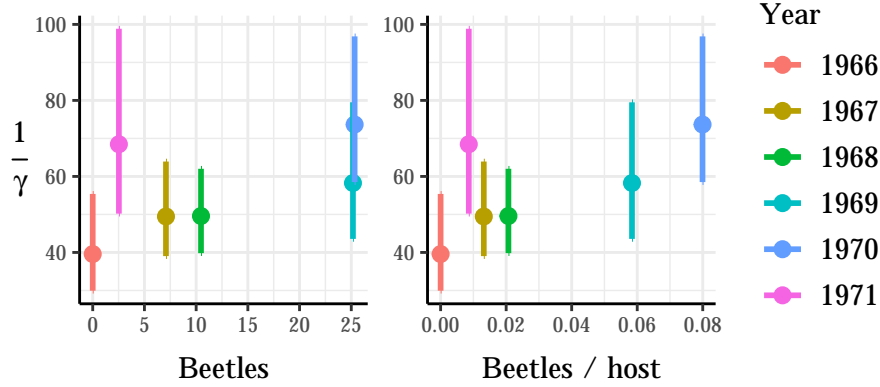


Figure B.3: The mean and 95% credible intervals of $1/\gamma$ — the idealized attack density in killed-tree sub-model — as a function of beetle pressure. To obtain multiple estimates of γ , the killed-tree sub-model was fit independently to each year of data. Two metrics of beetle pressure are used: *Beetles*, i.e., recently emerging female beetles (units: thousands per acre), and *Beetles/host*, i.e., the quotient of emerging female density and within-DBH-class surface area (units: females per acre per square meter). Data from Klein et al. (1978).

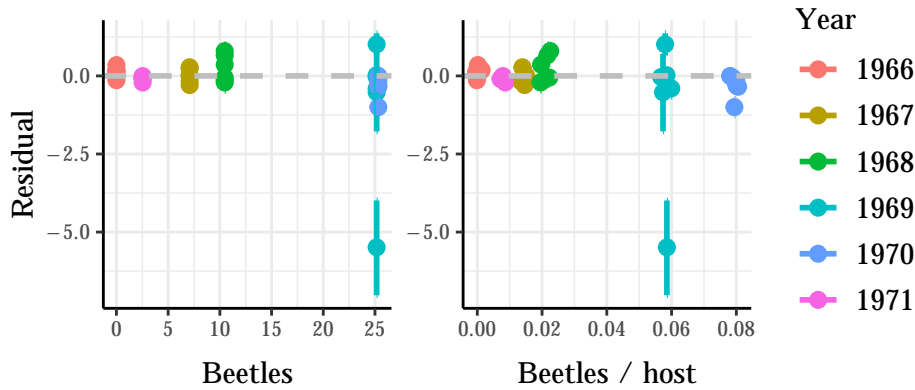


Figure B.4: Mean and 95% credible intervals of $(KTPA)_{j,y}$ residuals from the killed-tree sub-model, as a function of beetle pressure. Two metrics of beetle pressure are used: *Beetles*, i.e., recently emerging female beetles (units: thousands per acre), and *Beetles/host*, i.e., the quotient of emerging female density and within-DBH-class surface area (units: females per acre per square meter). Data from Klein et al. (1978).

B.4 Leave one year out cross validation

The statistical model successfully predicts in-sample data (Fig. B.5, panel A) and out-of-sample data. The exception is that the out-of-sample predictive intervals for 1970 are wide (Fig. B.5, panel B), which upon further investigation, was found to be the result of uncertain estimates of the stand-dependent dispersal mortality parameters, λ_0 and λ_1 (Fig. B.5, panel C).

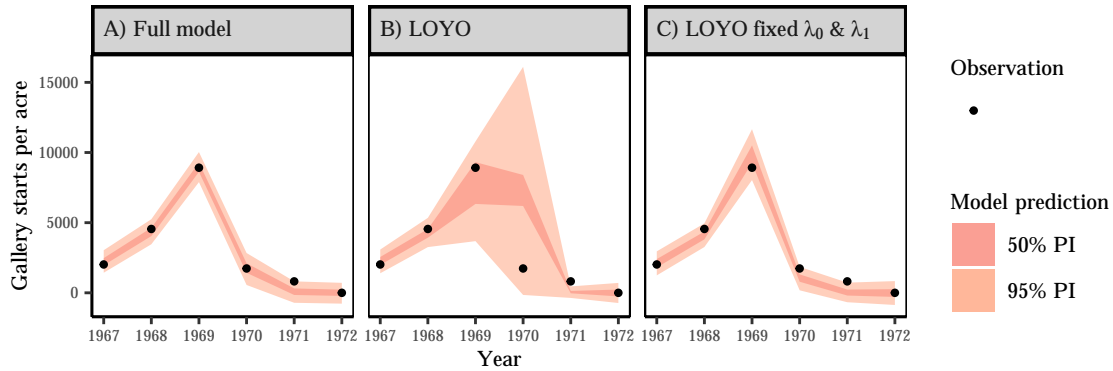


Figure B.5: Observations of successful attack density in the [Klein et al.](#) dataset (operationalized as gallery starts), with superimposed model-based predictive intervals (PIs). Panel A shows in-sample predictions for the full statistical model; panel B shows out-of-sample, leave-one-year-out (LOYO) predictions, where the model is not trained on the focal year’s data; and panel C shows LOYO predictions when the stand-dependent dispersal mortality parameters (λ_0 and λ_1) are fixed at the medians of their respective marginal posterior distributions (see Table 1). Panels B & C demonstrate that data from a single beetle generation (1969–1970) has an overwhelming influence on the estimation of λ_0 and λ_1 , but that all other parameter estimates are robust.

The estimation of stand-dependent dispersal mortality parameters is highly dependent on the data from 1969–1970. This would be indicative of overfitting (i.e., fitting the noise) *if* the decrease in attack density in 1970 was the result of noise, rather than stand-dependent dispersal mortality. The obvious source of statistical noise is the weather, but the weather leading up to the summer of 1970 was unexceptional (Figs. B.7 & B.6). Taken together, evidence for the presence of stand-dependent dispersal mortality (Section 1.2.2) and the absence of anomalous weather patterns imply that the model did not overfit.

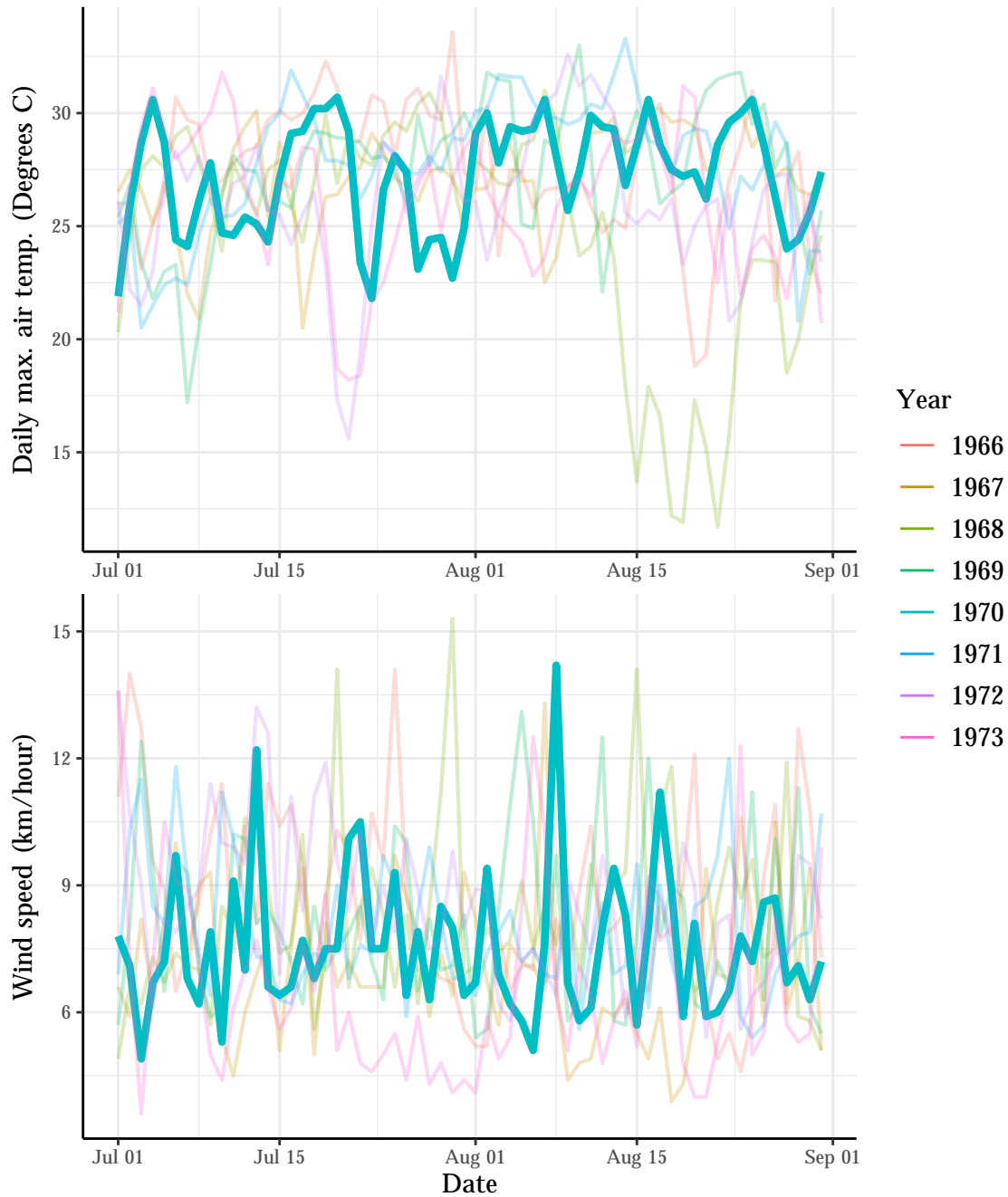


Figure B.6: In 1970, emergence density was high but subsequent attack density was low. Anomalous weather conditions during the flight period could be responsible for this pattern, but the relevant weather variables were unexceptional in 1970 (the bold, teal line). The maximum summer temperature was consistently greater than 18.3°C, the lower limit for beetle flight (McCambridge, 1971). The estimated wind speed often exceeded 8 km/hour, the proposed upper threshold for beetle flight (Gray et al., 1972); however, the wind speeds in 1970 were not anomalous in comparison to the other outbreak years. Weather data was obtained from the *Biosim* program (Régnière et al., 2014).

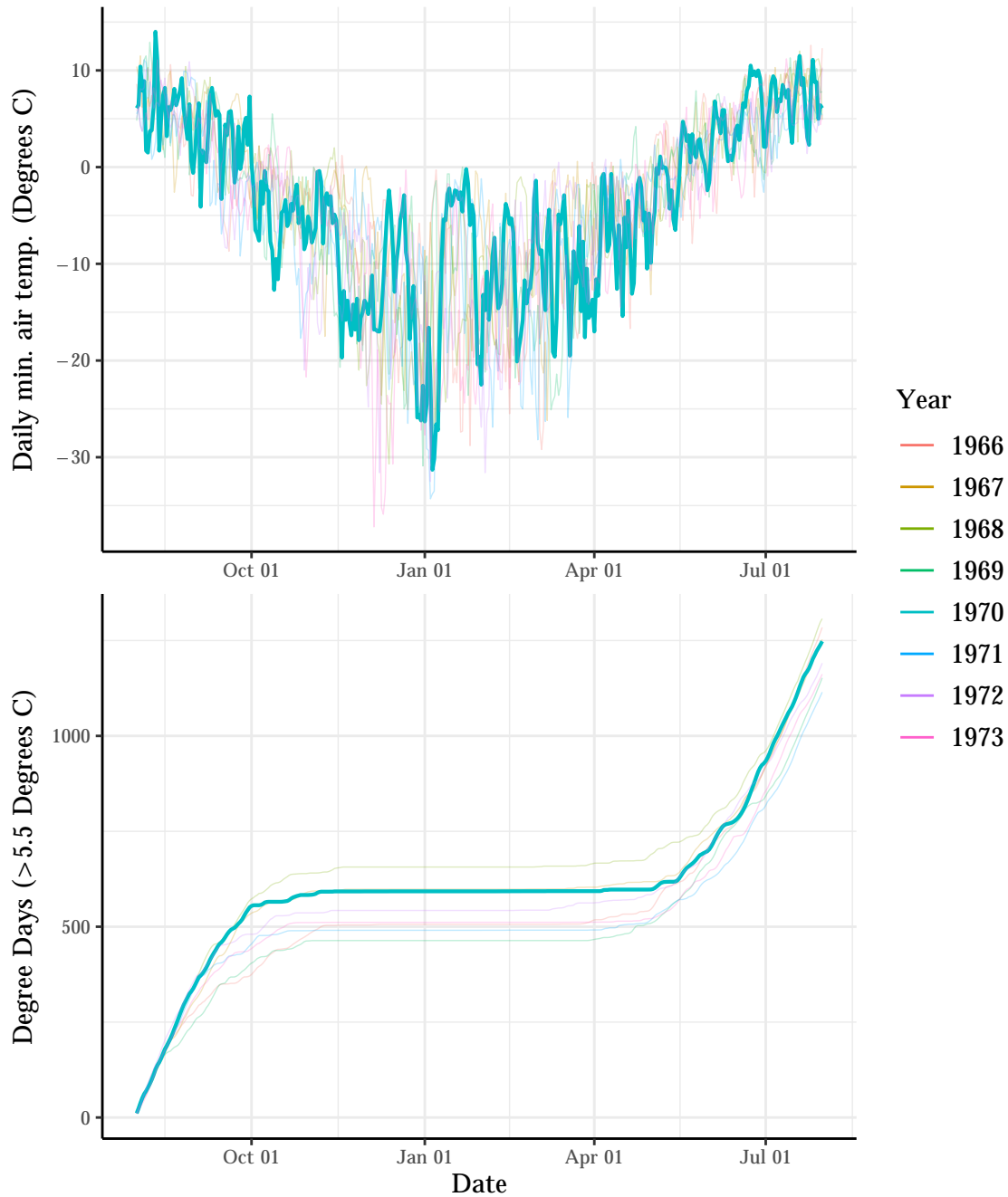


Figure B.7: In 1970, emergence density was high but subsequent attack density was low. The decline could theoretically be attributed to poor environmental conditions that weakened the beetles, despite not being lethal (because they still emerged). However, the developmental period leading up to 1970 had unexceptional weather conditions. The minimum winter temperature is related to larval mortality (here, sub-lethal damage), and degree days are related to emergence and univoltinism. The minimum winter temperature is approximately -30°C , which is substantially greater than the proposed threshold of -40°C (Safranyik, 1998) for significant overwintering mortality. There are approximately 1250 degree days from Aug. 1 to Jul. 31, far beyond the proposed threshold of 833 for the population to be univoltine (Reid, 1962). Weather data was obtained from the *Biosim* program (Régnière et al., 2014).

B.5 The Allee effect depends only on beetle density

Our model states that the success probability (i.e., the probability that an attacked tree is successfully killed) only depends on beetle density. Several previous papers have modeled the success probability as an increasing function of the quotient of beetles and susceptible trees, a simplifying assumption made for mathematical tractability. In this appendix, we argue that these models 1) are unrealistic, and 2) themselves show that the quotient of beetles and trees is superfluous for modeling the Allee effect, as a practical matter.

A good example of a model with non-separable beetles and trees is provided by [Goodsman et al. \(2017\)](#). In this model, the densities of beetles and susceptible trees are denoted B and S , respectively. In each generation, only an α proportion of susceptible trees are attacked. As the authors write, “In reality, because of the clustered nature of attacks in space, most trees in a stand are not attacked and attacks are focused on a small subset of trees ([Logan et al., 1998](#)) some of which may receive many more attacks than others.” The probability that an attacked tree is killed is an increasing function of $m = B/S$.

Each attacked tree receives a number of beetles that is drawn from a negative binomial distribution. The distribution is parameterized with the mean number of beetles, $m = B/(\alpha S)$, and a dispersion parameter k (note that we are redefining some parameters from the main text). Both parameters modulate aggregation — small k and small α both correspond to high aggregation, where a small number of trees receive a large number of beetles. Finally, a tree is killed if the number of beetles it receives is greater than the threshold parameter ϕ . With these dynamics, the probability of success (i.e., the probability that an attacked tree is killed) is the probability mass across all attacks with more than ϕ beetles:

$$F(m; \phi, k) = \sum_{i=\phi+1}^{\infty} NB(i; m, k). \quad (38)$$

This is the complementary CDF of the negative binomial distribution.

While this model may be attractive from a mathematical point of view, it has several unrealistic assumptions: the proportion of attacked trees, α , does not scale with the number of beetles; the per-surface-area attack density may be arbitrarily large, when in reality it is constrained by gallery defense and anti-aggregation pheromones; and brood size does not increase once the attack threshold ϕ is met (see [Raffa and Berryman, 1983](#), Fig. 6 for counter-evidence). More seriously, the model leads to unrealistic population dynamics. If aggregation is too strong (i.e. $k \ll 1$), then the beetles will always be able to find the few fractional trees that slip into the susceptible age class each year; this leads to a large stochastic equilibrium of beetles that is much larger than endemic population seen in nature. The solution, it would seem, is to accept that aggregation is not so strong. But weak aggregation makes it difficult for beetles to invade a mature forest; $m = B/S$ is small, and the beetles are spread evenly across trees, so the threshold ϕ is never exceeded. Counter-intuitively, the beetles get worse at invading as a forest becomes denser since $m = B/S$ becomes smaller. In our experience, with realistic values of ϕ and α , it is difficult to find values of k where beetles experience realistic boom-bust dynamics — where beetle populations will be able to invade, but will later recede to an endemic state.

While acknowledging certain limitations in the [Goodsman et al. \(2017\)](#) model, we will accept it as a premise to illustrate that the probability of mass attack success is predominantly influenced by beetle density. Our Allee effect sub-model with a single parameter (Appendix A.8) is well-approximated by the comparatively parameter-rich model of [Goodsman et al. \(2016\)](#), when the latter model’s parameters are given realistic values.

We examine the relationship between the success probability, here given by Eq. 38, and our three state variables: B , S , and $m = B/S$. More specifically, we examine how the nature of this relationship changes as the parameters α and k change. Figure B.8 shows that the probability of success only shows a weak dependence on S when the dispersion parameter is large (i.e.

$k > 1$) and the attacked fraction of trees is small (i.e. $\alpha \ll 1$). This is precisely the parameter combination that best corresponds to reality (Table B.1; Fig. B.9): beetles spread themselves evenly (i.e. $k > 1$) across a small fraction of susceptible trees (i.e. $\alpha \ll 1$), which they can successfully kill. Success probability remains high unless S is unrealistically large.

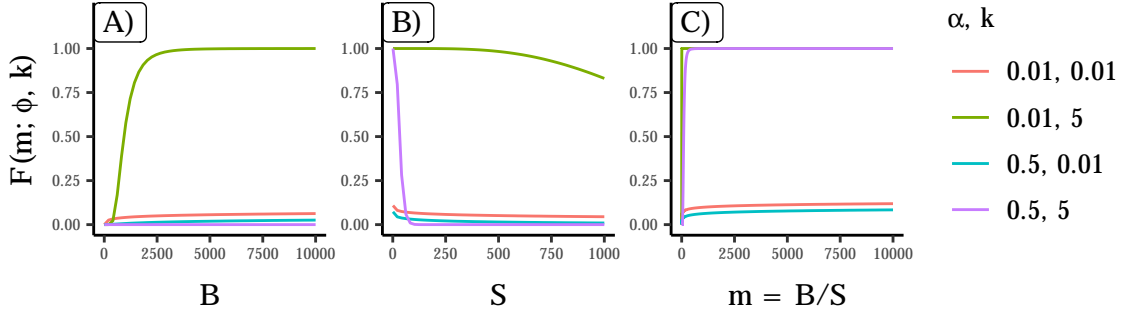


Figure B.8: The probability that an attack tree is killed, calculated via [Goodsman et al.’s 2017](#) model (Eq. 38), as a function of B (female beetles per acre), S (susceptible trees per acre), and $m = B/S$. The range for beetle density was selected based on the [Klein et al.](#) dataset, and the range for susceptible tree density was selected based on the literature: the density of lodgepole pine forests with susceptible trees rarely exceeds 1500 trees/ha, or equivalently, ≈ 600 trees/acre ([Nigh et al., 2008](#); [Pfeifer et al., 2011](#); [Meddens et al., 2011](#)). For panels A and B, the other state variable is fixed at $S = 500$ and $B = 3000$ respectively. To reduce the parameter space that we must numerically explore, we fix $\phi = 176$, which is the attack density threshold given by [Raffa and Berryman \(1983\)](#) — approximately 40 females per square meter — times the susceptible surface area of a 10-inch tree — approximately 4.4 square meters.

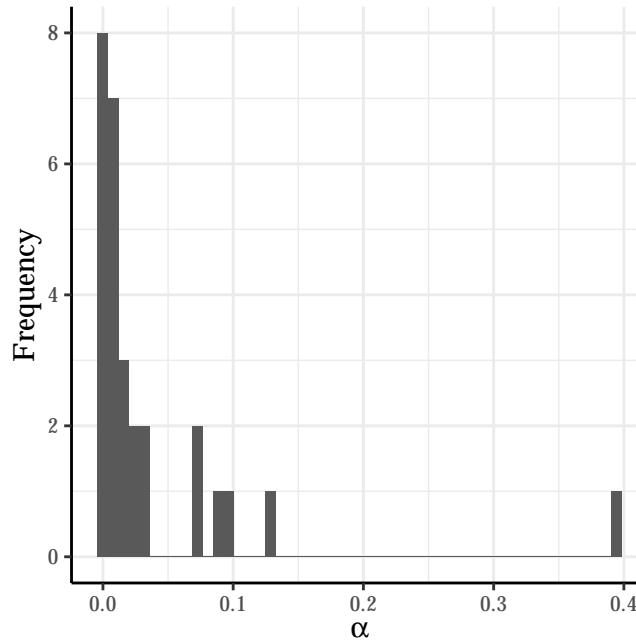


Figure B.9: Estimates of α , the proportion of susceptible trees that are attacked. The data are sourced from [Boone et al. \(2011, Table 1\)](#). The median is 0.009.

Source	$\bar{\mu}$	$\mu_{2.5\%}$	$\mu_{97.5\%}$	\bar{k}	$k_{2.5\%}$	$k_{97.5\%}$
Peterman, 1974, Thesis, Fig. 4, Plot: Elk	119.6	104.6	136.6	9.7	5.2	16.1
Peterman, 1974, Thesis, Fig. 4, Plot: Lean	84.8	75.3	95.6	3.9	2.8	5.2
Peterman, 1974, Thesis, Fig. 4, Plot: Pars	75.1	63.3	89.1	2.9	1.9	4.1
Peterman, 1974, Thesis, Fig. 4, Plot: Terr	76.5	66.5	87.7	3.6	2.5	5.1
Safranyik, 1968, Thesis, Fig. 32, Plot: Elk creek	32.1	23.3	43.9	6.5	1.7	16.9
Safranyik, 1968, Thesis, Fig. 32, Plot: Horsethief creek	23.8	20.9	26.9	23.8	7.3	68.8
Shepard, 1965, Can. Ento., Fig. 4	46.4	37.4	57.7	3.2	1.7	5.3
Waring and Pitman, 1985, Ecol. Fig. 1	92.6	78.6	110.2	2.1	1.5	2.9

Table B.1: Mean and dispersion parameters (μ and k respectively) for the negative binomial distribution, fit to the distribution of attack density (units: females per square meter) across successfully and unsuccessfully attacked trees. Posterior means and 95% credible intervals endpoints are displayed. The data are sourced from [Peterman \(1974\)](#); [Safranyik \(1968\)](#); [Shepard \(1965\)](#); [Waring and Pitman \(1985\)](#). The dispersion parameter k may be scale-dependent, so it is important to note the sizes of the study areas. All studies were conducted at the stand level, but the sizes of the study areas are not directly comparable due to disparate sampling methodologies (i.e., transect vs hierarchical spatial sampling).

Appendix C Model fitting details and diagnostics

We checked a standard suite of summary statistics to provide evidence that the Markov Chains had converged to the global posterior and were efficiently sampling. In particular, $R < 1.1$ for all parameters (i.e., all chains had mixed), the effective sample size per iteration was greater than 0.001 (i.e., efficient sampling), the energy Bayesian fraction of missing information (E-BFMI) was less than 0.2 (i.e., the model was not severely misspecified), and the proportion of divergent trajectories was far less than 1% (i.e., the posterior geometry did not lead do biased estimation). This diagnostic analysis is provided in the R markdown file *model_diagnostics.Rmd* and its output *model_mcmc_diagnostc_printoff.txt*, in the supplementary files. See [Gelman et al. \(2014, Ch. 6\)](#) for more information on the aforementioned summary statistics.

To show that the marginal prior distributions had negligible influence on the posterior distribution, we computed the posterior contraction,

$$\text{post. contraction} = 1 - \frac{\mathbb{V}_{\text{post}}}{\mathbb{V}_{\text{prior}}}. \quad (39)$$

This is a parameter-specific metric that shows the influence of the data on parameter estimation. For nearly every parameter in every model, the prior contraction was above 0.9, implying negligible prior influence. The exception is the Allee threshold parameter in the complex outbreak dynamics threshold. The posterior contraction analysis is provided in the R markdown file *model_diagnostics.Rmd* and its output *model_post_contract_printoff.txt*, in the supplementary files.

The low value of the posterior contraction for the parameter a indicates that the [Klein et al.](#) data is not informative with respect to estimating the Allee effect. This is unsurprising, as discerning the Allee effect is challenging without data from trees that were attacked but not successfully killed (see Section 1.2.1), data which is absent in [Klein et al.’s 1978](#) publication. However, the Allee threshold estimate is not devoid of information, since the prior distribution was derived from the Allee effect sub-model fit to the [Boone et al.](#) dataset (see Table C.2 & Appendix A.8).

Parameter	Short description	Mean	SD	CI _{2.5%}	CI _{97.5%}
β_0	pref.~DBH intercept	-3.42	0.773	-4.84	-1.93
β_1	pref.~DBH slope	0.453	0.0688	0.319	0.580
$\sigma_{\text{pref}0}$	pref. baseline noise	0.628	0.0830	0.484	0.814
$\sigma_{\text{pref}1}$	pref. sampling noise	0.154	0.112	0.00663	0.417
γ	dead tree~attack slope	0.0151	0.000878	0.0134	0.0168
σ_{dead}	dead tree noise	0.00508	0.000657	0.00398	0.00653
ζ_0	emerge~DBH intercept	-9.86	49.2	-106	87.8
ζ_1	emerge~DBH slope	25.4	5.21	15.3	35.5
σ_{exit}	emerge noise	3.61	1.52	1.76	7.42
s_0	max dispersal survival	0.477	0.0701	0.363	0.639
σ_0	residual noise	363	88.7	225	568
λ_{resid}	dispersal threshold	0.652	0.0353	0.579	0.708
λ_1	dispersal sensitivity	49.7	96.6	17.2	262
a	Allee threshold	432	363	13.5	1338.88825
K	forest carrying capacity	904	313	413	1630.37825
m	annual tree mortality	0.0518	0.00637	0.0376	0.0634
Derived quantity	Short description	Mean	SD	CI _{2.5%}	CI _{97.5%}
σ_{tree}	tree abund. noise	0.482	0.211	0.240	1.02
$-\beta_1/\beta_0$	susc. DBH threshold	7.46	0.666	5.98	8.47
$1/\gamma$	attack density	66.3	3.88	59.4	74.4
$\zeta_0 + \zeta_1 * 10$	emerge density (10 in. DBH)	244	25.1	191	296
$K - \sum_{t=0}^{17} (1 - m)^t m K$	Overstory density	338	86.0	193	529

Table C.1: Summary statistics for *all* model parameters, including the Mean, standard deviation, and parameter credible intervals (CI_{2.5%}, CI_{97.5%}). Here, the parameters come from the full hierarchical model (Appendix A) fit to the Klein et al. dataset. The table also includes derived quantities, including the DBH of the smallest susceptible trees, the model-estimated attack density (gallery starts per square meter), and the emergence density (females per square meter) on a tree with a 10-inch DBH, which is approximately the average DBH of attacked trees in the Klein et al. dataset. Finally, the table contains fixed parameters, whose values were obtained via literature search. For parameter units, and the summary statistics of sub-model noise parameters, see supplementary Table A.1.

Parameter	Short description	Mean	SD	CI _{2.5%}	CI _{97.5%}
a	Allee threshold	2492	569	1631	3809
σ_{Allee}	Pr. success noise	0.207	0.03	0.158	0.275

Table C.2: Summary statistics for Allee effect model parameters, including the Mean, standard deviation, and parameter credible intervals (CI_{2.5%}, CI_{97.5%}). Here, the parameters come from the Allee effect sub-model (Appendix A.8) fit to the Boone et al. dataset.

Appendix D Landscape analysis of bark beetle damage

Here, we analyze the relationship between bark beetle damage and host tree biomass across western North America, resulting in Figure 9 (in the main text). We focused on entirety of British Columbia and regions 1–6 of the United States (defined by the United States Forest Service), as these areas contain the majority of bark beetle data and initiated data collection earlier than other regions. The temporal scope of our analysis begins with the earliest start date for Aerial Detection Survey (ADS) data in each region, or 1962 when ADS data preceded this date, since surveys were not comprehensive before 1962. Specifically, the start years are:

Region 1 (1962), Region 2 (1994), Region 3 (1997), Region 4 (1991), Region 5 (1996), Region 6 (1962), British Columbia (1962), and Alberta (1998). All regions have an end date of 2021.

Bark beetle damage is estimated using publicly available Aerial Detection Survey (ADS) data. This comprehensive dataset is collected annually through aerial surveillance of all coniferous forests within defined regions. Trained surveyors fly over these areas, delineating polygons that represent the extent of observed forest damage while simultaneously estimating damage severity (e.g., percentage of trees affected within each polygon). Due to variations in severity metrics across space and time, we simplified our analysis by measuring bark beetle damage as the total affected area, summing affected polygon areas across all years and regions. Host tree species information primarily comes from [Wood \(1982\)](#), with additional references for the North American spruce beetle ([USDA Forest Service, 2011](#); [British Columbia Government, nd](#)) and the southern pine beetle ([North Carolina Forest Service, nd](#); [USDA Forest Service, 2009](#)). Host-trees are given in [Table D.1](#). For host-tree biomass data, we utilized multiple sources. In British Columbia, we used species-specific estimates of total live above-ground biomass from [Beaudoin et al. \(2014\)](#). In the United States, we calculated biomass by multiplying relative abundances from Individual Tree Species Parameter (ITSP) maps ([Ellenwood et al., 2015](#)) by total biomass data from [Blackard et al. \(2008\)](#).

Our methodology involved classifying all bark beetles in the ADS data into three categories: irruptive (also referred to as excitable or aggressive), pulse-driven (semi-aggressive or opportunistically aggressive), and non-outbreaking (non-aggressive or lower-stem beetles). This classification is based on subjective judgments gleaned from the literature, as there is no single diagnostic feature of irruptive bark beetle species. We designated the following species as irruptive: mountain pine beetle, European spruce beetle, southern pine beetle, western pine beetle, and western balsam bark beetle, supported by [Singh et al. \(2024\)](#), [Howe et al. \(2022a\)](#), [Howe et al. \(2022b\)](#), [Lantschner and Corley \(2023\)](#), [Biedermann et al. \(2019\)](#), [Koontz et al. \(2021\)](#), and [Weed et al. \(2015\)](#). Pulse-driven species were defined as species that could outbreak but were not known to be irruptive (using [Table 1](#) in [Lantschner and Corley \(2023\)](#), [Table 8.1](#) in [Six and Bracewell \(2015\)](#), and [Table 4.1](#) in [Weed et al. \(2015\)](#)) Non-outbreaking species are provided by [Howe et al. \(2022b\)](#); all remaining beetle species in the ADS data were assumed to be non-outbreaking.

BB Common Name	BB Genus Species	Host Common Name	Host Genus Species	Notes
roundheaded pine beetle	Dendroctonus adjunctus	Mexican white pine	Pinus ayacahuite	Mexico & CentAm
		Mexican mountain pine	Pinus hartwegii	Mexico & CentAm
		Chihuahua pine	Pinus leiophylla	Mexico & S. NM/AZ
		Montezuma pine	Pinus montezumae	Mexico & CentAm
		ponderosa pine	Pinus ponderosa	BC & W. USA
		smooth-bark Mexican pine	Pinus pseudostrabus	Mexico & CentAm
		thinleaf pine	Pinus maximinoi	Mexico & CentAm
western pine beetle	Dendroctonus brevicornis	ponderosa pine	Pinus ponderosa	BC & W. USA
Jeffrey pine beetle	Dendroctonus jeffreyi	Jeffrey pine	Pinus jeffreyi	CA, NV, OR, NW Mexico
		ponderosa pine	Pinus ponderosa (very rare)	BC & W. USA
lodgepole pine beetle	Dendroctonus murrayanae	jack pine	Pinus banksiana	CAN: BC-NS, USA: MN-ME
		lodgepole pine	Pinus contorta	W. NorAm
		eastern white pine	Pinus strobus	NL to great lakes
mountain pine beetle	Dendroctonus ponderosae	Engelmann spruce	Picea engelmannii	W. NorAm
		whitebark pine	Pinus albicaulis	W. Can & W. USA
		foxtail pine	Pinus balfouriana	CA only
		jack pine	Pinus banksiana	
		lodgepole pine	Pinus contorta	
		Coulter/big-cone pine	Pinus coulteri	S. CA & NW Mexico
		pinyon pine	Pinus edulis	SW USA
		limber pine	Pinus flexilis	W NorAm
		Jeffrey pine	Pinus jeffreyi (rare)	
		sugar pine	Pinus lambertiana	OR to NW Mexico
		single-leaf pinon pine	Pinus monophylla	ID to NW Mexico
		western white pine	Pinus monticola	W. Can & USA
		ponderosa pine	Pinus ponderosa	BC & W. USA

BB Common Name	BB Genus Species	Host Common Name	Host Genus Species	Notes
		Chihuahua white pine	Pinus strobiformis	Mexico & SW USA
douglas-fir beetle	Dendroctonus pseudotsugae	western larch/tamarack bigcone spruce/bigcone Douglas-fir Douglas-fir western hemlock	Larix occidentalis (rare) Pseudotsuga macrocarpa Pseudotsuga menziesii Tsuga heterophylla	NW Can & USA CA only W. NorAm NW Can and USA incl AK
spruce beetle	Dendroctonus rufipennis	spruce species	All Picea species in its range (mostly engelmann and white spruce)	
eastern larch beetle	Dendroctonus simplex	eastern larch/tamarack	Larix laricina	All Can, AK & NE USA
red turpentine beetle	Dendroctonus valens	white fir eastern larch/tamarack Norway spruce white spruce red spruce lodgepole pine Coulter/big-cone pine shortleaf pine pinyon pine Mexican mountain pine Jeffrey pine sugar pine Lawson's pine Chihuahua pine western white pine Sierra lodgepole pine	Abies concolor Larix laricina Picea excelsa Picea glauca Picea rubens Pinus contorta Pinus coulteri Pinus echinata Pinus edulis Pinus hartwegii Pinus jeffreyi Pinus lambertiana Pinus lawsonii Pinus leiophylla Pinus monticola Pinus murrayana	W. USA Introduced NE USA & Can All Can, AK, & N. USA NE USA, Quebec-NS SE USA Mexico

BB Common Name	BB Genus Species	Host Common Name	Host Genus Species	Notes
		Mexican yellow pine	Pinus oocarpa	Mexico & CentAm
		ponderosa pine	Pinus ponderosa	BC & W. USA
		smooth-bark Mexican pine	Pinus pseudostrobus	
		Monterey pine	Pinus radiata	Coastal CA & Mexico
		red pine	Pinus resinosa	E Can & NE USA
		pitch pine	Pinus rigida	E. USA
		California foothill pine	Pinus sabiniana	California only
		Chihuahua white pine	Pinus strobiformis	
		eastern white pine	Pinus strobus	
		Scotch pine	Pinus sylvestris	Introduced
		thinleaf pine	Pinus maximinoi	
		Virginia pine	Pinus virginiana	E. USA
NA	Dryocoetes autographus	fir species	Abies spp.	
		Engelmann spruce	Picea engelmannii	
		white spruce	Picea glauca	
		lodgepole pine	Pinus contorta	
		western white pine	Pinus monticola	
		eastern white pine	Pinus strobus	
		Douglas-fir	Pseudotsuga menziesii	
		western hemlock	Tsuga heterophylla	
western balsam bark beetle	Dryocoetes confusus	pacific silver fir	Abies amabilis (rare)	W. BC, WA, OR
		white fir	Abies concolor (rare)	
		subalpine fir	Abies lasiocarpa	
		Engelmann spruce	Picea engelmannii	
pinyon ips	Ips confusus	Colorado pinyon pine	Pinus edulis	
		single-leaf pinyon pine	Pinus monophylla	
emarginate Ips	Ips emarginatus	lodgepole pine	Pinus contorta (rare)	

BB Common Name	BB Genus Species	Host Common Name	Host Genus Species	Notes
		Jeffrey pine western white pine ponderosa pine	Pinus jeffreyi Pinus monticola Pinus ponderosa	BC & W. USA
blue spruce engraver	Ips hunteri	Engelmann spruce blue spruce	Picea engelmannii (rare) Picea pungens	
California fivespined Ips	Ips paraconfusus	knobcone pine lodgepole pine Coulter/big-cone pine Jeffrey pine sugar pine ponderosa pine	Pinus attenuata Pinus contorta (rare) Pinus coulteri Pinus jeffreyi Pinus lambertiana Pinus ponderosa	BC & W. USA
northern spruce engraver	Ips perturbatus	white spruce	Picea glauca	
pine engraver	Ips pini	jack pine lodgepole pine Jeffrey pine ponderosa pine eastern white pine	Pinus banksiana Pinus contorta Pinus jeffreyi Pinus ponderosa Pinus strobus	BC & W. USA
western cedar bark beetle	Phloeosinus spp.	Rocky Mountain juniper Utah juniper one-seed juniper	Juniperus scopulorum Juniperus osteosperma Juniperus monosperma	
NA	Pityophthorus pseudotsugae	white fir grand fir subalpine fir red fir Engelmann spruce sugar pine Douglas-fir	Abies concolor Abies grandis Abies lasiocarpa Abies magnifica Picea engelmannii Pinus lambertiana Pseudotsuga menziesii	

BB Common Name	BB Genus Species	Host Common Name	Host Genus Species	Notes
fir root bark beetle	Pseudohylesinus granulatus	western hemlock	Tsuga heterophylla	
		pacific silver fir	Abies amabilis	
		grand fir	Abies grandis	
		subalpine fir	Abies lasiocarpa	
		red fir	Abies magnifica	
Douglas-fir pole beetle	Pseudohylesinus nebulosus	noble fir	Abies procera	
		western hemlock	Tsuga heterophylla	
silver fir beetle	Pseudohylesinus sericeus	Douglas-fir	Pseudotsuga menziesii	
		western hemlock	Tsuga heterophylla (rare)	
Douglas-fir engraver	Scolytus unispinosus	pacific silver fir	Abies amabilis	
		grand fir	Abies grandis	
		noble fir	Abies procera	
		Douglas-fir	Pseudotsuga menziesii	
fir engraver	Scolytus ventralis	western hemlock	Tsuga heterophylla	
		Douglas-fir	Pseudotsuga menziesii	
Mediterranean oak borer	Xyleborus monographus	white fir	Abies concolor	
		grand fir	Abies grandis	
southern pine beetle	Dendroctonus frontalis	red fir	Abies magnifica	
		blue oak	Quercus douglasii	
southern pine beetle	Dendroctonus frontalis	valley oak	Quercus lobata	
		shortleaf pine	Pinus echinata	
		loblolly pine	Pinus taeda	
		pitch pine	Pinus rigida	
southern pine beetle	Dendroctonus frontalis	pond pine	Pinus serotina	
		Virginia pine	Pinus virginiana	

Appendix E Additional supplementary figures

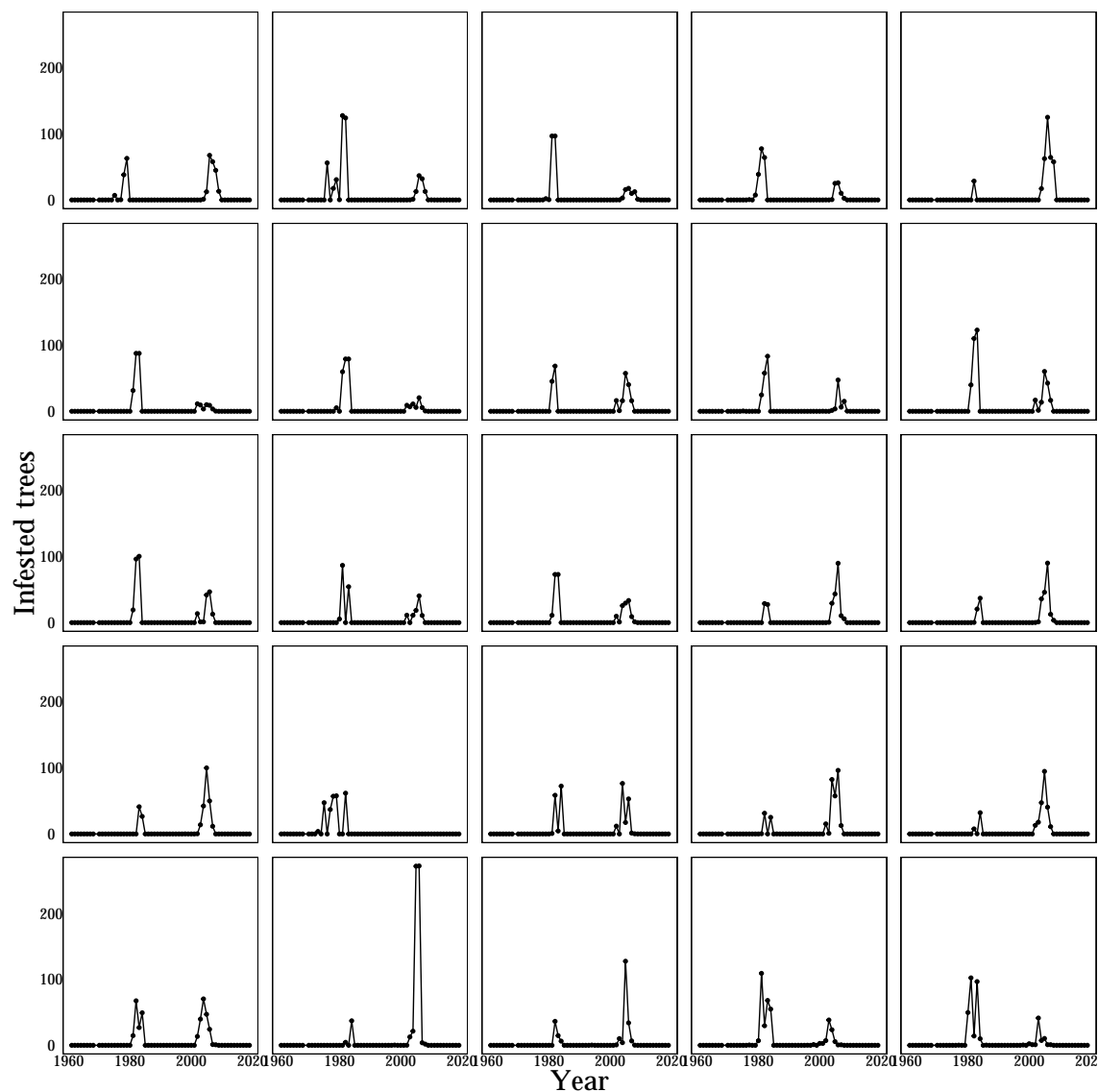
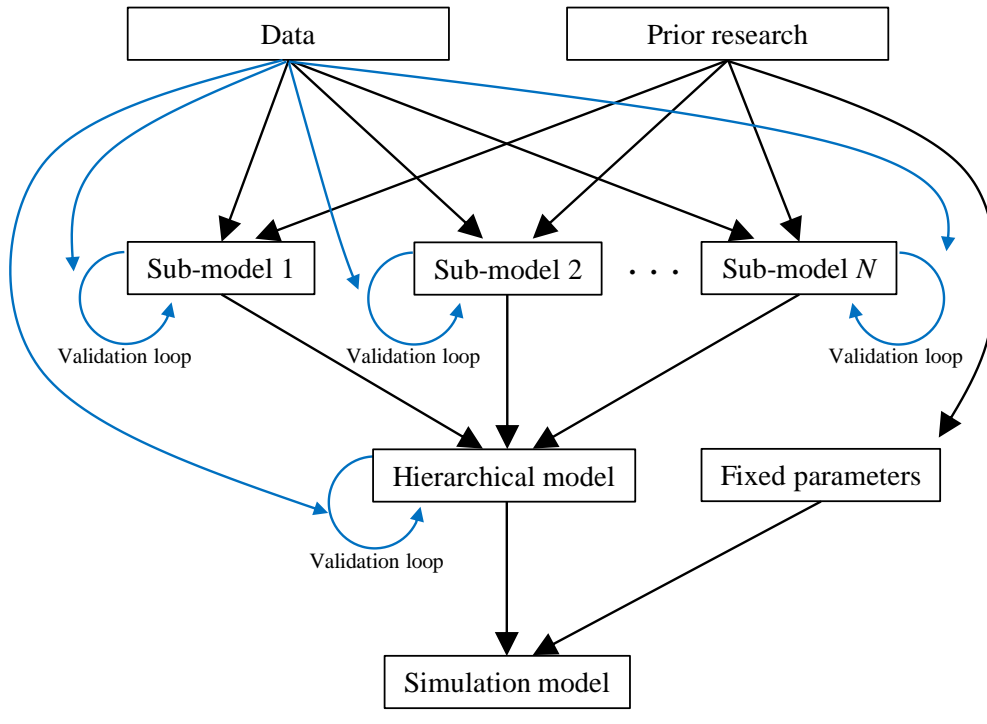


Figure E.1: Sample time series of MPB-infested trees from British Columbia’s Aerial Overview Surveys. Each panel is a randomly selected 1 km² patch from a subset of locations where cumulative infestations were in the upper quartile. To estimate the number of infested trees, we multiply the proportion of infested stems by $\frac{\text{Live aboveground biomass (units: Mg/ha)}}{10}$, which is an approximation for pine stem density that was validated by Koch et al. (2021, Appendix A), using the data and analyses of Nigh et al. (2008). The biomass data is sourced from Beaudoin et al. (2014).

Part 1: Model building



Part 2: Causal analysis

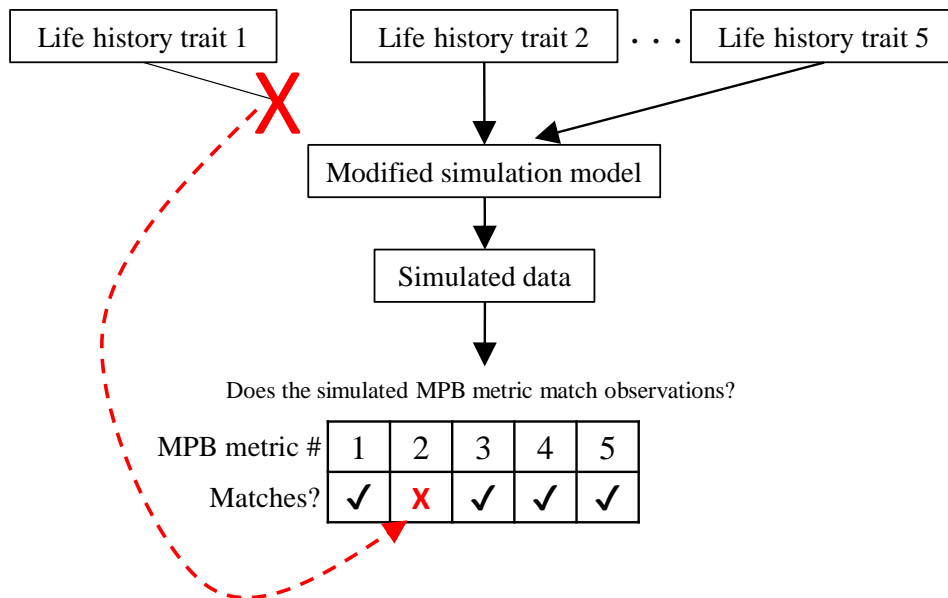


Figure E.2: Graphical representation of our inferential approach. First, we develop and validate a realistic model of MPB dynamics. Second, we perform a causal analysis in which we turn biological features on or off. In the example of the causal analysis, the red crosses respectively indicate that feature # 1 has been off, and that the simulated system does not match reality with respect to Metric #2 (e.g., outbreak periodicity). The dashed red arrow indicates that feature #1 is responsible for realistic values of Metric #2.

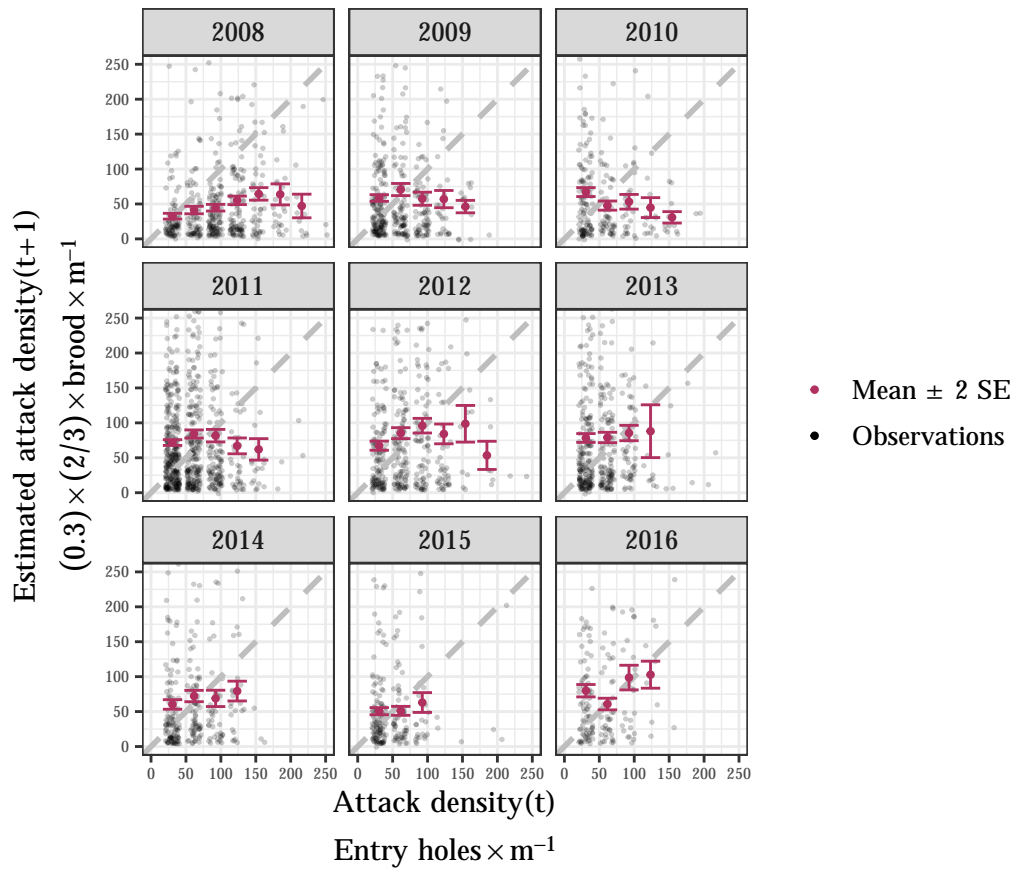


Figure E.3: Population maps provide evidence for compensatory density dependence at the tree level. The data comes from Alberta’s disk surveys (described by [Government of Alberta, 2016](#), and published by [Goodsman et al., 2018](#)). The estimate for attack density at time $t + 1$ involves the constants $(2/3)$ (the average proportion of the brood that will be female) and 0.3 (an estimate of dispersal-phase mortality from the [Klein et al. \(1978\)](#) dataset, see Fig. E.4).

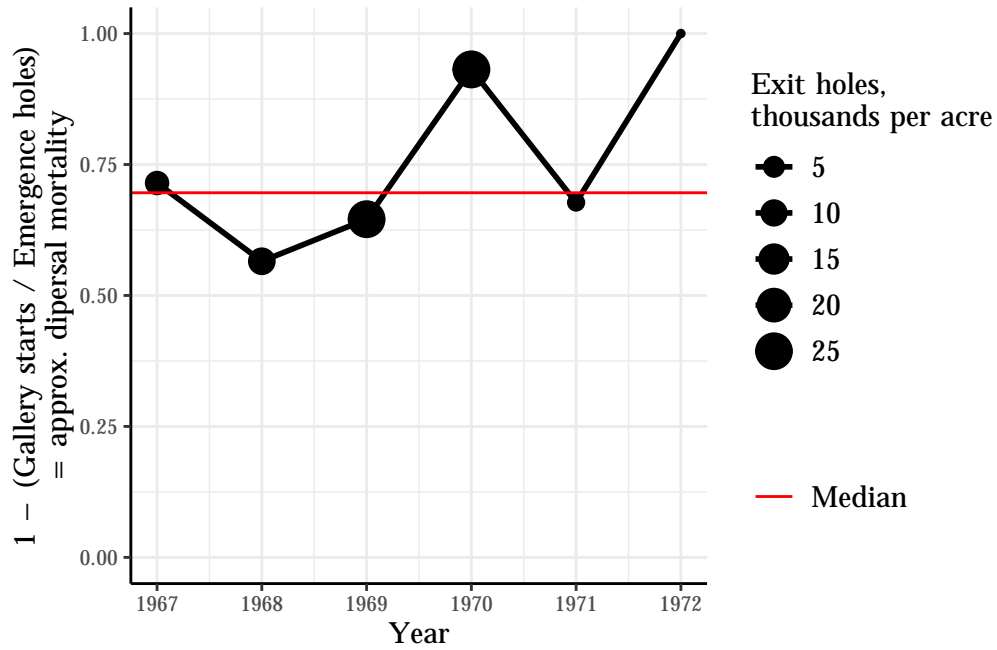


Figure E.4: An approximation of dispersal mortality as a function of time in the [Klein et al.](#) data. The dispersal mortality is approximated as the quotient of gallery starts and preceding emergence holes. The quotient captures both dispersal mortality and mortality from unsuccessful attacks (i.e., the Allee effect, Eq. 3). Therefore, the approximation will be better when emergence density is larger (i.e., before 1971), because the Allee effect will be less important and the relative influence of inter-patch dispersal will be less important. The first three years can be used to approximate the baseline dispersal mortality (i.e., $1 - s_0$ in Eq. 1).

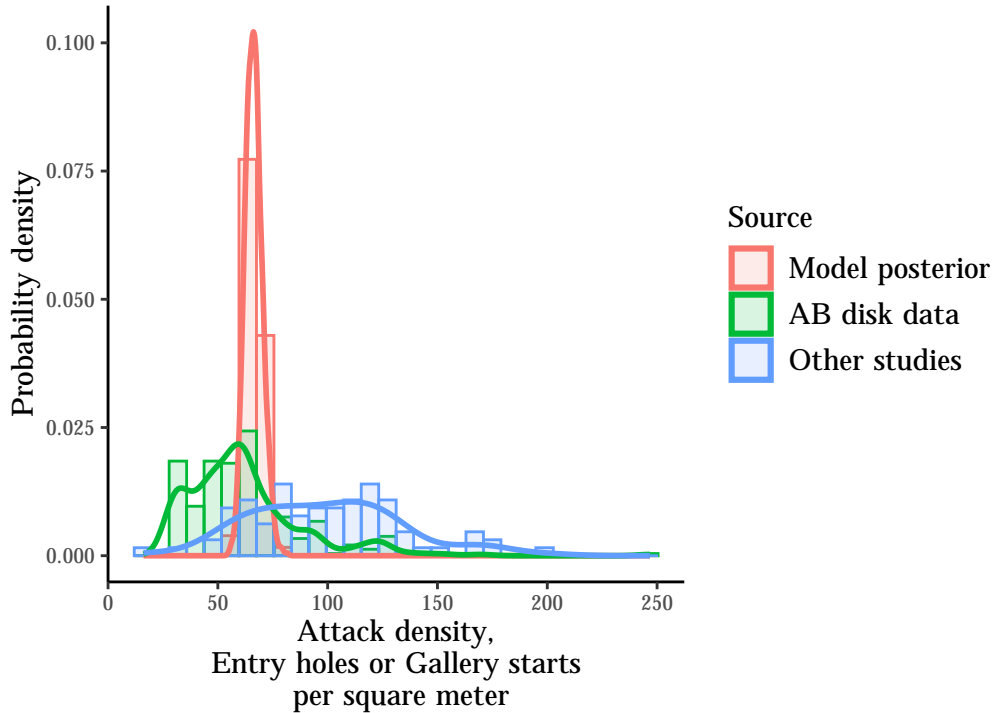


Figure E.5: Frequency distributions of attack density. The *Model posterior* category gives the marginal posterior of $1/\gamma$ from our statistical model of the [Klein et al.](#) outbreak. The *AB disk data* category contains the within-site means of attack density from 300 different sites across Alberta ([Government of Alberta, 2016](#)). The *Other studies* category includes estimates obtained via entry holes or gallery starts from a number of studies, mostly United States Forest Service report: [Tishmack et al. \(2005\)](#); [Mccambridge \(1967\)](#); [Negr3n \(2018\)](#); [Reid \(1963\)](#); [Raffa and Berryman \(1983\)](#); [Rasmussen \(1980\)](#); [Shepard \(1965\)](#); [Knight \(1959\)](#); [De Leon \(1939\)](#); [Safranyik \(1988\)](#); [Safranyik and Vithayasai \(1971\)](#); [Safranyik \(1968\)](#); [Parker \(1979\)](#); [Schmid \(1972\)](#); [Blackman \(1931\)](#); [Whiteside \(1937\)](#); [Washburn and Cole \(1959\)](#); [author N/A \(1963\)](#); [Peterman \(1974\)](#); [Klein et al. \(1978\)](#); [Safranyik and Linton \(1991\)](#).

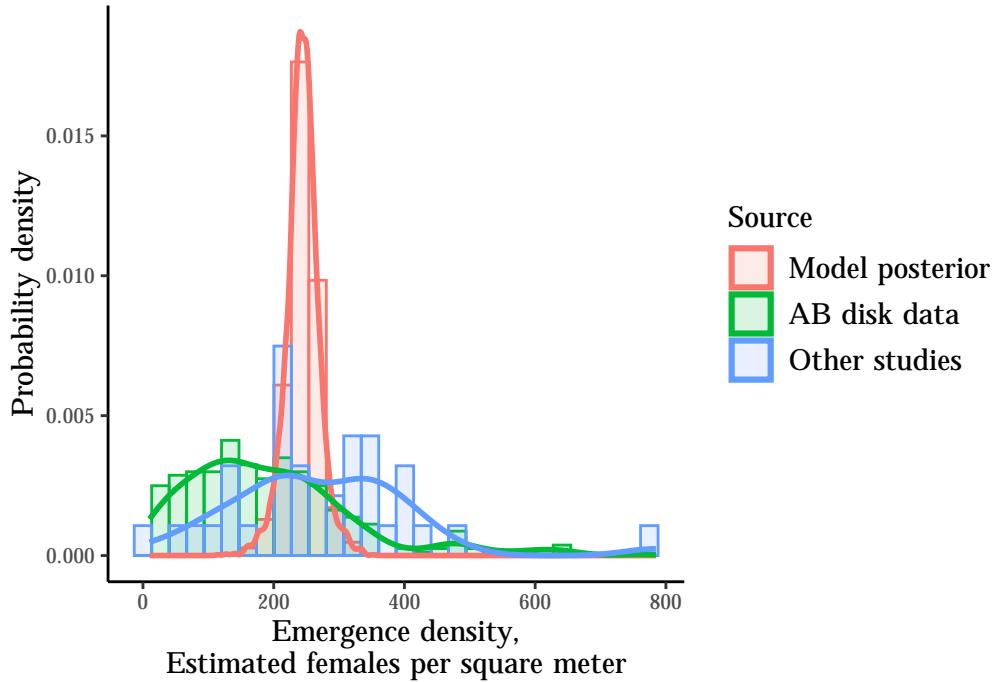


Figure E.6: Frequency distributions of female emergence density. Females are estimated with $(2/3) \times (3/2) \times$ emergence holes, or with $(2/3) \times$ emerging beetles or spring brood size. Note that $(2/3)$ is the typical proportion of females in a brood (Reid, 1962; Cole et al., 1976), and $(3/2)$ is the average number of beetles emerging from each hole (Safranyik and Linton, 1985; Peterman, 1974, Fig. 13). The *Model posterior* category gives the marginal posterior of $\zeta_0 + \zeta_1 * 10$, the emergence density on a 10-inch DBH tree; 10 inches is approximately the average DBH of MPB-killed trees in the Klein et al. dataset. The *AB disk data* category contains estimates of emergence from 300 different sites across Alberta (Government of Alberta, 2016). The *Other studies* category includes estimates from a number of studies, mostly United States Forest Service reports: Tishmack et al. (2005); Negrón (2018); Reid (1963); Raffa and Berryman (1983); Rasmussen (1980); De Leon (1939); Safranyik (1988); Cole (1969); Schmid (1972); Whiteside (1937); Beal (1938); Peterman (1974); Klein et al. (1978); Safranyik and Linton (1985, 1991).

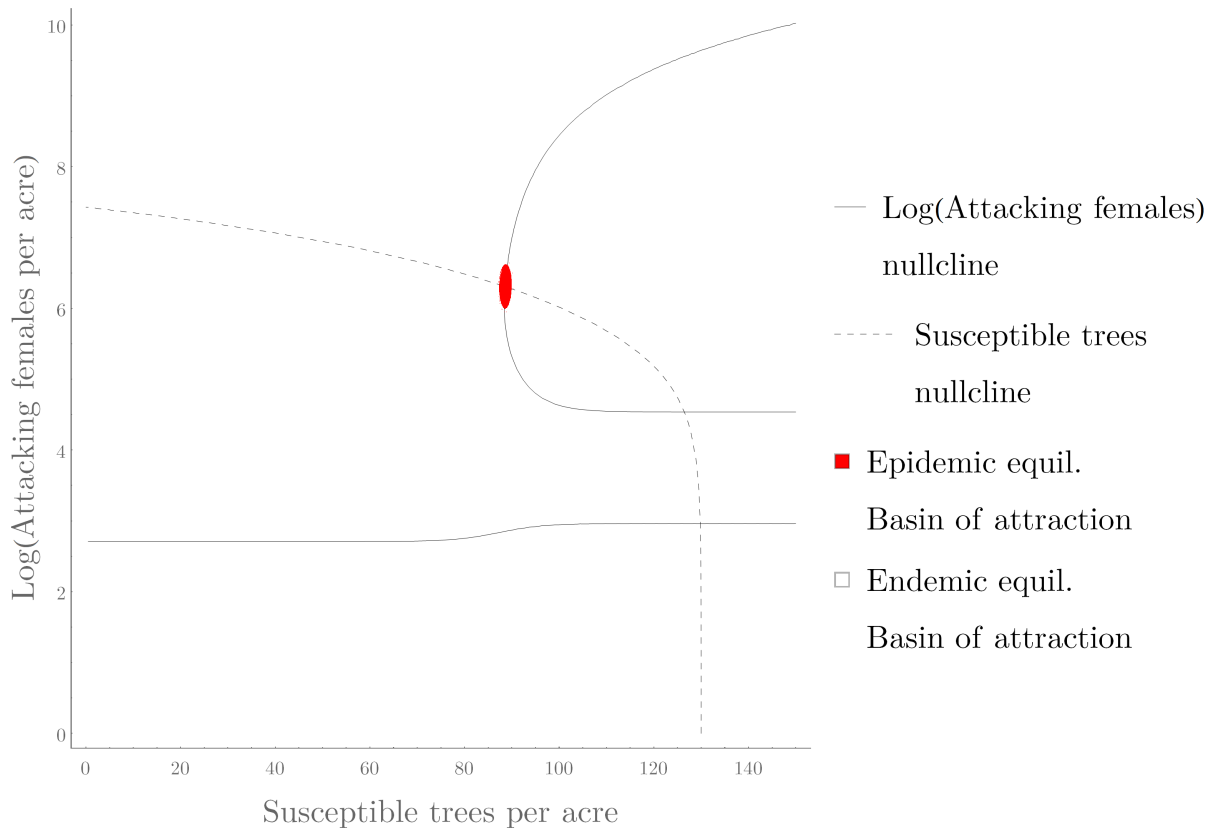


Figure E.7: The stable epidemic equilibrium (i.e., the intersection of the nullclines with the highest beetle density) has a very small basin of attraction. All other initial conditions lead to the endemic equilibrium.

References

- Alfaro, R. I., Campbell, E., Hawkes, B. C., et al. (2009). Historical frequency, intensity and extent of mountain pine beetle disturbance in british columbia. Technical report, Pacific Forestry Centre Canada.
- Alfaro, R. I., Campbell, R., Vera, P., Hawkes, B., Shore, T., et al. (2003). Dendroecological reconstruction of mountain pine beetle outbreaks in the chilcotin plateau of british columbia. In *Mountain Pine Beetle Symposium: Challenges and Solutions*, pages 245–256. Information Report BC-X-399.
- Amman, G. and Logan, J. (1998). Silvicultural control of mountain pine beetle: prescriptions and the influence of microclimate. *American Entomologist*, 44(3):166–178.
- Amman, G. D. (1969). Mountain pine beetle emergence in relation to depth of lodgepole pine bark. Technical report, United States Department of Agriculture, Forest Service, Intermountain Forest and Range Experiment Station.
- Amman, G. D. (1975). *Abandoned mountain pine beetle galleries in lodgepole pine*, volume 197. Intermountain Forest and Range Experiment Station.
- Amman, G. D. (1980). Incidence of mountain pine beetle abandoned galleries in lodgepole pine. Technical report, United States Department of Agriculture, Forest Service, Intermountain Forest and Range Experiment Station.
- Amman, G. D. (1983). Mountain pine beetle dynamics in lodgepole pine forests: Part ii.

- population dynamics. Technical report, United States Department of Agriculture, Forest Service, Intermountain Forest and Range Experiment Station.
- Amman, G. D. (1984). Mountain pine beetle (coleoptera: Scolytidae) mortality in three types of infestations. *Environmental Entomology*, 13(1):184–191.
- Amman, G. D., McGregor, M. D., and Dolph, Jr., R. E. (1985). Mountain pine beetle. Technical report, United States Department of Agriculture, Forest Service.
- Anderson, M. D. (2003). *Pinus contorta* var. *latifolia*. Fire Effects Information System, [Online]. Accessed Dec. 12, 2023.
- Anderson, R. S., Smith, S. J., Lynch, A. M., and Geils, B. W. (2010). The pollen record of a 20th century spruce beetle (*dendroctonus rufipennis*) outbreak in a colorado subalpine forest, usa. *Forest Ecology and Management*, 260(4):448–455.
- Andreassen, H. P., Sundell, J., Ecke, F., Halle, S., Haapakoski, M., Henttonen, H., Huitu, O., Jacob, J., Johnsen, K., Koskela, E., et al. (2021). Population cycles and outbreaks of small rodents: ten essential questions we still need to solve. *Oecologia*, 195:601–622.
- Antos, J. A. and Parish, R. (2002). Structure and dynamics of a nearly steady-state subalpine forest in south-central british columbia, canada. *Oecologia*, 130:126–135.
- Arango-Velez, A., El Kayal, W., Copeland, C. C., Zaharia, L. I., Lusebrink, I., and Cooke, J. E. (2016). Differences in defence responses of *pinus contorta* and *pinus banksiana* to the mountain pine beetle fungal associate *grosmannia clavigera* are affected by water deficit. *Plant, Cell & Environment*, 39(4):726–744.
- Asaro, C., Nowak, J. T., and Elledge, A. (2017). Why have southern pine beetle outbreaks declined in the southeastern us with the expansion of intensive pine silviculture? a brief review of hypotheses. *Forest Ecology and Management*, 391:338–348.
- Audley, J. P., Fettig, C. J., Munson, A. S., Runyon, J. B., Mortenson, L. A., Steed, B. E., Gibson, K. E., Jørgensen, C. L., McKelvey, S. R., McMillin, J. D., et al. (2021). Dynamics of beetle-killed snags following mountain pine beetle outbreaks in lodgepole pine forests. *Forest Ecology and Management*, 482:118870.
- author N/A (1963). Mountain pine beetle conditions forest service region 4, november 1963. Technical report, United States Department of Agriculture, Forest Service.
- Axelsson, J. N., Alfaro, R. I., and Hawkes, B. C. (2009). Influence of fire and mountain pine beetle on the dynamics of lodgepole pine stands in british columbia, canada. *Forest Ecology and Management*, 257(9):1874–1882.
- Axelsson, J. N., Alfaro, R. I., and Hawkes, B. C. (2010). Changes in stand structure in uneven-aged lodgepole pine stands impacted by mountain pine beetle epidemics and fires in central british columbia. *The Forestry Chronicle*, 86(1):87–99.
- Barclay, H., Safranyik, L., and Linton, D. (1998). Trapping mountain pine beetles *dendroctonus ponderosae* (coleoptera: Scolytidae) using pheromone-baited traps: effects of trapping distance. *Journal of the Entomological Society of British Columbia*, 95:25–32.
- Bartos, D. L. (1989). Microclimate, an alternative to tree vigor as a basis for mountain pine beetle infestations. Technical report, United States Department of Agriculture, Forest Service, Intermountain Research Station.

- Beal, J. A. (1938). Progress report of a study of the black hills beetle in southeastern wyoming and central colorado summer of 1937. Technical report, United States Department of Agriculture, Forest Service, Rocky Mountain Forest and Range Experiment Station.
- Beaudoin, A., Bernier, P., Guindon, L., Villemaire, P., Guo, X., Stinson, G., Bergeron, T., Magnussen, S., and Hall, R. (2014). Mapping attributes of canada’s forests at moderate resolution through k nn and modis imagery. *Canadian Journal of Forest Research*, 44(5):521–532.
- Bentz, B. (2019). Mountain pine beetle and great basin bristlecone pine: a complicated story. *Mountain Views*, pages 28–32.
- Bentz, B., Amman, G., and Logan, J. (1993). A critical assessment of risk classification systems for the mountain pine beetle. *Forest Ecology and Management*, 61(3-4):349–366.
- Bentz, B. and Mullins, D. (1999). Ecology of mountain pine beetle (coleoptera: Scolytidae) cold hardening in the intermountain west. *Environmental Entomology*, 28(4):577–587.
- Bentz, B. J. (1996). Localized spatial and temporal attack dynamics of the mountain pine beetle in lodgepole pine. Technical report, United States Department of Agriculture, Forest Service, Intermountain Research Station.
- Bentz, B. J., Millar, C. I., Vandygriff, J. C., and Hansen, E. M. (2022). Great basin bristlecone pine mortality: Causal factors and management implications. *Forest Ecology and Management*, 509:120099.
- Berryman, A. (1979). Dynamics of bark beetle populations: analysis of dispersal and redistribution. *Mitteilungen der Schweizerischen Entomologischen Gesellschaft*, 52(2/3):227–234.
- Berryman, A. A. (1974). Dynamics of bark beetle populations: towards a general productivity model. *Environmental Entomology*, 3(4):579–585.
- Berryman, A. A. (1976). Theoretical explanation of mountain pine beetle dynamics in lodgepole pine forests. *Environmental entomology*, 5(6):1225–1233.
- Berryman, A. A. (1978). A synoptic model of the lodgepole pine/mountain pine beetle interaction and its potential application in forest management. In *Theory and practice of mountain pine beetle management in lodgepole pine forests*, pages 95–108. United States Department of Agriculture, Forest Service.
- Berryman, A. A. (1996). What causes population cycles of forest lepidoptera? *Trends in Ecology & Evolution*, 11(1):28–32.
- Biedermann, P. H., Müller, J., Grégoire, J.-C., Gruppe, A., Hagge, J., Hammerbacher, A., Hofstetter, R. W., Kandasamy, D., Kolarik, M., Kostovcik, M., et al. (2019). Bark beetle population dynamics in the anthropocene: challenges and solutions. *Trends in ecology & evolution*, 34(10):914–924.
- Billings, R. F., Gara, R. I., and Hrutford, B. F. (1976). Influence of ponderosa pine resin volatiles on the response of dendroctonus ponderosae to synthetic trans-verbenol. *Environmental Entomology*, 5(1):171–179.
- Birgersson, G., Schlyter, F., Löfqvist, J., and Bergström, G. (1984). Quantitative variation of pheromone components in the spruce bark beetle ips typographus from different attack phases. *Journal of Chemical Ecology*, 10:1029–1055.

- Björklund, N. and Lindgren, B. S. (2009). Diameter of lodgepole pine and mortality caused by the mountain pine beetle: factors that influence their relationship and applicability for susceptibility rating. *Canadian journal of forest research*, 39(5):908–916.
- Bjørnstad, O. N., Nisbet, R. M., and Fromentin, J.-M. (2004). Trends and cohort resonant effects in age-structured populations. *Journal of animal ecology*, pages 1157–1167.
- Blackard, J., Finco, M., Helmer, E., Holden, G., Hoppus, M., Jacobs, D., Lister, A., Moisen, G., Nelson, M., Riemann, R., et al. (2008). Mapping us forest biomass using nationwide forest inventory data and moderate resolution information. *Remote sensing of Environment*, 112(4):1658–1677.
- Blackman, M. W. (1931). The black hills beetle. Technical report, Syracuse University, New York State College of Forestry.
- Bleiker, K. and Six, D. (2007). Dietary benefits of fungal associates to an eruptive herbivore: potential implications of multiple associates on host population dynamics. *Environmental Entomology*, 36(6):1384–1396.
- Bleiker, K. and Van Hezewijk, B. (2016). Flight period of mountain pine beetle (coleoptera: Curculionidae) in its recently expanded range. *Environmental Entomology*, 45(6):1561–1567.
- Bleiker, K. P. (2019). Risk assessment of the threat of mountain pine beetle to canada’s boreal and eastern pine resources. Technical report, Pacific Forestry Centre Canada.
- Bleiker, K. P., Ethier, C. A., and Van Hezewijk, B. H. (2023). Suitability of a historical, novel, and occasional host for mountain pine beetle (coleoptera: Curculionidae). *Forests*, 14(5):989.
- Bleiker, K. P., O’Brien, M. R., Smith, G. D., and Carroll, A. L. (2014). Characterisation of attacks made by the mountain pine beetle (coleoptera: Curculionidae) during its endemic population phase. *The Canadian Entomologist*, 146(3):271–284.
- Bone, C. and Altaweel, M. (2014). Modeling micro-scale ecological processes and emergent patterns of mountain pine beetle epidemics. *Ecological modelling*, 289:45–58.
- Boone, C. K., Aukema, B. H., Bohlmann, J., Carroll, A. L., and Raffa, K. F. (2011). Efficacy of tree defense physiology varies with bark beetle population density: a basis for positive feedback in eruptive species. *Canadian Journal of Forest Research*, 41(6):1174–1188.
- Breshears, D. D., Cobb, N. S., Rich, P. M., Price, K. P., Allen, C. D., Balice, R. G., Romme, W. H., Kastens, J. H., Floyd, M. L., Belnap, J., et al. (2005). Regional vegetation die-off in response to global-change-type drought. *Proceedings of the National Academy of Sciences*, 102(42):15144–15148.
- Briggs, C. J. and Hoopes, M. F. (2004). Stabilizing effects in spatial parasitoid–host and predator–prey models: a review. *Theoretical population biology*, 65(3):299–315.
- British Columbia Government (2016). Provincial-level projection of the current mountain pine beetle outbreak: Current projection results (year 13). Technical report, British Columbia Ministry of Forests Lands and Natural Resource Operations.
- British Columbia Government (n.d.). Spruce beetle management in british columbia. <https://www2.gov.bc.ca/gov/content/industry/forestry/managing-our-forest-resources/forest-health/forest-pests/bark-beetles/spruce-beetle>. Accessed: 2024-09-24.
- Brush, M. and Lewis, M. A. (2023). Coupling mountain pine beetle and forest population dynamics predicts transient outbreaks that are likely to increase in number with climate change. *Bulletin of Mathematical Biology*, 85(11):108.

- Brush, M. and Lewis, M. A. (2024). Eruptive insect outbreaks from endemic populations under climate change. *bioRxiv*, pages 2024–06.
- Buonanduci, M. S., Morris, J. E., Agne, M. C., Battaglia, M. A., and Harvey, B. J. (2023). Fine-scale spatial heterogeneity shapes compensatory responses of a subalpine forest to severe bark beetle outbreak. *Landscape Ecology*, 38(1):253–270.
- Burnell, D. (1977). A dispersal-aggregation model for mountain pine beetle in lodgepole pine stands. *Researches on Population Ecology*, 19:99–106.
- Burton, P. J. (2010). Striving for sustainability and resilience in the face of unprecedented change: the case of the mountain pine beetle outbreak in british columbia. *Sustainability*, 2(8):2403–2423.
- Carroll, A., Régnière, J., Logan, J., Taylor, S., Bentz, B., and Powell, J. (2006a). Impacts of climate change on range expansion by the mountain pine beetle. Technical report, Pacific Forestry Centre Canada.
- Carroll, A. L., Aukema, B., Raffa, K., Linton, D., Smith, G. D., and Lindgren, B. (2006b). Mountain pine beetle outbreak development: the endemic—incipient epidemic transition. Mpmi project # 1.03, Natural Resources Canada, Canadian Forest Service.
- Carroll, A. L., Safranyik, L., et al. (2003). The bionomics of the mountain pine beetle in lodgepole pine forests: establishing a context. In *Mountain pine beetle symposium: Challenges and solutions*, pages 21–32. Citeseer.
- Carroll, A. L., Shore, T. L., Safranyik, L., et al. (2006c). Direct control: theory and practice. In Safranyik, L. and Wilson, B., editors, *Detection, mapping, and monitoring of the mountain pine beetle*, pages 155–172. Natural Resources Canada, Canadian Forest Service, Pacific Forestry Centre.
- Cerezke, H. F. (1989). Mountain pine beetle aggregation semiochemical use in alberta and saskatchewan, 1983–1987. In Amman, G. D., editor, *Proceedings—Symposium on Management of Lodgepole Pine to Minimize Losses to the Mountain Pine Beetle, General Technical Report INT-262*, Kalispell, Montana. United States Department of Agriculture, Forest Service, Ogden, Utah.
- Chiu, C. C., Keeling, C. I., and Bohlmann, J. (2018). Monoterpenyl esters in juvenile mountain pine beetle and sex-specific release of the aggregation pheromone trans-verbenol. *Proceedings of the National Academy of Sciences*, 115(14):3652–3657.
- Chojnacky, D. C., Bentz, B. J., and Logan, J. A. (2000). Mountain pine beetle attack in ponderosa pine: Comparing methods for rating susceptibility. Technical report, United States Department of Agriculture, Forest Service, Rocky Mountain Research Station.
- Cole, H. M., Andrus, R. A., Butkiewicz, C., Rodman, K. C., Santiago, O., Tutland, N. J., Waupoichick, A., and Hart, S. J. (2022). Outbreaks of douglas-fir beetle follow western spruce budworm defoliation in the southern rocky mountains, usa. *Forests*, 13(3):371.
- Cole, W. E. (1969). Mountain pine beetle infestations in relation to lodgepole pine diameters. Technical report, United States Department of Agriculture, Forest Service, Intermountain Forest and Range Experiment Station.
- Cole, W. E., Amman, G. D., and Jensen, C. E. (1976). Mathematical models for the mountain pine beetle–lodgepole pine interaction. *Environmental Entomology*, 5(1):11–19.

- Corbett, L. J., Withey, P., Lantz, V., and Ochuodho, T. (2016). The economic impact of the mountain pine beetle infestation in british columbia: provincial estimates from a cge analysis. *Forestry: An International Journal of Forest Research*, 89(1):100–105.
- Coulson, R. N., Amman, G. D., Dahlsten, D. L., DeMars Jr, C., and Stephen, F. (1985). Forest-bark beetle interactions: bark beetle population dynamics. *Integrated Pest Management in Pine-Bark Beetle Ecosystems*, pages 61–80.
- Creeden, E. P., Hicke, J. A., and Buotte, P. C. (2014). Climate, weather, and recent mountain pine beetle outbreaks in the western united states. *Forest Ecology and Management*, 312:239–251.
- Crowley, P. H. (1981). Dispersal and the stability of predator-prey interactions. *The American Naturalist*, 118(5):673–701.
- Cudmore, T. J. et al. (2009). *Geographic variation in the effect of lodgepole pine characteristics on mountain pine beetle attacks and productivity in British Columbia*. University of Northern British Columbia.
- Cunningham, C. A., Jenkins, M. J., and Roberts, D. W. (2005). Attack and brood production by the douglas-fir beetle (coleoptera: Scolytidae) in douglas-fir, *pseudotsuga menziesii* var. *glauca* (pinaceae), following a wildfire. *Western North American Naturalist*, pages 70–79.
- de la Giroday, H.-M. C., Carroll, A. L., Lindgren, B. S., and Aukema, B. H. (2011). Incoming! association of landscape features with dispersing mountain pine beetle populations during a range expansion event in western canada. *Landscape Ecology*, 26:1097–1110.
- De Leon, D. (1939). The biology and control of the black hills beetle (*dendroctonus ponderosae* hopk.) summary of studies in colorado and wyoming 1935-1938. Technical report, United States Department of Agriculture, Forest Service.
- De Roos, A., Metz, J., Evers, E., and Leipoldt, A. (1990). A size dependent predator-prey interaction: who pursues whom? *Journal of Mathematical Biology*, 28:609–643.
- Deneubourg, J. L., Grégoire, J. C., and Le Fort, E. (1990). Kinetics of larval gregarious behavior in the bark beetle *dendroctonus micans* (coleoptera: Scolytidae). *Journal of Insect Behavior*, 3:169–182.
- Dodds, K. J. and Ross, D. W. (2002). Sampling range and range of attraction of *dendroctonus pseudotsugae* pheromone-baited traps. *The Canadian Entomologist*, 134(3):343–355.
- Duncan, J. P., Powell, J. A., Gordillo, L. F., and Eason, J. (2015). A model for mountain pine beetle outbreaks in an age-structured forest: Predicting severity and outbreak-recovery cycle period. *Bulletin of mathematical biology*, 77:1256–1284.
- Dymond, C. C., Tedder, S., Spittlehouse, D. L., Raymer, B., Hopkins, K., McCallion, K., and Sandland, J. (2014). Diversifying managed forests to increase resilience. *Canadian Journal of Forest Research*, 44(10):1196–1205.
- Ellenwood, J. R., Krist, F. J. J., and Romero, S. A. (2015). *National Individual Tree Species Atlas*. United States Department of Agriculture, Forest Service, United States.
- Ellner, S. and Turchin, P. (1995). Chaos in a noisy world: new methods and evidence from time-series analysis. *The American Naturalist*, 145(3):343–375.
- Evenden, J. C. and Gibson, A. L. (1940). A destructive infestation in lodgepole pine stands by the mountain pine beetle. *Journal of Forestry*, 38(3):271–275.

- Fettig, C. J., Asaro, C., Nowak, J. T., Dodds, K. J., Gandhi, K. J., Moan, J. E., and Robert, J. (2022). Trends in bark beetle impacts in north america during a period (2000–2020) of rapid environmental change. *Journal of Forestry*, 120(6):693–713.
- Forest Health Protection (2011). Spruce beetle. Technical report, USDA Forest Service. https://www.fs.usda.gov/Internet/FSE_DOCUMENTS/stelprdb5303039.pdf.
- Freund, J. A., Mieruch, S., Scholze, B., Wiltshire, K., and Feudel, U. (2006). Bloom dynamics in a seasonally forced phytoplankton–zooplankton model: trigger mechanisms and timing effects. *Ecological complexity*, 3(2):129–139.
- Fryer, J. L. (2018). *Pinus ponderosa* var. *benthamiana*, p. p. var. *ponderosa*: Ponderosa pine. Fire Effects Information System, [Online]. Accessed Dec. 12, 2023.
- Fuchs, M. and Borden, J. (1985). Pre-emergence insecticide applications for control of the mountain pine beetle, *dendroctonus ponderosae* (coleoptera: Scolytidae). *Journal of the Entomological Society of British Columbia*, 82:25–28.
- Gelman, A., Carlin, J. B., Stern, H. S., Dunson, D. B., Vehtari, A., and Rubin, D. B. (2014). *Bayesian data analysis*. Chapman and Hall/CRC, 3rd edition.
- Gelman, A. and Hill, J. (2007). *Data analysis using regression and multilevel/hierarchical models*. Cambridge University Press New York, NY, USA, 1st edition.
- Gibson, K. E. and Bennett, D. D. (1978). Damage assessment of a mountain pine beetle infestation, targhee national forest, idaho. Technical report, United States Department of Agriculture, Forest Service.
- Gibson, K. E., McGregor, M. D., and Bennett, D. D. (1979). An evaluation of a developing mountain pine beetle infestation in centennial valley, montana, 1979. Technical report, United States Department of Agriculture, Forest Service.
- Glibert, P. M., Berdalet, E., Burford, M. A., Pitcher, G. C., and Zhou, M. (2018). *Global ecology and oceanography of harmful algal blooms*. Springer.
- Goodsman, D., Cooke, B., and Lewis, M. (2017). Positive and negative density-dependence and boom-bust dynamics in enemy-victim populations: a mountain pine beetle case study. *Theoretical Ecology*, 10(2):255–267.
- Goodsman, D. W., Grosklos, G., Aukema, B. H., Whitehouse, C., Bleiker, K. P., McDowell, N. G., Middleton, R. S., and Xu, C. (2018). The effect of warmer winters on the demography of an outbreak insect is hidden by intraspecific competition. *Global Change Biology*, 24(8):3620–3628.
- Goodsman, D. W., Koch, D., Whitehouse, C., Evenden, M. L., Cooke, B. J., and Lewis, M. A. (2016). Aggregation and a strongallee effect in a cooperative outbreak insect. *Ecological Applications*, 26(8):2623–2636.
- Government of Alberta (2016). Mountain pine beetle detection and management in alberta. Technical report, Government of Alberta, Agriculture and Forestry. Accessed: 2024-09-05.
- Gray, B., Billings, R., Gara, R., and Johnsey, R. (1972). On the emergence and initial flight behaviour of the mountain pine beetle, *dendroctonus ponderosae*, in eastern washington 1. *Zeitschrift für Angewandte Entomologie*, 71(1-4):250–259.
- Grégoire, J.-C. (1988). The greater european spruce beetle. In *Dynamics of forest insect populations: patterns, causes, implications*, pages 455–478. Springer.

- Hamel, D. R., McGregor, M. D., and Bert, M. J. (1975). Status of mountain pine beetle infestations, yellowstone national park, wyoming, 1974. Technical report, United States Department of Agriculture, Forest Service.
- Hansen, E. M. (2014). Forest development and carbon dynamics after mountain pine beetle outbreaks. *Forest Science*, 60(3):476–488.
- Hassell, M. P., Lawton, J. H., and May, R. (1976). Patterns of dynamical behaviour in single-species populations. *The Journal of Animal Ecology*, pages 471–486.
- Hastings, A., Abbott, K. C., Cuddington, K., Francis, T., Gellner, G., Lai, Y.-C., Morozov, A., Petrovskii, S., Scranton, K., and Zeeman, M. L. (2018). Transient phenomena in ecology. *Science*, 361(6406):eaat6412.
- Hastings, A., Abbott, K. C., Cuddington, K., Francis, T. B., Lai, Y.-C., Morozov, A., Petrovskii, S., and Zeeman, M. L. (2021). Effects of stochasticity on the length and behaviour of ecological transients. *Journal of the Royal Society Interface*, 18(180):20210257.
- Heath, R. and Alfaro, R. I. (1990). Growth response in a douglas-fir/lodgepole pine stand after thinning of lodgepole pine by the mountain pine beetle: a case study. *Journal of the Entomological Society of British Columbia*, 87:16–21.
- Heavilin, J., Powell, J., and Logan, J. A. (2007). Dynamics of mountain pine beetle outbreaks. *Plant disturbance ecology: The process and the response*, pages 527–533.
- Hidalgo, H. G. (2004). Climate precursors of multidecadal drought variability in the western united states. *Water Resources Research*, 40(12).
- Hiratsuka, Y., Cerezke, H. F., Moody, B. H., Petty, J., and Still, G. N. (1982). Forest insect and disease conditions in alberta, saskatchewan, manitoba, and the northwest territories in 1981 and predictions for 1982. Information Report NOR-X-239, Natural Resources Canada, Canadian Forest Service, Edmonton, Alberta.
- Hodge, J., Cooke, B., and McIntosh, R. (2017). A strategic approach to slow the spread of mountain pine beetle across canada. Technical report, Forest Pest Working Group of the Canadian Council of Forest Ministers.
- Hodgkin, A. L. and Huxley, A. F. (1952). A quantitative description of membrane current and its application to conduction and excitation in nerve. *The Journal of physiology*, 117(4):500.
- Holling, C. S. (1959). The components of predation as revealed by a study of small-mammal predation of the european pine sawfly¹. *The canadian entomologist*, 91(5):293–320.
- Holt, R. D. (2008). Theoretical perspectives on resource pulses. *Ecology*, 89(3):671–681.
- Homicz, C. S., Fettig, C. J., Munson, A. S., and Cluck, D. R. (2022). Forest insect and disease leaflet 1. Forest Insect and Disease Leaflet 1, USDA Forest Service.
- Hood, S. and Bentz, B. (2007). Predicting postfire douglas-fir beetle attacks and tree mortality in the northern rocky mountains. *Canadian Journal of Forest Research*, 37(6):1058–1069.
- Hopping, G. R. and Beall, G. (1948). The relation of diameter of lodgepole pine to incidence of attack by the bark beetle *dendroctonus monticolae* hopkins. *The Forestry Chronicle*, 24(2):141–145.
- Howe, M., Carroll, A., Gratton, C., and Raffa, K. F. (2021). Climate-induced outbreaks in high-elevation pines are driven primarily by immigration of bark beetles from historical hosts. *Global Change Biology*, 27(22):5786–5805.

- Howe, M., Peng, L., and Carroll, A. (2022a). Landscape predictions of western balsam bark beetle activity implicate warm temperatures, a longer growing season, and drought in widespread irruptions across british columbia. *Forest Ecology and Management*, 508:120047.
- Howe, M., Raffa, K. F., Aukema, B. H., Gratton, C., and Carroll, A. L. (2022b). Numbers matter: how irruptive bark beetles initiate transition to self-sustaining behavior during landscape-altering outbreaks. *Oecologia*, 198(3):681–698.
- Huang, S. (1999). Ecoregion-based individual tree height-diameter models for lodgepole pine in alberta. *Western Journal of Applied Forestry*, 14(4):186–193.
- Huber, D. P., Aukema, B. H., Hodgkinson, R. S., and Lindgren, B. S. (2009). Successful colonization, reproduction, and new generation emergence in live interior hybrid spruce picea engelmannii × glauca by mountain pine beetle dendroctonus ponderosae. *Agricultural and Forest Entomology*, 11(1):83–89.
- Huppert, A., Blasius, B., and Stone, L. (2002). A model of phytoplankton blooms. *The American Naturalist*, 159(2):156–171.
- Huppert, A., Olinky, R., and Stone, L. (2004). Bottom-up excitable models of phytoplankton blooms. *Bulletin of Mathematical Biology*, 66:865–878.
- Hynum, B. G. and Berryman, A. A. (1980). Dendroctonus ponderosae (coleoptera: Scolytidae): Pre-aggregation landing and gallery initiation on lodgepole pine1. *The Canadian Entomologist*, 112(2):185–191.
- Jackson, P. L., Straussfogel, D., Lindgren, B. S., Mitchell, S., and Murphy, B. (2008). Radar observation and aerial capture of mountain pine beetle, dendroctonus ponderosae hopk.(coleoptera: Scolytidae) in flight above the forest canopy. *Canadian Journal of Forest Research*, 38(8):2313–2327.
- Jarvis, D. S. and Kulakowski, D. (2015). Long-term history and synchrony of mountain pine beetle outbreaks in lodgepole pine forests. *Journal of Biogeography*, 42(6):1029–1039.
- Johns, R., Flaherty, L., Carleton, D., Edwards, S., Morrison, A., and Owens, E. (2016). Population studies of tree-defoliating insects in canada: a century in review. *The Canadian Entomologist*, 148(S1):S58–S81.
- Johnson, D. M., Liebhold, A. M., Tobin, P. C., and Bjørnstad, O. N. (2006). Allee effects and pulsed invasion by the gypsy moth. *Nature*, 444(7117):361–363.
- Johnston, D. and Wu, S. M.-s. (1994). *Foundations of Cellular Neurophysiology*. MIT Press.
- Jones, K. (2019). *Influence of semiochemical cues on mountain pine beetle flight and subsequent effect of flight on host colonisation processes*. PhD thesis, University of Alberta.
- Jones, K. L., Rajabzadeh, R., Ishangulyyeva, G., Erbilgin, N., and Evenden, M. L. (2020). Mechanisms and consequences of flight polyphenisms in an outbreaking bark beetle species. *Journal of Experimental Biology*, 223(12):jeb219642.
- Kärve, S. and Schroeder, L. M. (2010). A comparison of outbreak dynamics of the spruce bark beetle in sweden and the mountain pine beetle in canada (curculionidae: Scolytinae). *Entomologisk tidskrift*, 131(3):215–224.
- Kautz, M., Imron, M. A., Dworschak, K., and Schopf, R. (2016). Dispersal variability and associated population-level consequences in tree-killing bark beetles. *Movement ecology*, 4:1–12.

- Klein, W. H., Parker, D. L., and Jensen, C. E. (1978). Attack, emergence, and stand depletion trends of the mountain pine beetle in a lodgepole pine stand during an outbreak. *Environmental Entomology*, 7(5):732–737.
- Kluttsch, J. G., Negrón, J. F., Costello, S. L., Rhoades, C. C., West, D. R., Popp, J., and Caissie, R. (2009). Stand characteristics and downed woody debris accumulations associated with a mountain pine beetle (*Dendroctonus ponderosae* Hopkins) outbreak in Colorado. *Forest Ecology and Management*, 258(5):641–649.
- Knight, F. B. (1959). Measuring trends of black hills beetle infestations. Technical report, United States Department of Agriculture, Forest Service.
- Koch, D., Lewis, M. A., and Lele, S. (2021). The signature of endemic populations in the spread of mountain pine beetle outbreaks. *Bulletin of Mathematical Biology*, 83(6):65.
- Kolb, T. E., Fettig, C. J., Ayres, M. P., Bentz, B. J., Hicke, J. A., Mathiasen, R., Stewart, J. E., and Weed, A. S. (2016). Observed and anticipated impacts of drought on forest insects and diseases in the United States. *Forest Ecology and Management*, 380:321–334.
- Koontz, M. J., Latimer, A. M., Mortenson, L. A., Fettig, C. J., and North, M. P. (2021). Cross-scale interaction of host tree size and climatic water deficit governs bark beetle-induced tree mortality. *Nature Communications*, 12(1):129.
- Koricheva, J., Klapwijk, M. J., and Björkman, C. (2012). Life history traits and host plant use in defoliators and bark beetles: implications for population dynamics. In Barbosa, P., Letourneau, D. K., and Agrawal, A. A., editors, *Insect outbreaks revisited*, pages 175–196. Wiley Online Library.
- Kozlov, M. V., Hunter, M. D., Koponen, S., Kouki, J., Niemelä, P., and Price, P. W. (2010). Diverse population trajectories among coexisting species of subarctic forest moths. *Population Ecology*, 52:295–305.
- Křivan, V., Lewis, M., Bentz, B. J., Bewick, S., Lenhart, S. M., and Liebhold, A. (2016). A dynamical model for bark beetle outbreaks. *Journal of Theoretical Biology*, 407:25–37.
- Kurz, W. A., Dymond, C., Stinson, G., Rampley, G., Neilson, E., Carroll, A., Ebata, T., and Safranyik, L. (2008). Mountain pine beetle and forest carbon feedback to climate change. *Nature*, 452(7190):987–990.
- Lantschner, M. V. and Corley, J. C. (2023). Spatiotemporal outbreak dynamics of bark and wood-boring insects. *Current Opinion in Insect Science*, 55:101003.
- Latty, T. M. (2007). *Pioneer behaviour in mountain pine beetles (Dendroctonus ponderosae)*. PhD thesis, University of Calgary.
- Lewis, D. (1979). Counterfactual Dependence and Time’s Arrow. *Noûs*, 13(4):455.
- Lewis, K. J. and Hartley, I. D. (2006). Rate of deterioration, degrade, and fall of trees killed by mountain pine beetle. *Journal of Ecosystems and Management*, 7(2).
- Lewis, M. A., Nelson, W., and Xu, C. (2010). A structured threshold model for mountain pine beetle outbreak. *Bulletin of mathematical biology*, 72:565–589.
- Logan, J., Bolstad, P., Bentz, B., and Perkins, D. (1995). Assessing the effects of changing climate on mountain pine beetle dynamics. In *Interior west global change workshop. General Technical Report RM-262*, pages 92–105. United States Department of Agriculture, Forest Service.

- Logan, J. A. and Powell, J. A. (2001). Ghost forests, global warming, and the mountain pine beetle (coleoptera: Scolytidae). *American Entomologist*, 47(3):160–173.
- Logan, J. A., White, P., Bentz, B. J., and Powell, J. A. (1998). Model analysis of spatial patterns in mountain pine beetle outbreaks. *Theoretical Population Biology*, 53(3):236–255.
- Lotan, J. E., Brown, J. K., and Neuenschwander, L. F. (1985). Role of fire in lodgepole pine forests. *Lodgepole pine: the species and its management. Cooperative Extension Service, Washington State University, Pullman*, pages 133–152.
- Louca, S. and Doebeli, M. (2015). Detecting cyclicity in ecological time series. *Ecology*, 96(6):1724–1732.
- Ludwig, D., Jones, D. D., Holling, C. S., et al. (1978). Qualitative analysis of insect outbreak systems: the spruce budworm and forest. *Journal of animal ecology*, 47(1):315–332.
- Lund, J. (1950). Studies on asterionella formosa hass: Ii. nutrient depletion and the spring maximum. *The Journal of Ecology*, pages 15–35.
- Maclauchlan, L. (2016). Quantification of dryocoetes confusus-caused mortality in subalpine fir forests of southern british columbia. *Forest Ecology and Management*, 359:210–220.
- Maclauchlan, L. E., Harder, L., Borden, J. H., and Brooks, J. E. (2003). Impact of the western balsam bark beetle, dryocoetes confusus swaine (coleoptera: Scolytidae), at the sicamous creek research site, and the potential for semiochemical based management in alternative silviculture systems. *Journal of the Entomological Society of British Columbia*, 100:27–41.
- Maclauchlan, L. E., Stock, A. J., and Brooks, J. E. (2023). Infestation phases and impacts of dryocoetes confusus in subalpine fir forests of southern british columbia. *Forests*, 14(2):363.
- MacQuarrie, C. J. and Cooke, B. J. (2011). Density-dependent population dynamics of mountain pine beetle in thinned and unthinned stands. *Canadian journal of forest research*, 41(5):1031–1046.
- Mantua, N. J. and Hare, S. R. (2002). The pacific decadal oscillation. *Journal of oceanography*, 58:35–44.
- Massey, C. L. and Wygant, N. D. (1954). Biology and control of the engelmann spruce beetle in colorado. Technical report, US Department of Agriculture, Forest Service, Washington DC.
- Mata, S. (2003). Growth of lodgepole pine stands and its relation to mountain pine beetle susceptibility. Technical report, United States Department of Agriculture, Forest Service, Rocky Mountain Research Station.
- Mawby, W., Hain, F., and Doggett, C. (1989). Endemic and epidemic populations of southern pine beetle: Implications of the two-phase model for forest managers. *Forest Science*, 35(4):1075–1087.
- McCabe, G. J., Palecki, M. A., and Betancourt, J. L. (2004). Pacific and atlantic ocean influences on multidecadal drought frequency in the united states. *Proceedings of the National Academy of Sciences*, 101(12):4136–4141.
- McCambridge, W. (1971). Temperature limits of flight of the mountain pine beetle, dendroctonus ponderosae. *Annals of the Entomological Society of America*, 64(2):534–535.
- Mccambridge, W. F. (1967). Nature of induced attacks by the black hills beetle, dendroctonus ponderosae (coleoptera: Scolytidae). *Annals of the Entomological Society of America*, 60(5):920–928.

- McGregor, M. D. (1973). Status of mountain pine beetle, gallatin district, gallatin national forest, 1973. Technical report, United States Department of Agriculture, Forest Service.
- McLane, S. C., Daniels, L. D., and Aitken, S. N. (2011). Climate impacts on lodgepole pine (*pinus contorta*) radial growth in a provenance experiment. *Forest Ecology and Management*, 262(2):115–123.
- McMillin, J. D., Allen, K. K., Long, D. F., Harris, J. L., and Negrón, J. F. (2003). Effects of western balsam bark beetle on spruce-fir forests of north-central wyoming. *Western Journal of Applied Forestry*, 18(4):259–266.
- Meddens, A. J., Hicke, J. A., and Ferguson, C. A. (2012). Spatiotemporal patterns of observed bark beetle-caused tree mortality in british columbia and the western united states. *Ecological Applications*, 22(7):1876–1891.
- Meddens, A. J., Hicke, J. A., and Vierling, L. A. (2011). Evaluating the potential of multi-spectral imagery to map multiple stages of tree mortality. *Remote Sensing of Environment*, 115(7):1632–1642.
- Mitchell, R. G. and Preisler, H. K. (1991). Analysis of spatial patterns of lodgepole pine attacked by outbreak populations of the mountain pine beetle. *Forest Science*, 37(5):1390–1408.
- Moeck, H. A. and Simmons, C. S. (1991). Primary attraction of mountain pine beetle, *dendroctonus ponderosae* hopk.(coleoptera: Scolytidae), to bolts of lodgepole pine. *The Canadian Entomologist*, 123(2):299–304.
- Molnar, A. (1965). Pathogenic fungi associated with a bark beetle on alpine fir. *Canadian Journal of Botany*, 43(5):563–570.
- Morozov, A. and Petrovskii, S. (2009). Excitable population dynamics, biological control failure, and spatiotemporal pattern formation in a model ecosystem. *Bulletin of Mathematical Biology*, 71:863–887.
- Morris, J. E., Buonanduci, M. S., Agne, M. C., Battaglia, M. A., and Harvey, B. J. (2022). Does the legacy of historical thinning treatments foster resilience to bark beetle outbreaks in subalpine forests? *Ecological Applications*, 32(1):e02474.
- Murdoch, W. W., Briggs, C. J., and Nisbet, R. M. (2003). *Consumer–Resource Dynamics*. Princeton University Press.
- Murray, J. D. (1989). *Mathematical Biology*. Springer-Verlag.
- Negrón, J. F. (2018). Biological aspects of mountain pine beetle in lodgepole pine stands of different densities in colorado, usa. *Forests*, 10(1):18.
- Negrón, J. F. (2020). Within-stand distribution of tree mortality caused by mountain pine beetle, *dendroctonus ponderosae* hopkins. *Insects*, 11(2):112.
- Negrón, J. F., Allen, K. K., Ambourn, A., Cook, B., and Marchand, K. (2017). Large-scale thinnings, ponderosa pine, and mountain pine beetle in the black hills, usa. *Forest Science*, 63(5):529–536.
- Negrón, J. F. and Huckaby, L. (2020). Reconstructing historical outbreaks of mountain pine beetle in lodgepole pine forests in the colorado front range. *Forest ecology and management*, 473:118270.

- Negron, J. F. and Klutsch, J. G. (2017). Probability of infestation and extent of mortality models for mountain pine beetle in lodgepole pine forests in colorado. Research Note RMRS-RN-77, U.S. Department of Agriculture, Forest Service, Rocky Mountain Research Station, Fort Collins, CO.
- Negrón, J. F., Lynch, A. M., Schaupp Jr, W. C., and Mercado, J. E. (2014). Douglas-fir tussock moth-and douglas-fir beetle-caused mortality in a ponderosa pine/douglas-fir forest in the colorado front range, usa. *Forests*, 5(12):3131–3146.
- Negron, J. F., Schaupp Jr, W. C., Gibson, K. E., Anhold, J., Hansen, D., Their, R., and Mocettini, P. (1999). Estimating extent of mortality associated with the douglas-fir beetle in the central and northern rockies. *Western Journal of Applied Forestry*, 14(3):121–127.
- Negron, J. F., Wilson, J. L., and Anhold, J. A. (2000). Stand conditions associated with round-headed pine beetle (coleoptera: Scolytidae) infestations in arizona and utah. *Environmental Entomology*, 29(1):20–27.
- Negrón, J. F. (2008). Roundheaded pine beetle, *Dendroctonus adjunctus* blandford (coleoptera: Curculionidae, scolytinae). In Capinera, J. L., editor, *Encyclopedia of Entomology*. Springer, Dordrecht.
- Nelson, K. N. (2009). *The effect of mountain pine beetle caused mortality on subalpine forest stand and landscape structure in Rocky Mountain National Park, CO*. PhD thesis, Colorado State University.
- Nigh, G. D., Antos, J. A., and Parish, R. (2008). Density and distribution of advance regeneration in mountain pine beetle killed lodgepole pine stands of the montane spruce zone of southern british columbia. *Canadian Journal of Forest Research*, 38(11):2826–2836.
- North Carolina Forest Service (n.d.). Southern pine beetle prevention cost-share program. https://www.ncforestservice.gov/forest_health/pdf/SouthernPineBeetle.pdf. Accessed: 2024-09-24.
- Nothnagle, P. J. and Schultz, J. C. (1987). What is a forest pest? In Barbosa, P. and Schultz, J. C., editors, *Insect Outbreaks*, pages 59–79. Academic Press, San Diego.
- Parker, D. L. (1973). Trend of a mountain pine beetle outbreak. *Journal of Forestry*, 71(11):698–700.
- Parker, D. L. (1979). Mountain pine beetle infestation characteristics in ponderosa pine, kaibab plateau, arizona, 1975-1977. Technical report, United States Department of Agriculture, Forest Service, Rocky Mountain Forest and Range Experiment Station.
- Pearsall, W. (1932). Phytoplankton in the english lakes: Ii. the composition of the phytoplankton in relation to dissolved substances. *The Journal of Ecology*, pages 241–262.
- Peterman, R. M. (1974). *Some aspects of the population dynamics of the mountain pine beetle, Dendroctonus ponderosae in lodgepole pine forests of British Columbia*. PhD thesis, University of British Columbia.
- Pfeifer, E. M., Hicke, J. A., and Meddens, A. J. (2011). Observations and modeling of above-ground tree carbon stocks and fluxes following a bark beetle outbreak in the western united states. *Global Change Biology*, 17(1):339–350.
- Pope, D., Coulson, R., Fargo, W., Gagne, J., and Kelly, C. (1980). The allocation process and between-tree survival probabilities in dendroctonus frontalis infestations. *Researches on population Ecology*, 22:197–210.

- Powell, J. A. and Bentz, B. J. (2009). Connecting phenological predictions with population growth rates for mountain pine beetle, an outbreak insect. *Landscape Ecology*, 24:657–672.
- Powell, J. A. and Bentz, B. J. (2014). Phenology and density-dependent dispersal predict patterns of mountain pine beetle (*dendroctonus ponderosae*) impact. *Ecological Modelling*, 273:173–185.
- Powell, J. A., Garlick, M. J., Bentz, B. J., and Friedenber, N. (2018). Differential dispersal and the allee effect create power-law behaviour: Distribution of spot infestations during mountain pine beetle outbreaks. *Journal of Animal Ecology*, 87(1):73–86.
- Preisler, H. K. and Mitchell, R. G. (1993). Colonization patterns of the mountain pine beetle in thinned and unthinned lodgepole pine stands. *Forest Science*, 39(3):528–545.
- Pureswaran, D. S., Gries, R., Borden, J. H., and Pierce, Jr, H. D. (2000). Dynamics of pheromone production and communication in the mountain pine beetle, *dendroctonus ponderosae* hopkins, and the pine engraver, *ips pini* (say)(coleoptera: Scolytidae). *Chemoecology*, 10:153–168.
- Pureswaran, D. S., Johns, R., Heard, S. B., and Quiring, D. (2016). Paradigms in eastern spruce budworm (lepidoptera: Tortricidae) population ecology: a century of debate. *Environmental Entomology*, 45(6):1333–1342.
- Raffa, K. and Berryman, A. (1982). Gustatory cues in the orientation of *dendroctonus ponderosae* (coleoptera: Scolytidae) to host trees1. *The Canadian Entomologist*, 114(2):97–104.
- Raffa, K. and Berryman, A. (1983). The role of host plant resistance in the colonization behavior and ecology of bark beetles (coleoptera: Scolytidae). *Ecological monographs*, 53(1):27–49.
- Raffa, K. F. (1988). Host orientation behavior of *Dendroctonus ponderosae*: Integration of token stimuli and host defenses. In Mattson, W. J., Leveux, J., and Bernard-Dagan, C., editors, *Mechanisms of Woody Plant Resistance to Insects and Pathogens*, pages 369–390. Springer-Verlag, New York.
- Raffa, K. F. (2001). Mixed messages across multiple trophic levels: The ecology of bark beetle chemical communication systems. *Chemoecology*, 11:49–65.
- Raffa, K. F., Aukema, B. H., Bentz, B. J., Carroll, A. L., Hicke, J. A., Turner, M. G., and Romme, W. H. (2008). Cross-scale drivers of natural disturbances prone to anthropogenic amplification: the dynamics of bark beetle eruptions. *Bioscience*, 58(6):501–517.
- Ramakrishnan, R., Hradecký, J., Roy, A., Kalinová, B., Mendezes, R. C., Synek, J., Bláha, J., Svatoš, A., and Jirošová, A. (2022). Metabolomics and transcriptomics of pheromone biosynthesis in an aggressive forest pest *ips typographus*. *Insect Biochemistry and Molecular Biology*, 140:103680.
- Randall, C. B., Steed, B. E., and Bush, R. (2011). Revised r1 forest insect hazard rating system user guide for use with inventory data stored in fsveg and/or analyzed with the forest vegetation simulator. Technical report, United States Department of Agriculture, Forest Service, Region 1.
- Rasmussen, L. A. (1980). Emergence and attack behavior of the mountain pine beetle in lodgepole pine. Technical report, Department of Agriculture, Forest Service, Intermountain Forest and Range

- Reeve, J. D., Anderson, F. E., and Kelley, S. T. (2012). Ancestral state reconstruction for dendroctonus bark beetles: evolution of a tree killer. *Environmental entomology*, 41(3):723–730.
- Régnière, J. and Bentz, B. (2007). Modeling cold tolerance in the mountain pine beetle, dendroctonus ponderosae. *Journal of insect physiology*, 53(6):559–572.
- Régnière, J., Delisle, J., Pureswaran, D. S., and Trudel, R. (2013). Mate-finding allee effect in spruce budworm population dynamics. *Entomologia Experimentalis et Applicata*, 146(1):112–122.
- Régnière, J. and Nealis, V. (2007). Ecological mechanisms of population change during outbreaks of the spruce budworm. *Ecological Entomology*, 32(5):461–477.
- Régnière, J., Saint-Amant, R., Béchard, A., and Moutaoufik, A. (2014). *BioSIM 10: User's manual*. Laurentian Forestry Centre Québec, QC, Canada.
- Reid, R. (1962). Biology of the mountain pine beetle, dendroctonus monticolae hopkins, in the east kootenay region of british columbia i. life cycle, brood development, and flight periods1. *The Canadian Entomologist*, 94(5):531–538.
- Reid, R. W. (1958). The behaviour of the mountain pine beetle, dendroctonus monticolae hopk., during mating, egg laying, and gallery construction1. *The Canadian Entomologist*, 90(9):505–509.
- Reid, R. W. (1963). Biology of the mountain pine beetle, dendroctonus monticolae hopkins, in the east kootenay region of british columbia.: Iii. interaction between the beetle and its host, with emphasis on brood mortality and survival1. *The Canadian Entomologist*, 95(3):225–238.
- Reid, T. G. and Reid, M. L. (2008). Fluorescent powder marking reduces condition but not survivorship in adult mountain pine beetles. *The Canadian Entomologist*, 140(5):582–588.
- Robertson, C., Nelson, T. A., and Boots, B. (2007). Mountain pine beetle dispersal: the spatial–temporal interaction of infestations. *Forest Science*, 53(3):395–405.
- Robertson, C., Nelson, T. A., Jelinski, D. E., Wulder, M. A., and Boots, B. (2009). Spatial–temporal analysis of species range expansion: the case of the mountain pine beetle, dendroctonus ponderosae. *Journal of Biogeography*, 36(8):1446–1458.
- Rodman, K. C., Andrus, R. A., Carlson, A. R., Carter, T. A., Chapman, T. B., Coop, J. D., Fornwalt, P. J., Gill, N. S., Harvey, B. J., Hoffman, A. E., et al. (2022). Rocky mountain forests are poised to recover following bark beetle outbreaks but with altered composition. *Journal of Ecology*, 110(12):2929–2949.
- Rosenberger, D. W., Aukema, B. H., and Venette, R. C. (2017). Cold tolerance of mountain pine beetle among novel eastern pines: A potential for trade-offs in an invaded range? *Forest Ecology and Management*, 400:28–37.
- Royama, T. (1984). Population dynamics of the spruce budworm choristoneura fumiferana. *Ecological Monographs*, 54(4):429–462.
- Royama, T. (1997). Population dynamics of forest insects: are they governed by single or multiple factors? In Watt, A. D., Stork, N. E., and Hunter, M. D., editors, *Forests and insects*, pages 37–48. Chapman & Hall, London, UK.
- Rudinsky, J., Morgan, M., Libbey, L., and Putnam, T. (1974). Antiaggregative-rivalry pheromone of the mountain pine beetle, and a new arrestant of the southern pine beetle. *Environmental Entomology*, 3(1):90–98.

- Rudinsky, J. A. (1962). Ecology of Scolytidae. *Annual Review of Entomology*, 7:327–348.
- Rust, H. (1930). Relation of insectivorous birds to the mortality of the mountain pine beetle during the flight period. *United States Department of Agriculture Bureau of Entomology, Forest Insect Field Station, Coeur d'Alene, ID*.
- Safranyik, L. (1968). *Development of a technique for sampling mountain pine beetle populations in lodgepole pine*. PhD thesis, University of British Columbia.
- Safranyik, L. (1988). Estimating attack and brood totals and densities of the mountain pine beetle in individual lodgepole pine trees. *The Canadian Entomologist*, 120(4):323–331.
- Safranyik, L. (1989). Mountain pine beetle: biology overview. In *Proceedings: Symposium on the Management of Lodgepole Pine to Minimize Losses to the Mountain Pine Beetle*, pages 9–12. United States Department of Agriculture, Forest Service, Intermountain Forest and Range Experiment Station.
- Safranyik, L. (1998). Mortality of mountain pine beetle larvae, *dendroctonus ponderosae* (coleoptera: Scolytidae) in logs of lodgepole pine (*pinus contorta* var. *latifolia*) at constant low temperatures. *Journal of the Entomological Society of British Columbia*, 95:81–88.
- Safranyik, L. and Carroll, A. L. (2006). The biology and epidemiology of the mountain pine beetle in lodgepole pine forests. In Safranyik, L. and Wilson, B., editors, *Detection, mapping, and monitoring of the mountain pine beetle*, pages 3–66. Natural Resources Canada, Canadian Forest Service, Pacific Forestry Centre.
- Safranyik, L., Carroll, A. L., Régnière, J., Langor, D., Riel, W., Shore, T. L., Peter, B., Cooke, B. J., Nealis, V., and Taylor, S. W. (2010). Potential for range expansion of mountain pine beetle into the boreal forest of north america. *The Canadian Entomologist*, 142(5):415–442.
- Safranyik, L. and Linton, D. (1985). The relationship between density of emerged *dendroctonus ponderosae* (coleoptera: Scolytidae) and density of exit holes in lodgepole pine. *The Canadian Entomologist*, 117(3):267–275.
- Safranyik, L. and Linton, D. (1991). Unseasonably low fall and winter temperatures affecting mountain pine beetle and pine engraver beetle populations and damage in the british columbia chilcotin region. *Journal of the Entomological Society of British Columbia*, 88:17–21.
- Safranyik, L., Linton, D., Silversides, R., and McMullen, L. (1992). Dispersal of released mountain pine beetles under the canopy of a mature lodgepole pine stand. *Journal of Applied Entomology*, 113(1-5):441–450.
- Safranyik, L., Shrimpton, D., Whitney, H., et al. (1975). An interpretation of the interaction between lodgepole pine, the mountain pine beetle and its associated blue stain fungi in western canada. *Management of lodgepole pine ecosystems*, 1:406–428.
- Safranyik, L. and Vithayasai, C. (1971). Some characteristics of the spatial arrangement of attacks by the mountain pine beetle, *dendroctonus ponderosae* (coleoptera: Scolytidae), on lodgepole pine1: Appendix: Statistical analysis of the” hole-pairs” experiment. *The Canadian Entomologist*, 103(11):1607–1625.
- Sallé, A. and Raffa, K. F. (2007). Interactions among intraspecific competition, emergence patterns, and host selection behaviour in *ips pini* (coleoptera: Scolytinae). *Ecological Entomology*, 32:162–171.

- Schmid, J. (1972). *Emergence, attack densities and seasonal trends of mountain pine beetle (Dendroctonus ponderosae) in the Black Hills*, volume 211. Rocky Mountain Forest and Range Experiment Station, Forest Service, US
- Schmid, J. (1977). *Spruce beetle in the Rockies*, volume 49. Rocky Mountain Forest and Range Experiment Station, Forest Service, US
- Schmitz, R. F., McGregor, M. D., Amman, G. D., and Oakes, R. D. (1989). Effect of partial cutting treatments of lodgepole pine stands on the abundance and behavior of flying mountain pine beetles. *Canadian Journal of Forest Research*, 19(5):566–574.
- Schnorbus, M. (2011). A synthesis of the hydrological consequences of large-scale mountain pine beetle disturbance. Mountain Pine Beetle Working Paper 2010-01, Natural Resources Canada, Canadian Forest Service, Pacific Forestry Centre. MPBI Project # 7.53.
- Seybold, S. J., Bentz, B. J., Fettig, C. J., Lundquist, J. E., Progar, R. A., and Gillette, N. E. (2018). Management of western north american bark beetles with semiochemicals. *Annual Review of Entomology*, 63(1):407–432.
- Seybold, S. J., Huber, D. P., Lee, J. C., Graves, A. D., and Bohlmann, J. (2006). Pine monoterpenes and pine bark beetles: a marriage of convenience for defense and chemical communication. *Phytochemistry Reviews*, 5:143–178.
- Shepard, R. (1965). Distribution of attacks by dendroctonus ponderosae hopk. on pinus contorta dougl. var. latifolia englm. *Can. Entomol*, 97:207–215.
- Shepherd, R. (1966). Factors influencing the orientation and rates of activity of dendroctonus ponderosae hopkins (coleoptera: Scolytidae) 1. *The Canadian Entomologist*, 98(5):507–518.
- Shore, T. L., Safranyik, L., et al. (1992). Susceptibility and risk rating systems for the mountain pine beetle in lodgepole pine stands. Technical report, Natural Resources Canada, Canadian Forest Service, Pacific Forestry Centre.
- Singh, V. V., Naseer, A., Mogilicherla, K., Trubin, A., Zabihi, K., Roy, A., Jakuš, R., and Erbilgin, N. (2024). Understanding bark beetle outbreaks: exploring the impact of changing temperature regimes, droughts, forest structure, and prospects for future forest pest management. *Reviews in Environmental Science and Bio/Technology*, pages 1–34.
- Six, D. L. and Bracewell, R. (2015). Dendroctonus. In *Bark beetles*, pages 305–350. Elsevier.
- Stallcup, P. L., Baldwin, P. H., Wygant, N. D., Lechleitner, R. R., et al. (1963). A method for investigating avian predation on the adult black hills beetle. Master’s thesis, Colorado State University. Libraries.
- Stan Development Team (2020). RStan: the R interface to Stan. R package version 2.19.3.
- Stipe, L. (1974). Yearly trend of a mountain pine beetle infestation near spring creek park bridger-teton national forest. Technical report, United States Department of Agriculture, Forest Service.
- Stipe, L. (1976). Trends of a mountain pine beetle outbreak in a high elevation stand in yellowstone national park. Technical report, United States Department of Agriculture, Forest Service.
- Storer, A., Wainhouse, D., and Speight, M. (1997). The effect of larval aggregation behaviour on larval growth of the spruce bark beetle dendroctonus micans. *Ecological Entomology*, 22(1):109–115.

- Strogatz, S. H. (1994). *Nonlinear dynamics and chaos: With applications to physics, biology, chemistry, and engineering*. CRC press.
- Strohm, S., Tyson, R., and Powell, J. (2013). Pattern formation in a model for mountain pine beetle dispersal: linking model predictions to data. *Bulletin of mathematical biology*, 75:1778–1797.
- Sturdevant, N., Haavik, L., and Negrón, J. F. (2022). Douglas-fir tree mortality caused by the douglas-fir beetle in thinned and unthinned stands in montana, usa. *Forest Science*, 68(2):145–151.
- Sun, J., Lu, M., Gillette, N. E., and Wingfield, M. J. (2013). Red turpentine beetle: innocuous native becomes invasive tree killer in china. *Annual Review of Entomology*, 58(1):293–311.
- Taylor, C. M. (2012). Allee effects. In Hastings, A. M., editor, *Encyclopedia of theoretical ecology*, pages 32–38. University of California Press.
- Taylor, S. W., Carroll, A. L., Alfaro, R. I., Safranyik, L., et al. (2006). Forest, climate and mountain pine beetle outbreak dynamics in western canada. In Safranyik, L. and Wilson, B., editors, *Detection, mapping, and monitoring of the mountain pine beetle*, pages 67–94. Natural Resources Canada, Canadian Forest Service, Pacific Forestry Centre.
- Teste, F. P., Lieffers, V. J., and Landhäusser, S. M. (2011a). Seed release in serotinous lodgepole pine forests after mountain pine beetle outbreak. *Ecological Applications*, 21(1):150–162.
- Teste, F. P., Lieffers, V. J., and Landhäusser, S. M. (2011b). Viability of forest floor and canopy seed banks in *pinus contorta* var. *latifolia* (pinaceae) forests after a mountain pine beetle outbreak. *American Journal of Botany*, 98(4):630–637.
- Thalenhorst, W. (1958). *Grundzüge der Populationsdynamik des großen Fichtenborkenkäfers Ips typographus L.* Sauerländer.
- Tishmack, J., Mata, S., and Schmid, J. (2005). Mountain pine beetle emergence from lodgepole pine at different elevations near fraser, co. res. pap. rmrs-rn-27. Technical report, United States Department of Agriculture, Forest Service, Rocky Mountain Research Station.
- Tkacz, B. M. and Schmitz, R. F. (1986). Association of an endemic mountain pine beetle population with lodgepole pine infected by armillaria root disease in utah. Research note, United States Department of Agriculture, Forest Service, Intermountain Forest and Range Experiment Station, Ogden, Utah, United States of America.
- Truscott, J. and Brindley, J. (1994a). Equilibria, stability and excitability in a general class of plankton population models. *Philosophical Transactions of the Royal Society of London. Series A: Physical and Engineering Sciences*, 347(1685):703–718.
- Truscott, J. and Brindley, J. (1994b). Ocean plankton populations as excitable media. *Bulletin of Mathematical Biology*, 56(5):981–998.
- Trzcinski, M. K. and Reid, M. L. (2009). Intrinsic and extrinsic determinants of mountain pine beetle population growth. *Agricultural and Forest Entomology*, 11(2):185–196.
- Tunnock, S. et al. (1970). A chronic infestation of mountain pine beetles in lodgepole pine in glacier national park, montana. *Journal of the Entomological Society of British Columbia*, 67.
- USDA Forest Service (2009). Southern pine beetle. https://www.fs.usda.gov/Internet/FSE_DOCUMENTS/fsbdev2_042840.pdf. Accessed: 2024-09-24.

- USDA Forest Service (2011). Spruce beetle in the southern rocky mountains. https://www.fs.usda.gov/Internet/FSE_DOCUMENTS/stelprdb5303039.pdf. Accessed: 2024-09-24.
- Waring, R. and Pitman, G. (1983). Physiological stress in lodgepole pine as a precursor for mountain pine beetle attack 1. *Zeitschrift für angewandte Entomologie*, 96(1-5):265–270.
- Waring, R. H. and Pitman, G. B. (1985). Modifying lodgepole pine stands to change susceptibility to mountain pine beetle attack. *Ecology*, 66(3):889–897.
- Washburn, R. I. and Cole, W. E. (1959). Mountain pine beetle and black hills beetle conditions in the pine stands of forest service region 4. Technical report, United States Department of Agriculture, Forest Service.
- Weed, A. S., Ayres, M. P., and Bentz, B. J. (2015). Population dynamics of bark beetles. In *Bark beetles*, pages 157–176. Elsevier.
- Werner, R. A., Raffa, K. F., and Illman, B. L. (2006). Dynamics of phytophagous insects and their pathogens in alaskan boreal forests. *Alaska's Changing Boreal Forest*. Oxford University Press, London, pages 133–146.
- Whiteside, H. E. (1937). Progress report of a study of the black hills beetle emergence in southeastern wyoming summer of 1936. Technical report, United States Department of Agriculture, Forest Service.
- Wood, S. (1982). Bark and ambrosia beetles of north and central america (coleoptera: Scolytidae), a taxonomic monograph. *Great Basin naturalist memoirs*, 6(1).
- Wright, L., Berryman, A., and Wickman, B. (1984). Abundance of the fir engraver, *scolytus ventralis*, and the douglas-fir beetle, *dendroctonus pseudotsugae*, following tree defoliation by the douglas-fir tussock moth, *orgyia pseudotsugata*1. *The Canadian Entomologist*, 116(3):293–305.
- Wygant, N. D. (1940). *Effects of Low Temperatures on the Black Hills Beetle (Dendroctonus ponderosae Hopk.)*. PhD thesis, New York State College of Forestry, Syracuse, New York.
- Yan, Z., Sun, J., Don, O., and Zhang, Z. (2005). The red turpentine beetle, *dendroctonus valens leconte* (scolytidae): an exotic invasive pest of pine in china. *Biodiversity & Conservation*, 14:1735–1760.
- Zipfel, R. D., de Beer, Z. W., Jacobs, K., Wingfield, B. D., and Wingfield, M. J. (2006). Multi-gene phylogenies define *ceratocystiopsis* and *grosmannia* distinct from *ophiostoma*. *Studies in mycology*, 55(1):75–97.